Regulatory mechanism of nitrogen metabolism and stress response in the methylotrophic yeast *Candida boidinii*

Kosuke Shiraishi

2017

Contents

Introduction

Plant leaves cover a large area of global land surface, approximately 10^9 square kilometer[1]. Every leaf provides a habitat for colonization of microbes[2,3]. Many microbes form spores, either to survive under nutrient-limited conditions or to differentiate from spores into appressoria prior to invasion to host plants. Asporogenous microbes also inhabit and survive for long periods on leaf surfaces over the entire lifespan of a plant, i.e., during the growth from seed to adulthood, followed by aging and death[4]. Upon death of the host plant, microbes on the plant body return to the soil where the plant biomass is degraded by soil microbes, recycling the nutrients for use by the next generation. Some microbes found in the phyllosphere (the above-ground portions of plants used as microbial habitats) emerge from the soil during plant growth[5]. Despite its potential importance, information regarding microbe-plant interactions and microbial physiology, in the context of the whole plant lifespan, is very limited. Consequently, the actual nutrient sources used by microbes on the above parts of plant surfaces remain mostly unknown.

Methylotrophs are microbes that can utilize reduced one-carbon (C1) compounds, e.g., methane, methanol, or methylamine, as the sole carbon and energy source. Because methanol is abundant in the phyllosphere[6], methylotrophs are ubiquitous on plant leaf surfaces and dominate the phyllosphere population[7]. Recent study discovered that the plant-residing asporogenous methylotrophic yeast *Candida boidinii* can proliferate on growing plant leaves, assimilating methanol for its growth and survival[6]. However, the yeast nitrogen metabolism is still unknown in the phyllosphere.

Nitrogen, which is present in many biological molecules such as proteins and nucleic acids, is essential for growth and development of all organisms[8]. In the natural environment, nitrogen is present in a wide range of chemical forms including organic nitrogen, inorganic ammonium (NH_4^+), nitrate (NO_3^-), nitric oxide (NO), and nitrogen gas (N_2), and is continuously cycled among these forms. This process, called the nitrogen cycle, involves not only numerous types of microorganisms but also plants, animals, and humans[9].

Microbe-plant interactions are one of the key factors responsible for the global nitrogen cycle. The assimilation of nitrogen by microorganisms participating in microbe-plant symbioses has been studied mainly in the underground soil environment. These studies have revealed many strategies of microbial nitrogen assimilation including nitrogen fixation, nitrification, and denitrification mainly in the rhizosphere[10,11].

Compared with rhizospheric niche, microbes living on plant surface need to respond and adapt to a variety of stresses and environmental changes such as nutrient limitation, high fluxes of UV radiation, and changes of temperature, humidity, and wind direction[12]. In order to correspond to such uncomfortable conditions and variation in the external environments,

microorganisms must have developed their survival strategies and molecular functions.

In stress response, signal transduction is very important. When exposed to stresses, cells sense the stresses and activate the corresponding signal pathways. Subsequently, the downstream gene expression and/or protein activity are regulated for adaptation to the stress conditions. Mitogen-activated protein kinases (MAPK) are signaling proteins that are conserved from yeast to human. They are serine-threonine protein kinases that are activated by some stimuli, such as cytokines, growth factors, hormones, and cellular stress[13-15]. MAPK are catalytically inactive in their base form. In order to become active, they require phosphorylation events in their activation loops. When cells sense some stimuli, small GTPase Ras is activated for activation of the downstream signaling pathways, including MAPK cascade. Dephosphorylation of MAPK by MAPK phosphatase, on the other hand, leads to the inactivation of MAPK[16].

High osmolarity glycerol (Hog) pathway plays a central role in stress responses. It has been reported that Hog1 is activated in response to a variety of stress stimuli including high osmolarity, oxidative stress, heat stress, and arsenite, and contributes to the regulation of cell wall composition. However, intracellular dymanics of Hog1 is almost unknown under those stresses except for high osmotic stress condition.

In this thesis, I demonstrate that available nitrogen source for yeast survival changes from nitrate to methylamine and other nitrogen sources during the host plant aging and that nitrate reductase necessary for cell growth on young leaves is degraded via autophagy on aged leaves. I also describe that Hog1, a stress response factor, formes dot structures in the cytosol under heat stress condition, which contributes to the yeast heat tolerance.

Chapter I describes identification of the genes, *YNR1* encoding nitrate reductase (Ynr1) that is involved in nitrate metabolism and *AMO1* encoding amine oxidase (Amo1) responsible for the oxidation of methylamine, and characterization of their regulatory expression. According to RT-PCR analysis, the transcript level of *YNR1* was induced by nitrate and nitrite, and was not repressed by the coexistence of other nitrogen sources. In contrast, the transcript level of *AMO1*, which was induced by methylamine, was significantly repressed by the coexistence of ammonium or glutamine.

In the Chapter II, regulation of yeast nitrogen metabolism in the phyllosphere is studied. Quantitative PCR analysis, RT-PCR analysis and microscopic observation revealed that nitrate is utilized on young plant leaves, while methylamine becomes the primary nitrogen source on older plant leaves. Subsequently, intracellular dynamics of Ynr1 necessary for nitrate metabolism was investigated *in vitro*. It was found that Ynr1 was degraded via one of the selective autophagy pathways, Cvt (Cytoplasm-to-vacuole targeting) pathway, in response to the shift of available nitrogen source from nitrate to methylamine. In addition, when cells were transferred from nitrate to nitrate plus methylamine, Ynr1 was degraded in a

similar manner. These results suggest that Ynr1 is transported to the vacuole for degradation under the coexisting stage of nitrate and methylamine during the host plant life cycle.

Chapter III shows the intracellular dynamics of Hog1, one of the representative stress response factors. Intracellular localization of Hog1 was examined under heat and osmotic stress conditions using 4 different yeast species, *C. boidinii*, *Pichia pastoris*, *Saccharomyces cerevisiae* and *Schizosaccharomyces pombe*. It was found that all of the 4 yeast species except for *S. cerevisiae* showed dot structures of Hog1 in the cytosol under high temperature condition. Further analysis in *C. boidinii* disclosed that Hog1 was sequestered into stress granules, which contributes to the yeast heat tolerance.

Chapter I

Regulation of nitrate and methylamine metabolism in the methylotrophic yeast *Candida boidinii*

Abstract

The methylotrophic yeast *Candida boidinii* is capable of growth on methanol as a sole carbon and energy source. Recently, a new method was developed to gain insight into microbial life on the plant leaf surface and revealed that *C. boidinii* utilizes methanol as a carbon source in the phyllosphere. However, the yeast nitrogen metabolism and its regulation are unknown. Prior to investigating the yeast nitrogen metabolism on plant leaves, I performed *in vitro* experiments to investigate the regulatory profile of nitrate and methylamine in *C. boidinii*. The transcript level of nitrate reductase (Ynr1) gene was induced by nitrate and nitrite, and was not repressed by the coexistence with other nitrogen sources. In contrast, the transcript level of amine oxidase (Amo1) gene, which was induced by methylamine, was significantly repressed by the coexistence with ammonium or glutamine. These results suggest that the sensitivity to repression by other nitrogen sources was different between Ynr1 and Amo1.

Introduction

Utilization of nitrate as the source of nitrogen is restricted to relatively few species of yeast[17]. Since the classical model yeasts *Saccharomyces cerevisiae* and *Schizosaccharomyces pombe* are unable to assimilate nitrate, studies of nitrate utilization have been conducted mainly using the methylotrophic yeast *Hansenula polymorpha* in terms of the assimilation pathway, control of gene expression, and enzymatic properties. In *H. polymorpha*, nitrate is first reduced to nitrite by nitrate reductase (HpYnr1), and reduction of nitrite to ammonium is catalyzed by nitrite reductase (HpYni1). Both of these enzymatic reactions require NAD(P)H as an energy source[18]. Previously, HpYnr1 enzyme activity was shown to be regulated primarily at the level of transcription. HpYnr1 expression was induced by nitrate and nitrite, and it was significantly repressed by the coexistence with ammonium[19-21]. In addition, post-transcriptional regulation of HpYnr1 was investigated with respect to its enzymatic properties. Similar to the expression profile of HpYnr1, nitrate and nitrite enhanced the enzymatic activity, whereas it was repressed by the presence of ammonium[22]. To date, there has only been one study demonstrating the effect of methylamine on the regulation of nitrate reductase[22]. Metabolic responses to utilizable nitrogen sources at the transcript level, which are elicited by primary nitrogen sources (e.g. ammonium and glutamine) and lead to repression of genes at transcript level essential for assimilation of secondary sources, such as nitrate, are generally referred to as nitrogen metabolite repression (NMR).

Research has shown that the effects of nitrogen compounds on the enzymatic properties of nitrate reductase differ in other yeast species. In *Candida nitratophila*, glutamine but not ammonium suppressed nitrate reductase (CnYnr1) activity, whereas both compounds partially suppressed the nitrate reductase activity (HaYnr1) and enhanced the enzyme degradation of HaYnr1 in *Hansenula anomala*[23,24]. *Dekkera bruxellensis* showed high growth rates in mixed ammonia/nitrate media, and nitrate assimilation genes were slightly repressed by ammonia[25]. The transcript level of nitrate reductase was also investigated in *H. anomala*. In this yeast, the transcript level of *HpYNR1* in medium containing nitrate plus ammonium was similar to that in the nitrate medium[26], while the expression of *HpYNR1* in *H. polymorpha* was very low in medium supplemented with nitrate and ammonium[20,21].

Methylamine utilization in *H. polymorpha* has also been investigated in relation to peroxisome biogenesis[27]. In this yeast, a large number of peroxisomes developed when methylamine was utilized as a sole nitrogen source. In the assimilation pathway in *H. polymorpha*, methylamine is converted to ammonium by amine oxidase (HpAmo1), a peroxisomal enzyme that has peroxisome targeting signal type 2 (PTS2) at the amino terminus. During adaptation to methylamine, HpAmo1 was specifically synthesized and transported to peroxisomes with induction of the PTS2 pathway[28]. In addition, a recent study showed the

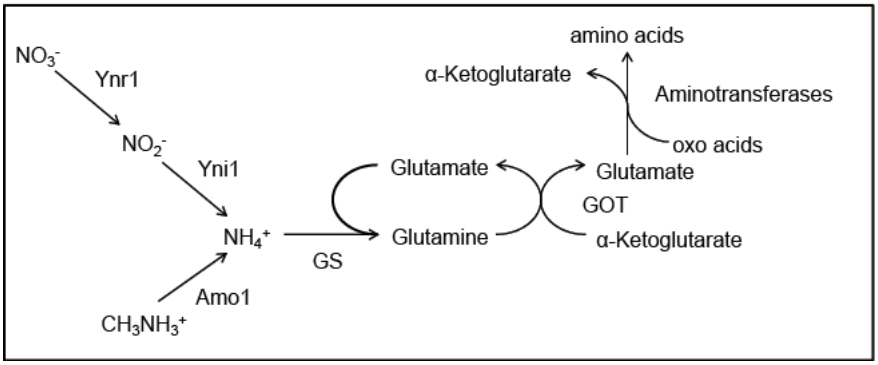

Figure 1-1. Nitrogen utilization pathway in the methylotrophic yeast *C. boidinii*. Ynr1, nitrate reductase; Yni1, nitrite reductase; Amo1, amine oxidase; GS: glutamine synthetase; GOT, glutamine oxoglutarate aminotransferase.

positive effect of methylamine on yeast lifespan[29]. Nevertheless, the regulatory profile of gene expression and enzyme activity involved in methylamine metabolism is not clear.

In this study, I examined the regulatory profile of key enzymes involved in nitrate and methylamine metabolism, nitrate reductase (Ynr1) and amine oxidase (Amo1), in response to various nitrogen sources in *Candida boidinii* (Figure 1-1). The results showed that Ynr1 and Amo1 were specifically induced by nitrate and methylamine, respectively, both at the enzyme-activity and transcript levels. I also found that effect of coexistence with other nitrogen sources on transcript regulation of Ynr1 and Amo1 genes was different each other.

Materials and methods

Yeast strains, vectors, and plasmids

C. boidinii strains, primers and plasmids used in this study are listed up in Table 1-1, Table 1-2 and Table 1-3, respectively. *C. boidinii* strain AOU1 was used as the wild-type strain. The *ynr1Δ* and *amo1Δ* strains were constructed by replacing the appropriate ORF of *C. boidinii* strain TK62 (*ura3*)[30] with the Zeocin™ resistance gene as a selective marker[31], using the modified lithium acetate method[32].

Table 1-1. Strains used in this study

Designation	Description	Genotype	References
AOU1	Wild type	Normal	Tani *et al.* (1985)
TK62	*Cbura3Δ*	*ura3*	Sakai *et al.* (1991)
KSC0001	*Cbura3Δynr1Δ*	*ynr1Δ*:: Zeo^r *ura3*	This study
KSC0002	*Cb ynr1Δ*	KSC0001 *ura3*:: SK+URA	This study
KSC0003	*Cbura3Δamo1Δ*	*amo1Δ*:: Zeo^r *ura3*	This study
KSC0004	*Cbamo1Δ*	KSC0003 *ura3*:: SK+URA	This study

Table 1-2. Primers used in this study

Designation	DNA sequence (5'→3')
Fw-YNRu-*Bam*HI	GGATCCCCCAATTAGTACTAAACACGGGCG
Rv-YNRu-*Xho*I	CTCGAGGGAGTTATGTGCTGGTGAATAAAG
Fw-YNRd-*Not*I	GCGGCCGCCTCGCTTATAAAAATCTTTTTGTCTTGTC
Rv-YNRd-*Bam*HI	GGATCCCTAGAAGGATATTGTATATGAGGTG
Fw-AMOu-*Bam*HI	GGATCCCTATTGAAAGGGAATTGCCTATCC
Rv-AMOd-XhoI	CTCGAGCCTAATTAGGTATATCAATCCACC
Fw-AMOd-*Not*I	GCGGCCGCGTCTTATATTTTTTCTTCTTCATC
Rv-AMOd-BamHI	GGATCCCTAGCTCTGATGTCTTAAAGTTATC
Fw-RT-ACT	CAGCAGTGGTGGAGAAAGTG
Rv-RT-ACT	TGCTGATGAATCTTGGTGGA
Fw-RT-YNR	TCGGCTAATCTCCAGGTGAC
Rv-RT-YNR	ATTGCTGCTCCATCAAGACC
FwRT-AMO	ACACCTGGAACACCAGCTTC
Rv-RT-AMO	TGGCCTTTTGCTGGCCTTTTGCTCACATGTCTTGCAGTCTAAAAATAAACA

Table 1-3. Plasmids used in this study

Designation	Description	References
pBluescript II SK+/Zeocassette™	*Zeo*^{r}	Kawaguchi *et al*. (2011)
SK+Zeo YNR1del	*YNR1*$_{up}$-*Zeo*^{r}-*YNR1*$_{down}$	This study
SK+Zeo AMO1del	*AMO1*$_{up}$-*Zeo*^{r}-*AMO1*$_{down}$	This study
SK+URA	*URA3*	This study

Culture conditions

Cells were grown at 28°C on YPD medium (1% Bacto-yeast extract, 2% Bacto-peptone, 2% glucose) and SD medium (0.17% yeast nitrogen base without amino acids and ammonium sulfate, 2% glucose, and nitrogen sources). Nitrogen sources were ammonium sulfate [$(NH_4)_2SO_4$], potassium nitrate [KNO_3], methylamine chloride [CH_3NHCl], sodium nitrite [$NaNO_2$], L-glutamine [$NH_2CO(CH_2)CH(NH_2)COOH$]. When a single nitrogen source was present, the concentration was 7.6 mM. When two compounds were used as nitrogen sources, 3.6 mM (as the molar concentration of N atom) of each compound was used. The pH of SD medium was adjusted to 6.0 with NaOH. Growth was monitored by measuring the optical density at 610 nm (OD_{610}).

Construction of the *YNR1* and *AMO1* disruptant strains

The upstream region (1.1 kb) and downstream (1.3 kb) region of the *YNR1* gene were amplified by PCR with the primer sets Fw-YNRu-*Bam*HI/Rv-YNRu-*Xho*I and Fw-YNRd-*Not*I/Rv-YNRd-*Bam*HI, respectively, using genomic DNA as a template. These PCR-amplified fragments were ligated into the *Xho*I-*Not*I backbone fragment of pBluescript II SK+/Zeocassette™. The resultant vector (6.5 kb) was linearized with *Bam*HI and used to transform *C. boidinii* strain TK62 using a modified version of the lithium acetate method[32]. Zeocin-resistant colonies were selected on YPD medium supplemented with Zeocin[31]. The upstream (1.3 kb) and downstream (1.5 kb) regions of the *AMO1* gene were amplified by PCR with the primer sets Fw-AMOu-*Bam*HI/Rv-AMOd-XhoI and Fw-AMOd-*Not*I/Rv-AMOd-BamHI, respectively. These PCR-amplified fragments were ligated into the *Xho*I-*Not*I backbone fragment of pBluescript II SK+/Zeocassette™. The resultant vector (6.9 kb) was linearized with *Bam*HI and used to transform *C. boidinii* strain TK62. The disruptions of these genes were confirmed by Southern blot analysis as previously described[33].

RNA analysis

In order to assure a high-quality gene expression data, RNA analysis was performed by taking advantage of the MIQE Guidelines[34] *C. boidinii* cells were grown on SD medium containing various nitrogen sources and harvested at the indicated time point. Total RNA was extracted using Yeast Processing Reagent (TaKaRa Bio, Otsu, Japan) and RNeasy mini Kit (Qiagen). The purity of the extracted RNA was assessed by the NanoDrop 1000 spectrophotometer (Thermo Scientific). Subsequently, cDNA was synthesized from 2 µg of total RNA using Random Primers (Promega) and ReverTra Ace (Toyobo, Tokyo, Japan) at the total volume of 20 µl according to the following parameters: pre-incubation, 10 min at 30°C and incubation 50 min at 40°C. After amplifying cDNA, RT-qPCR was performed in a 20-µl mixture in glass capillary tubes using a LightCycler (Roche Diagnostic). The PCR cycling reaction for the sample DNA was performed with 1x SYBR *Premix Ex Taq* RNase H plus (TaKaRa Bio) according to the following parameters: first cycle, 30 s of denaturation at 95°C; second cycle with 40 repetitions, 95°C for 5 s, 60°C for 20 s (all temperature transitions, 20°C s^{-1}). Transcript level of *YNR1* and *AMO1* was first quantified using *ACT1* as the control, and then, expressed as the relative value to those in ammonium media.

Preparation of cell-free extract

C. boidinii cells were first cultured on SD supplemented with 7.6 mM ammonium for 12 h, shifted to SD containing with 7.6 mM of the indicated nitrogen source, and then collected 4 h after the medium transfer. Cells (approximately 100 OD_{610} units of cells grown in SD medium) were then resuspended in 0.1 M potassium phosphate buffer (pH 7.5) and disrupted with 0.5-mm zirconia beads in a Multi-Beads Shocker (YASUI KIKAI Co., Ltd, Osaka, Japan). Cell debris was removed by centrifugation at 15,000 rpm for 10 min at 4uC, and the resultant supernatant (cell-free extract) was used for enzyme assays. Protein concentrations were determined by the Bradford method[35] using a protein assay kit (Bio-Rad Laboratories, Hercules, CA, USA), using bovine serum albumin as the standard.

Enzyme assay

For the measurement of Ynr1 activity, 650 µL assay mixtures containing potassium phosphate buffer and 250 µL cell-free extract were prepared in polystyrene cuvettes (light path, 10 mm). The cuvettes were incubated for 2–3 min at 28°C, and the absorbance at 340 nm was monitored. The reaction was then initiated by the addition of 100 µL of 100 mM potassium nitrate, and the rate of decrease in absorbance at 340 nm was measured against a blank containing all of the assay components except potassium nitrate. Ynr1 activity is expressed in U/mg (U; µmol/min). Amo1 activity was measured in a similar way as follows: 860 µL assay mixtures containing potassium phosphate buffer and 100 µL of cell-free extract were prepared

in polystyrene cuvettes. The cuvettes were incubated for 2–3 min at 28°C, and the absorbance at 405 nm was monitored. The reaction was then initiated by addition of 40 µL of 80 mM methylamine hydrochloride, and the rate of increase in absorbance at 405 nm was measured against a blank containing all assay components except methylamine hydrochloride. Amo1 activity is also expressed in U/mg (U; µmol/min).

Results and discussion

Identification and characterization of *YNR1* and *AMO1* in *C. boidinii*

Homology searches of the *C. boidinii* genome database revealed enzyme genes responsible for nitrate- and methylamine-utilization pathways predicted to yield ammonium. The genes encoding the initial steps for these pathways are *YNR1*, encoding the nitrate reductase Ynr1, and *AMO1*, encoding the amine oxidase Amo1 (Figure 1-1). These genes were first assigned based on the alignment with orthologous enzymes from the methylotrophic yeast *Hansenula polymorpha* (Figure 1-2 and 1-3). In order to reveal the functions of *YNR1* and *AMO1* in *C. boidinii*, these genes were disrupted by replacing the appropriate ORF with the Zeocin™ resistance gene as a selective marker. The *ynr1Δ* and *amo1Δ* strains could not utilize nitrate and methylamine, respectively, as the nitrogen source (Figure 1-4A, 1-4B and 1-4C). Furthermore, nitrate reductase and amine oxidase activities were lost in the *ynr1Δ* and *amo1Δ* strains, respectively (Table 1-4), confirming that these genes encode proteins with the corresponding activities.

Figure 1-2. Comparison of amino-acid sequences of nitrate reductase by alignment of CbYnr1 and HpYnr1. *YNR1* contains a 2667-bp ORF encoding a protein of 889 amino acids (Ynr1). The predicted amino acid sequence of *YNR1* has a high degree of identity (56%) to nitrate reductase of the yeast *H. polymorpha*.

```
CbAmo1      MERLAQISSQTTGSIAAPSRPAHPLDPLSIEEISAITAVVKNHFAGRQISFNTVTLREPTKKAFLEWKEQGGAFPPRNAYYVILEAGVPG
HpAmo1      MERLRQIASQATAASAAPPRPAHPLDPLSTAEIKAVTSTVKSYFAGKQISFNTVTLREPARKAYIQWKEQGGPLPPRLAYYVILEAGKPG
            **** **:**:*.: ***.********** **.*:*:.**.:***:***********::**:::******.:*** ********* **

CbAmo1      VKEGIVSVNNLSVIEVKSLEQVQPILTVEDLISTEDIIRKDPRVIEQCVISGIPANEMHKVYCDPWTIGFDERWGAGRRLQQALMYYRSD
HpAmo1      VKEGLVDLASLSVIETRALETVQPILTVEDLCATEDVIRNDPAVIEQCVLSGIPANEMHKVYCDPWTIGYDERWGTGKRLQQALVYYRSD
            ****:*.: .*****.::** ********** :***:**:** ******:******************:*****:*:******:*****

CbAmo1      EDDSQYSHPLDFCPIVDTEEKKVIFIDVPNRRRKVSKHKHSNFNPKDMIEKYGTLRTDGKPIDILQPEGVSFKMDGNVISWSNFNIHIGF
HpAmo1      EDDSQYSHPLDFCPIVDTEEKKVIFIDIPNRRRKVSKHKHANFYPKHMIEKVGAMRPEAPPINVTQPEGVSFKMTGNVMEWSNFKFHIGF
            **************************:***********:** **.**** *::*.:. **:: ********* ***:.****::****

CbAmo1      NYREGIVLSDISYNDHGNVRPLFHRISLSEMIVPYGSPDFPHQRKHALDIGEYGAGYMTNPLALGCDCKGVIHYLDAHFADRAGDPITVK
HpAmo1      NYREGIVLSDVSYNDHGNVRPIFHRISLSEMIVPYGSPEFPHQRKHALDIGEYGAGYMTNPLSLGCDCKGVIHYLDAHFSDRAGDPITVK
            **********:**********:***************:**********************:***************:**********

CbAmo1      HAVCIHEEDDGLLQKHSDFRDNFATSIVTRATKLIISQIFTAANYEYCIYWVFMQDGTIKLDVKLTGILNTYVLADGEESGPWGTKVYPG
HpAmo1      NAVCIHEEDDGLLFKHSDFRDNFATSIVTRATKLVISQIFTAANYEYCLYWVFMQDGAIRLDIRLTGILNTYILGDDEEAGPWGTRVYPN
            :********** ******************:************:********:*:**::********:*.*.**:*****:***.

CbAmo1      VNAHNHQHLFALRLHPRIDGDGNSVCTSDACSAEAPVGSPENMYGNGFYAKRTVFKTVADSETNYESSTGRTWDFFNPKKLNPYSGKPVS
HpAmo1      VNAHNHQHLFSLRIDPRIDGDGNSAAACDAKPSPYPLGSPENMYGNAFYSEKTTFKTVKDSLTNYESATGRSWDIFNPNKVNPYSGKPPS
            **********:**:.*********..:.** .:  *:*********.**:::*.**** ** *****:***:**:***:*:******* *

CbAmo1      YKLVSAQCPPLLAKPGALVYKRAPWANTTIKVVPFKEDRLYPSGDHVPQWSGDGNIGMRKWLGDKTDKIEDTDILVFHTFGISHFPAPED
HpAmo1      YKLVSTQCPPLLAKEGSLVAKRAPWASHSVNVVPYKDNRLYPSGDHVPQWSGDGVRGMREWIGDGSEKIENTDILFFHTFGITHFPAPED
            *****:******** *:** ******. :::***:*::**************** ***:*:** ::***:****.******:*******

CbAmo1      FPLMPAEPISLLMRPRHFFTENAGMDIVPSHAMTTTEARKATNLEVTSDTDKSSKLAFETTSACCGSTRFVKEK
HpAmo1      FPLMPAEPITLMLRPRHFFTENPGLDIQPSYAMTTSEAKRAVHKEAK---DKTSRLAFEGS--CCGK-------
            *********:*::*********.*:** **:****:**::*.: *.   **:*:**** :  ***.
```

Figure 1-3. Comparison of amino-acid sequences of amine oxidase by alignment of CbAmo1 and HpAmo1. *AMO1* contains a 2112-bp ORF encoding a protein of 704 amino acids (Amo1) with significant identity (76%) to amine oxidase of *H. polymorpha*. Close to the N terminus, Amo1 has a peroxisomal targeting signal type 2 (PTS2) motif.

Regulation of *YNR1* and *AMO1* expression

Next, I examined the regulation of *YNR1* and *AMO1* expression, as well as the activities of the corresponding enzymes, in response to ammonium, nitrate or methylamine. *YNR1* and *AMO1* were specifically induced by nitrate and methylamine, respectively, at both the transcript and (Table 1-5) enzyme-activity (Table 1-6) levels.

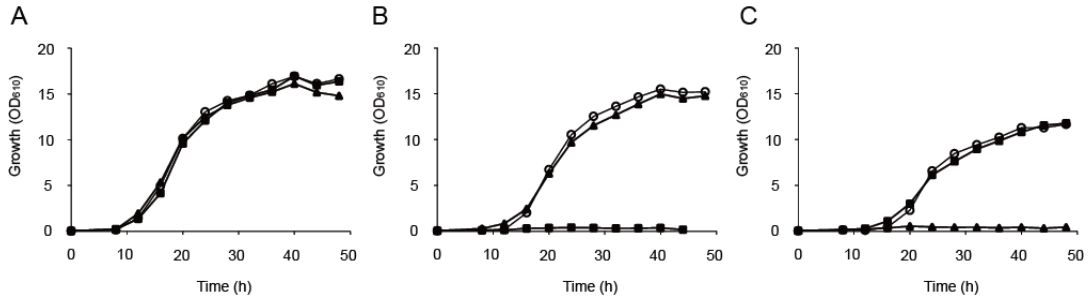

Figure 1-4. Ynr1 and Amo1 are necessary for yeast growth on nitrate and methylamine, respectively. Growth of the *C. boidinii* wild-type, *ynr1Δ*, and *amo1Δ* strain on SD medium containing (A) 3.8 mM $(NH_4)_2SO_4$, (B) 7.6 mM CH_3NH_3Cl, and (C) 7.6 mM KNO_3. Symbols: ○; wild-type, ■; *amo1Δ*, ▲; *ynr1Δ*.

Table 1-4. Ynr1 activity in the *ynr1Δ* strain and Amo1 activity in the *amo1Δ* strain

Enzyme	Strain	Activity : units (μmol/mg protein)
Ynr1	WT	54.4
	ynr1Δ	n.d.*
Amo1	WT	178
	amo1Δ	n.d.

* n.d.: not detected
Average values of duplicate measurements are shown.

Regulatory profile of nitrate reductase and amine oxidase by multiple nitrogen sources

To further investigate the regulatory profile of Ynr1 and Amo1, *C. boidinii* cells were incubated in media containing multiple nitrogen sources. First, I examined the transcript level of *YNR1* and *AMO1*. The *YNR1* transcript level increased in all four types of media supplemented with nitrate, whereas it remained at the basal low level in the medium supplemented with only methylamine, ammonium or glutamine (Figure 1-5A). The effect of nitrite, a reduced form of nitrate, on *YNR1* expression, was also investigated.

Table 1-5. Transcript level of *YNR1* and *AMO1* in response to various nitrogen sources

Nitrogen source	*YNR1*	*AMO1*
NH_4^+	1.0*	1.0*
NO_3^-	30.7	4.9×10^2
$CH_3NH_3^+$	3.2	2.2×10^4

*Transcriptional level of *YNR1* and *AMO1* was first quantified using *ACT1* as the control, and then, the transcript level was expressed as the relative value to those in ammonium media.
Average values of duplicate measurements are shown.

Table 1-6. Ynr1 and Amo1 activities in response to various nitrogen sources

Nitrogen source	Ynr1	Amo1
NH_4^+	2.0	n.d.*
NO_3^-	57	n.d.
$CH_3NH_3^+$	n.d.	152

* n.d .: not detected
Activity : units (μmol/mg protein)
Average values of duplicate measurements are shown.

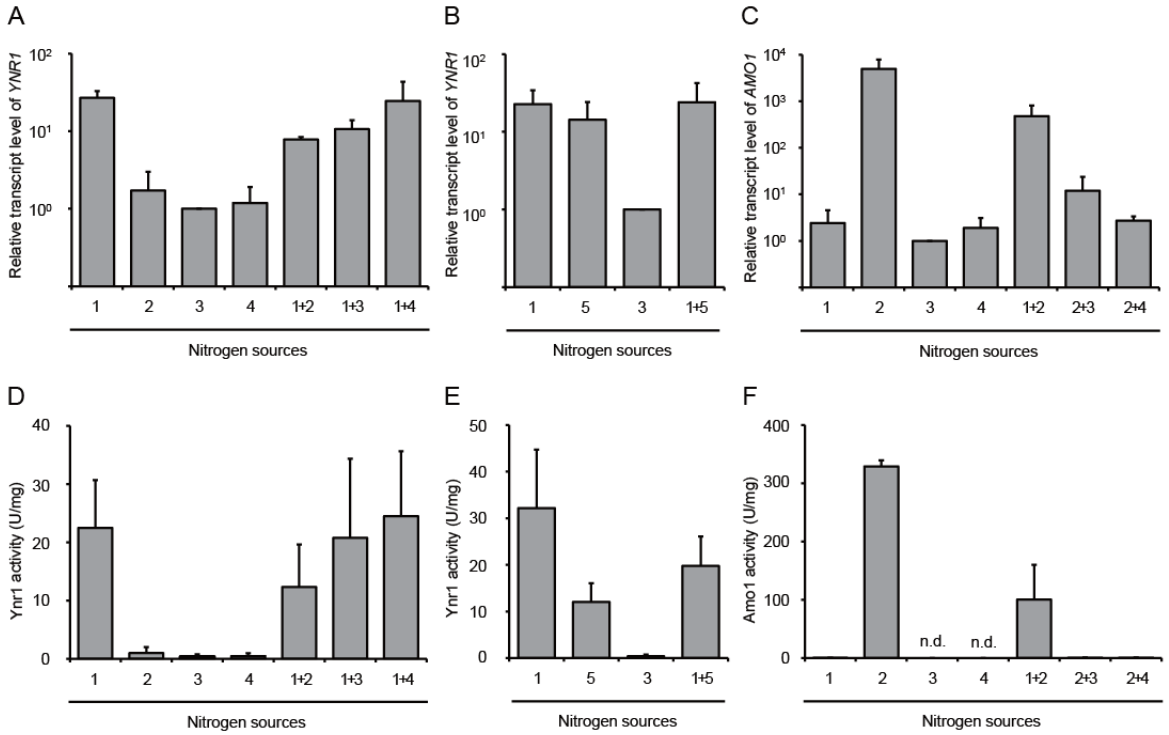

Figure 1-5. Regulation of Ynr1 and Amo1 in the presence of multiple nitrogen sources. *Candida boidinii* cells were first cultured on SD medium supplemented with ammonium (SD ammonium medium) and transferred to SDmedium containing different nitrogen sources. Four hours after themedium transition, cellswere collected for determination of Ynr1 activity, and the transcript levels of *YNR1* and *AMO1*. Amo1 activity was assayed with cells harvested 10 h after the medium shift. (A, B) Relative transcript level of *YNR1*. (C) Relative transcript level of *AMO1*. Each value was first quantified using *ACT1* as the internal control, and then the transcript level was expressed as the relative value to those in ammonium media. (D, E) Ynr1 activity. (F) Amo1 activity. Enzyme activities are expressed as U/mg (U; μmol/min). Each number shows the nitrogen source used: 1; nitrate, 2; methylamine, 3; ammonium, 4; glutamine and 5; nitrite. Bars are expressed as average values of three independent experiments and error bars show the standard deviations of these triplicate trials. ∗n.d.; not detected.

The *YNR1* transcript level was not affected by the coexistence with nitrite, and nitrite itself could induce the *YNR1* transcript as well as nitrate (Figure 1-5B). These results indicated that the expression of *YNR1* is induced by nitrate and nitrite but not by other nitrogen sources. On the other hand, the *AMO1* transcript was highly induced by methylamine and repressed by other nitrogen sources (Figure 1-5C). Ammonium and glutamine strongly repressed the methylamine-induced expression of *AMO1*, but repression by nitrate was partial. These results could be due to NMR and also this effect differs between preferable nitrogen sources (ammonium and glutamine) and the secondary nitrogen source (nitrate).

Next, I examined the enzyme activities of Ynr1 and Amo1. Ynr1 activity was found to be highly induced after 4 h of incubation with nitrate, nitrate plus methylamine, nitrate plus ammonium and nitrate plus glutamine, indicating that the coexistence with ammonium, methylamine or glutamine did not affect the Ynr1 activity by nitrate as expected by the *YNR1* transcript level (Figure 1-5D). When methylamine, ammonium or glutamine used as the sole

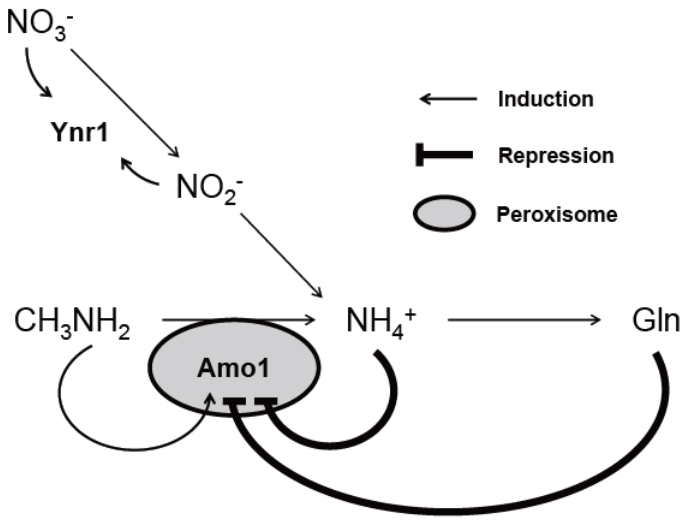

Figure 1-6. Schematic diagram of the regulatory profile of nitrate and methylamine metabolism in *C. boidinii*. Nitrate as well as nitrite increased the transcript and enzyme activity levels of nitrate reductase (Ynr1). Induction of amine oxidase (Amo1) by methylamine was repressed by the coexistence with ammonium or glutamine both at the transcript and enzyme activity levels.

nitrogen source, Ynr1 activity was very low although the low level of transcript was observed. Some post-translational event may exist for Ynr1 in activation of the enzyme. Ynr1 activity was also increased by nitrite and not inhibited by the coexistence with nitrite (Figure 1-5E). As previously described with the yeast *H. polymorpha*[19], Ynr1 and nitrite reductase might be coordinately regulated and that nitrite upregulates Ynr1 at its enzyme activity and transcript levels. In contrast to Ynr1, Amo1 activity after 10 h of cultivation in each medium was very low in the medium supplemented with methylamine plus ammonium or methylamine plus glutamine, although the yeast cells incubated with methylamine showed a high level of Amo1 activity (Figure 1-5F). And coexistence of nitrate with methylamine partially decreased Amo1 activity. According to these results, Ynr1 is regulated both at transcript and enzyme activity levels while Amo1 is regulated mainly at the transcript level. Nitrate induced expression of *YNR1* was not repressed by the coexistence with other nitrogen sources including methylamine. On the other hand, methylamine-induced expression of *AMO1* was completely repressed by coexistence with ammonium and glutamine and partially by nitrate (Figure 1-6). Therefore, the sensitivity to repression by other nitrogen sources was different between *YNR1* and *AMO1*.

Chapter II

Yeast nitrogen utilization in the phyllosphere during plant life span under regulation of autophagy

Abstract

Recently, microbe-plant interactions at the above-ground parts have attracted a great attention. This chapter describes nitrogen metabolism and regulation of autophagy in the methylotrophic yeast *Candida boidinii*, proliferating and surviving on the leaves of *Arabidopsis thaliana*. Quantitative analyses of yeast growth on the leaves of *A. thaliana* with the wild-type and several mutant yeast strains showed that on young leaves, nitrate reductase (Ynr1) was necessary for yeast proliferation, and the yeast utilized nitrate as nitrogen source. On the other hand, a newly developed methylamine sensor revealed appearance of methylamine on older leaves, and methylamine metabolism was induced in *C. boidinii*, and Ynr1 was subjected to degradation. Biochemical and microscopic analysis of Ynr1 *in vitro* during a shift of nitrogen source from nitrate to methylamine revealed that Ynr1 was transported to the vacuole being the cargo for biosynthetic cytoplasm-to-vacuole targeting (Cvt) pathway, and degraded. Overall, these results reveal changes in the nitrogen source composition for phyllospheric yeasts during plant aging, and subsequent adaptation of the yeasts to this environmental change mediated by regulation of autophagy.

Introduction

Nitrogen-source utilization of microorganisms in the field of microbe-host interaction have been studied mostly on underground part and researchers have revealed various kinds of microbial nitrogen metabolism such as nitrogen fixation, nitrification, and denitrification[10,11,36,37]. On the other hand, above-ground part of plants, especially in the phyllsopheric environment, which is assumed to be directly affected by plant daily cycle, e.g., photosynthetic metabolism, it remains unknown which of these nitrogen compounds are utilized by microbes, although proteomic analysis and growth test analysis using growing plant tissues showed several possible nitrogen sources for microbes[38,39].

The methylotrophic yeast *Candida boidinii* capable of growth on methanol as a sole carbon and energy source has been used as a model microorganism to study on the microbial life in the phyllosphere[6]. This yeast can utilize several nitrogen sources *in vitro*, e.g., ammonium, nitrate, and methylamine. Based on the research shown in the Chapter I, this yeast uses nitrate reductase (Ynr1) to reduce nitrate to nitrite, which is subsequently reduced to ammonium. Methylamine, on the other hand, is converted to ammonium by peroxisomal amine oxidase (Amo1). Generally in yeasts, ammonium assimilation is catalyzed by ATP-dependent glutamine synthase, yielding glutamine from α-ketoglutarate and ammonium. Glutamine serves as a general acceptor for amino groups from amino acids and other nitrogen compounds[40], and *C. boidinii* is thought to have a similar pathway for ammonium assimilation.

Because yeast methanol metabolism requires peroxisome biogenesis, peroxisomes are induced when cells are grown *in vitro* on methanol as the carbon source[41,42]. A shift to medium containing other carbon sources, or to nutrient-limited conditions, provokes degradation of peroxisomes via pexophagy, a type of selective autophagy[43]. On young plant leaves, methanol concentration exhibits a daily dynamic oscillation cycle (high during the dark period, low in the light period), and peroxisome biogenesis and pexophagy are dynamically regulated in response to the methanol cycle[6]. Previous research showed that pexophagy plays crucial roles in the proliferation of *C. boidinii* on plant leaves[6]. Other lines of evidence from fungal plant pathogens indicate that pexophagy is required for invasion of fungal cells into host plants[44].

Autophagy is a well-characterized catabolic pathway responsible for degradation of superfluous or dysfunctional cellular components[45]. This process contributes to intracellular remodeling, as well as removal of aggregates and damaged organelles. The most prevalent form of autophagy is starvation-induced macroautophagy, a nonselective system for bulk degradation of cytoplasmic components[46]. During this process, subcellular substrates are sequestered within double-membrane-bound structures called autophagosomes. These

structures fuse with vacuoles, leading to the degradation or recycling of their cargo[46].

In contrast to the bulk degradation system of macroautophagy, there also exist selective autophagic pathways, in which cytoplasmic cargoes are selectively recognized and transported to the vacuole for degradation[47]. One such selective pathway is pexophagy, described above, which is responsible for degradation of excess peroxisomes. Additional types of selective autophagy correspond to other organelles: mitophagy for mitochondria, lipophagy for lipid droplets, ribophagy for ribosomes, and ER-phagy for the endoplasmic reticulum[48-51]. In addition, yeasts have a constitutive biosynthetic pathway, the cytoplasm-to-vacuole targeting (Cvt) pathway, which is responsible for the transport of several vacuolar enzymes including aminopeptidase I (ApeI), aspartyl aminopeptidase (Ape4), and alpha mannosidase I (AmsI)[52-54]. ApeI, which is synthesized as a precursor ApeI (pre-ApeI), forms a large Cvt complex that is sequestered by a double-membrane structure, forming a Cvt vesicle. And after its delivery to the vacuole, pre-ApeI is matured by removal of the propeptide[55].

In this study, I investigated the nitrogen-utilization pathway of the methylotrophic yeast *C. boidinii* on plant leaves. Ynr1 was necessary for the proliferation of this yeast on young leaves. On older leaves, however, methylamine played more important role as nitrogen source, and Ynr1 was transported to the vacuole and degraded**.** Analyses of the dynamics of Ynr1 after the nitrogen-source switch revealed that Ynr1 protein is transported to the vacuole for degradation via the autophagic vesicles of biosynthetic Cvt pathway. These results elucidate yeast nitrogen metabolism and the regulation of autophagy on plant leaves in response to the life stages of the host plant.

Materials and methods

Yeast strains, vectors, and plasmids

C. boidinii strains, primers and plasmids used in this study are listed up in Table 2-1, Table 2-2 and Table 2-3, respectively. *C. boidinii* strain AOU1 was used as the wild-type strain. The *atg11*Δ and *atg17*Δ *C. boidinii* strains were constructed by replacing the appropriate ORF of *C. boidinii* strain TK62 (*ura3*)[30] with the Zeocin™ resistance gene as a selective marker[31], using the modified lithium acetate method[32]. The primer sets used for disruption of these genes are Fw-ATG11u-*Pst*I/Rv-ATG11u-*Not*I and Fw-ATG17u-*Eco*RI/ Rv-ATG17u-*Bam*HI for their upstream regions, and Fw-ATG11d-*Xho*I/ Rv-ATG11d-*Pst*I and Fw-ATG17d-*Cla*I/Rv-ATG17d-*Eco*RI for their downstream regions, respectively. The vector pACT1-Venus, encoding Venus under the control of the *ACT1* promoter[6], was transformed into the *ynr1Δ* and *amo1Δ* strains. The strain expressing Venus-Ynr1 fusion protein under the control of the *YNR1* promoter was used for fluorescence microscopy and immunoblot analysis. The plasmid pEX-Venus-Atg8, encoding Venus-Atg8 under the control of the *ATG8* promoter[6], the plasmid pACT1-Venus-Ape1, encoding Venus-Ape1 under the control of the *ACT1* promoter, and the plasmid pACT1-Ape4-Venus, encoding Ape4-Venus under the control of the *ACT1* promoter were also transformed into the wild-type strain. The PYNR strain and the PAMO strain which express Venus under the *YNR1* promoter and the *AMO1* promoter, respectively, were used for expression tests on plant leaves. pACT1 PTS2-GFP was constructed in the following manner. The GFP ORF was PCR-amplified using pGFP-C1 vector (Clontech) as a template with CbPot1 derived PTS2 DNA sequence (unpublished) with the primer set Fw-PTS2-GFP /Rv-PTS2-GFP. Subsequently, the PCR-amplified fragment was digested with *Sal*I and *Pst*I, and cloned into pACT1 vector, yielding pACT1 PTS2-GFP. Then, pACT1 PTS2-GFP was introduced into TK62 after digestion with *EcoT22*I. For quantitative reverse-transcriptional PCR (qRT-PCR), I used primer sets Fw-RT-ACT/Rv-RT-ACT, Fw-RT-YNR/Rv-RT-YNR, and Fw-RT-AMO/Rv-RT-AMO in order to amplify cDNA of *ACT1*, *YNR1* and *AMO1*, respectively.

Culture conditions

Cells were grown at 28°C on YPD medium (1% Bacto-yeast extract, 2% Bacto-peptone, 2% glucose) and SD medium (0.17% yeast nitrogen base without amino acids and ammonium sulfate, 2% glucose, and nitrogen sources). Nitrogen sources were ammonium sulfate [$(NH_4)_2SO_4$], potassium nitrate [KNO_3], methylamine chloride [CH_3NHCl], sodium nitrite [$NaNO_2$], urea [$(H_2N)_2CO$], L-alanine [$CH_3CH(NH_2)COOH$], L-glutamine [$NH_2CO(CH_2)CH(NH_2)COOH$], trimethylamine [$N(CH_3)_3$], and choline chloride [$(CH_3)_3NCHCH_2CH_2OHCl$]. When a single nitrogen source was present, the concentration

Table 2-1. Strains used in this study

Designation	Description	Genotype	References
AOU1	Wild type	Normal	Tani *et al.* (1985)
TK62	*Cbura3Δ*	*ura3*	Sakai *et al.* (1991)
BUL	*Cbura3Δ leu2Δ*	*ura3 leu2*	Sakai *et al* (1992)
KSC0001	*Cbura3Δynr1Δ*	*ynr1Δ*:: Zeo^r *ura3*	This study
KSC0002	*Cb ynr1Δ*	KSC0001 *ura3*:: SK+URA	This study
KSC0003	*Cbura3Δamo1Δ*	*amo1Δ*:: Zeo^r *ura3*	This study
KSC0004	*Cbamo1Δ*	KSC0003 *ura3*:: SK+URA	This study
KSC0005	*Cbura3Δ atg1Δ*	*atg1Δ*:: Zeo^r *ura3*	Kawaguchi *et al.* (2011)
KSC0006	*Cbura3Δ atg8Δ*	*atg8Δ*:: Zeo^r *ura3*	Kawaguchi *et al.* (2011)
KSC0007	*Cbura3Δ atg11Δ*	*atg11Δ*:: Zeo^r *ura3*	This study
KSC0008	*Cbura3Δ atg17Δ*	*atg17Δ*:: Zeo^r *ura3*	This study
KSC0009	TK62 VENUS-CbYNR1	TK62 *ura3*:: pACT1 Venus	This study
KSC0010	*ynr1Δ* VENUS-CbYNR1	KSC0001 *ura3*:: pACT1 Venus	This study
KSC0011	*amo1Δ* VENUS-CbYNR1	KSC0002 *ura3*:: pACT1 Venus	This study
KSC0012	TK62 VENUS	TK62 *ura3*:: pYNR1 Venus	This study
KSC0013	TK62 VENUS	TK62 *ura3*:: pAMO1 Venus	This study
KSC0014	TK62 VENUS-CbYNR1	TK62 *ura3*:: pEX Venus-Ynr1	This study
KSC0015	*atg1Δ* VENUS-CbYNR1	KSC0005 *ura3*:: pEX Venus-Ynr1	This study
KSC0016	*atg8Δ* VENUS-CbYNR1	KSC0006 *ura3*:: pEX Venus-Ynr1	This study
KSC0017	*atg11Δ* VENUS-CbYNR1	KSC0007 *ura3*:: pEX Venus-Ynr1	This study
KSC0018	*atg17Δ* VENUS-CbYNR1	KSC0008 *ura3*:: pEX Venus-Ynr1	This study
KSC0019	BUL mCHERRY-CbYNR1 VENUS-CbAPE1	BUL *ura3*:: pACT1 Venus-Ape1 *leu2*:: pEXL mCherry-Ynr1	This study
KSC0020	BUL mCHERRY-CbYNR1 CbAPE4-VENUS	BUL *ura3*:: pACT1 Venus-Ape4 *leu2*:: pEXL mCherry-Ynr1	This study
KSC0021	BUL mCHERRY-CbYNR1 VENUS-CbATG8	BUL *ura3*:: pEX Venus- ATG8 *leu2*:: pEXL mCherry-Ynr1	This study
KSC0022	BUL mCHERRY-CbYNR1 CbATG11-VENUS	BUL *ura3*:: pEX Atg11-Venus *leu2*:: pEXL mCherry-Ynr1	This study
KSC0023	TK62 PTS2-GFP	TK62 *ura3*:: pACT1 PTS2-GFP	This study

Table 2-2. Primers used in this study

Designation	DNA sequence (5'→3')
Fw-ATG11u-*Pst*I	CTGCAGGCATTGCTTCTTTGGGAC
Rv-ATG11u-*Not*I	GCGGCCGCTTTGTCTATGAGTTGAC
Fw-ATG11d-*Xho*I	CTCGAGGACAATGCAGTTGACCG
Rv-ATG11d-*Pst*I	CTGCAGCAACGAAGATGCCAACTTG
Fw-ATG17u-*Eco*RI	GGAATTCCTCTGTTAAACAATAAATCCGTAGCC
Rv-ATG17u-*Bam*HI	CGGGATCCGTAATTCTCAAATTCATGG
Fw-ATG17d-*Cla*I	CCATCGATCTATGTACATGATATATATATAATATAT
Rv-ATG17d-*Eco*RI	GGAATTCCAATTTAAAAGATTGTACTGTGATAG
Fw-PYNR	TGGCCTTTTGCTGGCCTTTTGCTCACATGTCTTGCAGTCTAAAAATAAACA
Rv-PYNR	CACCTTTAGAAACCATGTCGACTTATGAATTATATTTGGAGTTAT
Fw-PAMO	CTTTTGCTCACATGTAGTAAAGACGGACAACTATAATTGA
Rv-PAMO	CTTCACCTTTAGAAACCATGTCGACTTTTATGATATTATATAATAAAG
Fw-YNR1-*AflIII* inf	CTTTTGCTCACATGTGACTTCATATTGGAAAATGCCACTAAAATT
Rv-YNR1-*PstI* inf	GATTAAATTCCCTGCAGTTAAAAAGCAACACAGTATTCTTCACCAAA
Fw-YNR1-*SacI* inv	GAGCTCATGATTGTAGCATCAGGTACAGAT
Rv-YNR1-*KpnI* inv	GGTACCTATGAATTATATTTGGAGTTATGTGCTGGT
Fw-VENUS-*KpnI* inf	TAATTCATAGGTACCATGGTTTCTAAAGGTGAAGAATTATTCA
Rv-VENUS-*SacI* inf	TACAATCATGAGCTCTTTATATAATTCATCCATACCTAAAGTAATACC
Fw-APE1-*Pst*I inf	AATTATATAAACTGCAGATGGTTGGTGCTCACACAGATT
Rv-APE1-PstI inf	GATTAAATTCCCTGCAGCTAATCTTGGATACCATCGACTAAAATTTTTGGT
Fw-Tact-*Pst*I inv	GAGCTCCTGCAGGGAATTTAATC
Rv-VENUS-*Pst*I inv	TTTTCTGCAGTTTATATAATTCATCCATACCTAAAGTAATACCAGC
Fw-APE4-*Sal*I inf	ATATTACAAAAGTCGACATGGTTGGTGCTCACACAGATT
Rv-APE4-*Sal*I inf	TTAGAAACCATGTCGACAAATTTTGGTTCTAATTCATTGTATCTTTCGAAATATTG
Fw-PTS2-GFP	ACGCGTCGACATGGAAAGACTCTCTCAGATTAATTCTCATCTCGGTACCATGGGTAA AGGAGAAGAACTTTT
Rv-PTS2-GFP	AACTGCAGTTAACCTCCGGACTTGTATAG
Fw-RT-ACT	CAGCAGTGGTGGAGAAAGTG
Rv-RT-ACT	TGCTGATGAATCTTGGTGGA
Fw-RT-YNR	TCGGCTAATCTCCAGGTGAC
Rv-RT-YNR	ATTGCTGCTCCATCAAGACC
FwRT-AMO	ACACCTGGAACACCAGCTTC
Rv-RT-AMO	TGGCCTTTTGCTGGCCTTTTGCTCACATGTCTTGCAGTCTAAAAATAAACA

Table 2-3. Plasmids used in this study

Designation	Description	References
pBluescript II SK+/Zeocassette™	*Zeo*^{r}	Kawaguchi *et al*. (2011)
SK+Zeo YNR1del	*YNR1*$_{up}$-*Zeo*^{r}-*YNR1*$_{down}$	This study
SK+Zeo AMO1del	*AMO1*$_{up}$-*Zeo*^{r}-*AMO1*$_{down}$	This study
SK+URA	*URA3*	This study
pACT1 Venus	P_{ACT1}-*VENUS, URA3*	Kawaguchi *et al*. (2011)
pYNR1 Venus	P_{YNR1}-*VENUS, URA3*	This study
pAMO1 Venus	P_{AMO1}-*VENUS, URA3*	This study
pEX Venus-Ynr1	P_{YNR1}-*VENUS-YNR1, URA3*	This study
pACT1 Venus-Ape1	P_{ACT1}-*VENUS-APE1, URA3*	This study
pACT1 Ape4-Venus	P_{YNR1}-*APE4-VENUS, URA3*	This study
pEX Venus-Atg8	P_{ATG8}-*VENUS-ATG8, URA3*	Kawaguchi *et al*. (2011)
pEX Atg11-Venus	P_{ATG11}-*ATG11-VENUS, URA3*	This study
pACT1 PTS2-GFP	P_{ACT1}-*PTS2-GFP, URA3*	This study

was 7.6 mM. When two compounds were used as nitrogen sources, 3.6 mM (as the molar concentration of N atom) of each compound was used. The pH of SD medium was adjusted to 6.0 with NaOH. Growth was monitored by measuring the optical density at 610 nm (OD_{610}).

Construction of the *C. boidinii* P_{YNR}- and P_{AMO}-reporter strains

Putative promoter regions of *YNR1* and *AMO1* genes were amplified by PCR with the primer sets Fw-PYNR/Rv-PYNR and Fw-PAMO/Rv-PAMO, respectively. These 1.0-kb PCR-amplified fragments were fused with a fragment from pACT1-Venus digested with *Afl*III/*Sal*I, using the In-fusion HD ® cloning kit, which yielded two expression vectors of Venus under the regulations of P_{YNR} or P_{AMO} promoters.

Generation of *C. boidinii* strains expressing Venus-Ynr1 fusion protein

A fragment of the 1.0-kb 5' untranslated region and 2.7-kb *YNR1* coding region was amplified by PCR with the primer set Fw-YNR1-*Afl*III inf/Rv-YNR1-*Pst*I inf. The PCR product was fused with the 5.7-kb *Afl*III-*Pst*I fragment of pACT1-Venus[6] to form pEX-Ynr1 by In-fusion HD ® cloning kit (TaKaRa, Kyoto, Japan). Next, a 9.4-kb fragment was amplified by inverse PCR with the generated plasmid as a template DNA, using the primer set Fw-YNR1-*Sac*I inv/Rv-YNR1-*Kpn*I inv. The Venus-coding region was PCR amplified with the primer set Fw-VENUS-*Kpn*I inf/Rv-VENUS-*Sac*I inf. These two fragments were fused to form pEX-Venus-Ynr1. The resulting plasmid was linearized with AfeI and then introduced into the

wild-type host strain, *atg1Δ*, *atg11Δ*, and *atg30Δ* mutant strains.

VENUS-APE1* and *APE4-VENUS* expressions in *C. boidinii

A backbone vector pACTL-Venus, encoding Venus under the control of the *ACT1* promoter with *LEU2*[33] as Leucine auxotrophic marker was constructed by ligation of an AatII-*Nar*I fragment from pACT1-Venus (Kawaguchi *et al*, 2011) with an *Aat*II-*Nar*I fragment of *LEU2* gene. For the construction of the plasmid for *VENUS-APE1* expression, a 1.3-kb *APE1* fragment was amplified by PCR with the primer set Fw-APE1-*Pst*I inf/Rv-APE1-*PstI* inf. Next, a 8.8-kb fragment was amplified by inverse PCR with the pACTL-Venus plasmid as a template DNA, using the primer set Fw-Tact-*Pst*I inv/Rv-VENUS-*Pst*I inv. These two fragments were fused to form pACTL-Venus-APE1 with the In-fusion HD ® cloning kit. The plasmid for *APE4-VENUS* expression, termed pACTL-APE4-Venus, was constructed from a *Sal*I-digested fragment of pACT1-Venus and an *APE4*-coding region that was amplified with the primer set Fw-APE4-*Sal*I inf/Rv-APE4-*Sal*I inf, using the In-fusion HD ® cloning kit.

Host plant growth condition and yeast inoculation on plant leaves

A. thaliana plants were cultivated on mini-pots of cultivable lock-fiber (Nittobo) with Hoagland solution in growth chambers, as previously described[6]. *C. boidinii* cells were cultured to OD_{610} = 1.0. To follow yeast proliferation on the leaves of *A. thaliana*, 1 µl of yeast cell suspension (OD_{610} = 0.5) was spotted onto the upper sides of the leaves. To observe Venus and/or mCherry expression in *C. boidinii*, 5 µl of yeast suspension (OD_{610} = 0.5) was sprayed onto the upper sides of the leaves. To prepare the samples for qRT-PCR, yeast suspension was sprayed onto *A. thaliana* leaves and incubated for 5 days. For these experiments, I used two different age of leaves. Young plant leaves, which were used in the Figure 2-1, 2-2, 2-3, and 2-11, were growing leaves 2-3 weeks after the germination. And aged plant leaves, which were used in the Figure 2-3 and 2-11, were wilting leaves 2-3 months after the germination.

Comparison of yeast populations on *A. thaliana*

After *C. boidinii* cells were inoculated on the leaves of *A. thaliana*, 5 leaves were collected. Isolation of genomic DNA of *C. boidinii* and quantitation of the yeast populations on plant leaves were performed as previously described[6].

RNA preparation from cells grown on plants

Fifty to sixty leaves of *A. thaliana* onto which *C. boidinii* cells had been inoculated were harvested in tubes and frozen using liquid nitrogen. Total cellular RNA was extracted using ISOGEN, and qRT-PCR was performed as previously described[6].

Preparation of cell-free extract

C. boidinii cells were first cultured on SD supplemented with 7.6 mM ammonium for 12 h, shifted to SD containing with 7.6 mM of the indicated nitrogen source, and then collected 4 h after the medium transfer. Cells (approximately 100 OD_{610} units of cells grown in SD medium) were then resuspended in 0.1 M potassium phosphate buffer (pH 7.5) and disrupted with 0.5-mm zirconia beads in a Multi-Beads Shocker (YASUI KIKAI Co., Ltd, Osaka, Japan). Cell debris was removed by centrifugation at 15,000 rpm for 10 min at 4°C, and the resultant supernatant (cell-free extract) was used for enzyme assays. Protein concentrations were determined by the Bradford method (Bradford, 1976) using a protein assay kit (Bio-Rad Laboratories, Hercules, CA, USA), using bovine serum albumin as the standard.

Enzyme assay

Ynr1 activity was measured according to Boer *et al.*[56] with slight modifications. The assay mixture contained potassium phosphate buffer (final concentration 0.1 M, pH 7.5), 10 µL of 10 mM DTT, 10 µL of 1 mM FAD, 10 µL of 20 mM NADPH, and 250 µL cell-free extract in a final volume of 1 mL in a polystyrene cuvette (light path, 10 mm). The cuvettes were incubated for 2–3 min at 28°C, and the absorbance at 340 nm was monitored. The reaction was then initiated by the addition of 100 µL of 100 mM potassium nitrate, and the rate of decrease in absorbance at 340 nm was measured against a blank containing all the assay components expect potassium nitrate. Ynr1 activity is expressed in units (µmol/mg protein). Amo1 activity was measured as follows: the assay mixture contained potassium phosphate buffer (final concentration 0.1 M, pH 7.0), 15 µL of 50 mM 2,2'-azinobis-(3-ethylbenzthiazoline)- 6-sulfonate (ABTS), 15 µL of 100 units/mL horseradish peroxidase, and 100 µL of cell-free extract in a final volume of 1 mL in a polystyrene cuvette (light path, 10 mm). The cuvettes were incubated for 2–3 min at 28°C, and the absorbance at 405 nm was monitored. The reaction was then initiated by addition of 40 µL of 80 mM methylamine hydrochloride, and the rate of increase in absorbance at 405 nm was measured against a blank containing all assay components except methylamine hydrochloride. Amo1 activity is expressed in units (µmol/mg protein).

Immunoblot analysis

To prepare samples for immunoblot analysis, cells were grown to $A_{610} = 1.0$ on nitrate medium, and then shifted to SD containing either 10 mM methylamine or no nitrogen source. Cells equivalent to 5 OD_{610} units were collected at the appropriate time points, washed once with water, suspended in lysate buffer containing 0.25 N NaOH and 150 mM β-mercaptoethanol, and incubated at 4°C for 10 min. Next, trichloroacetic acid (final concentration, 10%) was added. The samples were vortexed, incubated at 4°C for 10 min, and

centrifuged. Subsequently, the pellet was washed twice with acetone and resuspended in a buffer containing 50 mM Tris-HCl, pH 7.5. The samples were denatured by boiling in SDS sample buffer, separated on 12% SDS-PAGE gels, and electrotransferred to nitrocellulose membranes. Blots were blocked for 1 h in 5% skim milk in TBS-T buffer (25 mM Tris, 220 mM NaCl, 27mM KCl, 0.1% Tween 20, pH 8.0). These blots were incubated for 1 h with polyclonal anti-GFP antibody (Life Technologies) at 1:1000 dilution in TBS-T buffer, and then washed three times with TBS-T. Subsequently, blots were incubated for 1 h with anti–rabbit IgG antibody (life technologies) at 1:10000 dilution in TBS-T, and then washed again three times in TBS-T. Immunoreactive bands were detected with the Western Lightning Chemiluminescence Reagent Plus (Perkin-Elmer Life Science), and the signals were detected using the Light-Capture II system (ATTO). To ascertain the reproducibility, each of immunoblot analysis was conducted at least twice.

Fluorescence microscopy

Confocal microscopy was carried out using a Zeiss LSM510 META/Axiovert 200 laser-scanning confocal inverted microscope equipped with a Plan Fluor 100×/1.45 NA oil objective. Venus fluorescence was obtained with a multiline (458, 477, 488, and 514 nm) argon laser and a 530–600 nm filter for emission. An HFT 405/514 beam splitter was used as a connecting filter. Fluorescence microscopy was performed using an IX81 inverted microscope (Olympus) equipped with an Uplan-Apochromat 100×/1.35 NA oil iris objective lens. Venus and mCherry signals were acquired using a Plan Fluor 100× lens (Carl Zeiss) with pinhole set to 1.02 airy units for YFP acquisition. Fluorescence observations of cells cultured *in vitro* were repeated at least twice and three shots at different fields were taken in each time. For fluorescence microscopy of the cells on the plant surface, 3 different leaves were harvested for the observation. At least five shots at different fields were taken per one leaf.

Morphometric analysis

Cell count analysis was performed in which the numbers of cells ($n > 50$, n; number of cells in one field) observed under fluorescent microscopy ($f > 3$, f; a field of vision) were counted, and independent examinations were repeated at least three times.

Results

C. boidinii utilizes nitrate on growing *A. thaliana* leaves

A previous study established a technique for evaluating proliferation of *C. boidinii* on plant leaves using a combination of qPCR and fluorescent microscopy[6]. In this study, I used that technique to compare the growth of the *ynr1Δ* and *amo1Δ* strains on young *A. thaliana* leaves (2–3 weeks after germination) with that of a corresponding strain expressing Venus under the control of the constitutive *ACT1* promoter. In the wild-type and *amo1Δ* strains, concomitant with increases in the cell numbers observed under fluorescence microscopy (Figure 2-1A), 4–8 fold increases in the copy numbers of *VENUS* gene integrated in the *C. boidinii* genome were detected after 13 days of inoculation, indicating proliferation of the strains on the leaves. On the other hand, such proliferation was not observed for the *ynr1Δ* strain (Figure 2-1A and 2-1B). These results indicated that *YNR1* is necessary for *C. boidinii* proliferation on growing young *A. thaliana* leaves, and that *C. boidinii* can utilize nitrate as a nitrogen source.

YNR1, but not *AMO1*, is expressed on young leaves

Next, I constructed strains expressing Venus under the control of the *YNR1* promoter (strain PYNR) or the *AMO1* promoter (strain PAMO), and then examined their promoter activities on young plant leaves. At 4 h of incubation after spotting onto the upper side of growing young leaves, the cells were observed under a fluorescent microscope. Strain PYNR exhibited clear cytosolic fluorescence, whereas strain PAMO did not (Figure 2-2A). Thus, *YNR1* was expressed on young leaves of *A. thaliana*, whereas *AMO1* was not. Therefore, I hypothesized that *YNR1* expression is induced by nitrate present on plant leaves.

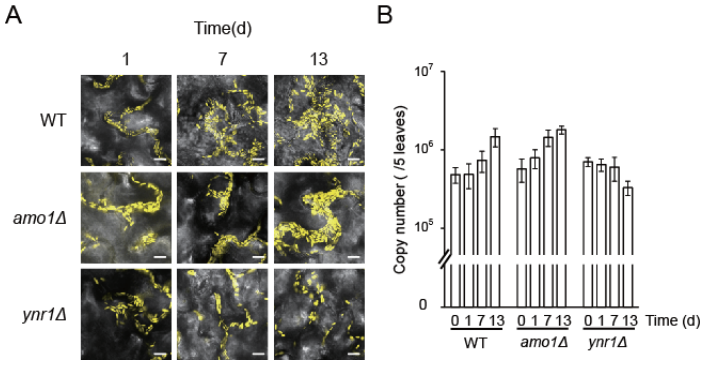

Figure 2-1. Ynr1 is necessary for yeast proliferation on *A. thaliana* leaves. (A) Confocal microscope images of Venus-labeled wild-type, *amo1Δ*, and *ynr1Δ* strain on growing *A. thaliana* leaves. *C. boidinii* cells were spotted on young Arabidopsis leaves (2–3 weeks after germination) and observed on the indicated day. Bar, 10 μm. (B) Quantitation of *C. boidinii* cell populations on the *A. thaliana* leaves by qPCR method. The leaves onto which the *C .boidinii* strains were inoculated were retrieved at the indicated time points, and were subjected to qPCR that amplified *VENUS* gene integrated in the *C. boidinii* genome. The Error bars show standard deviations of triplicate measurements.

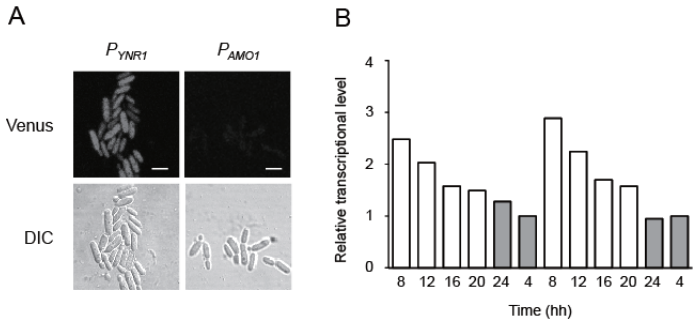

Figure 2-2. Expression of *YNR1* and *AMO1* on young leaves of *A. thaliana*. (A) Microscopic images of *C. boidinii* inoculated onto the surface of a young leaf. Venus fluorescent protein was expressed under the control of the *YNR1* or *AMO1* promoter. DIC represents the image from differential interference contrast microscopy. Bar, 5 μm. (B) mRNA levels of *YNR1* during the daily light–dark cycle. Transcript level of *YNR1* is expressed as the relative value to the sample collected at 4 h. Gray bars indicate the dark period. Average values of duplicate experiments are shown.

The genes for methanol utilization exhibit a daily periodicity in their expression, reflecting the oscillation in methanol concentration: high expression during the dark period and low levels during the light period. For example, the transcript level of *DAS1*, which encodes peroxisomal dihydroxyacetone synthase, is ~3-fold higher in the dark period than the light period[6]. Therefore, I investigated whether the transcript level of *YNR1* changes during the daily cycle. To this end, the total RNA was extracted from *C. boidinii* proliferating on leaf surfaces, and subjected to qRT-PCR analysis. The transcript level of *YNR1* increased 2.8-fold, peaking at 8 hh (4 h after the start of light period), decreasing gradually to its minimum at 4 hh (8 h after the start of dark period) (Figure 2-2B). These findings indicate that *YNR1* expression also fluctuates on young plant leaves during the daily cycle.

AMO1 expression and alteration of Venus-Ynr1 localization on aged leaves

During the plant life cycle (growth, maturation, wilting, and death), microbes in the phyllosphere must adapt to host aging–dependent changes in the leaf environment. On young growing leaves, methanol concentration in the phyllosphere oscillates in a daily cycle, this oscillation disappears in wilting leaves, and the concentration steadily rises as wilting progresses and the leaf dies. On old leaves, yeasts are unable to proliferate; instead, they survive by using their highly developed peroxisomes as protein-storage organelles[6].

Using strain PAMO, I investigated whether *AMO1* was expressed on wilting plant leaves (2–3 months after germination). Cytosolic fluorescence was detectable on wilting leaves (Figure 2-3A), suggesting that methylamine metabolism is induced in *C. boidinii* on an aged or dead host plant. Using a standard curve of fluorescence intensity, based on agar plates containing various concentrations of methylamine (Figure 2-3B), I determined that methylamine concentration at the phyllosphere was 4.78×10^{-3} mM.

To determine the localization of Ynr1 on aged plants, I constructed a strain expressing a Venus-Ynr1 fusion protein under the control of the *YNR1* promoter. Expression of

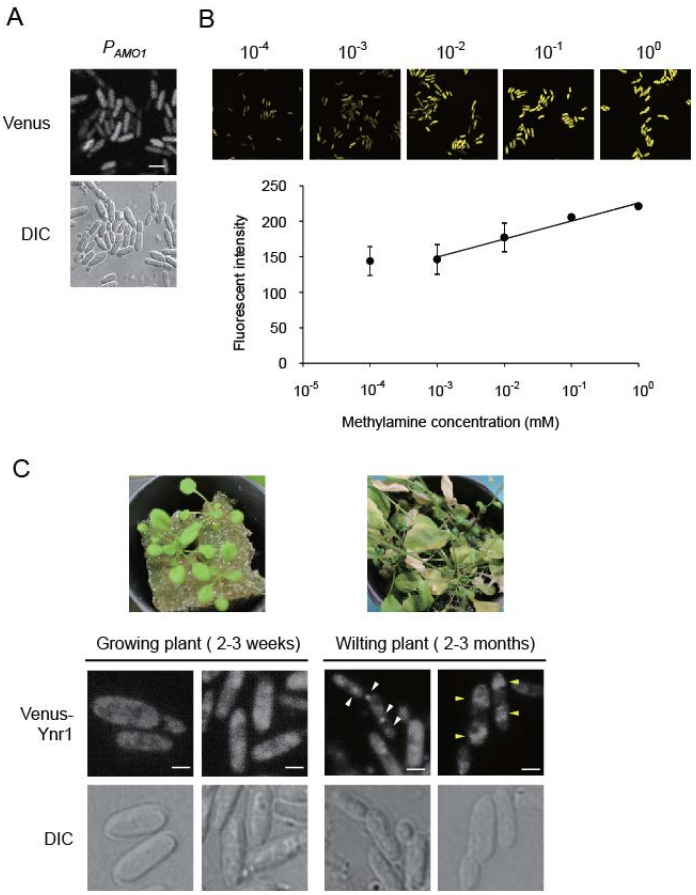

Figure 2-3. Expression of *YNR1* and *AMO1* on aged leaves of *A. thaliana*. (A) Microscopic images of *C. boidinii* inoculated onto the surface of a wilting leaf. Venus fluorescent protein was expressed under the control of the *AMO1* promoter. Bar, 5 µm. (B) Standard curve for Venus fluorescence intensity vs. methylamine concentrations. *C. boidinii* strain expressing Venus under the control of AMO1 promoter (the PAMO strain) was used for measurement of local methylamine concentrations. Cells were inoculated onto SD-agar plates containing different concentrations of methylamine (10^{-4} – 1 mM). At four hours after the inoculation, *C. boidinii* cells were collected and observed by fluorescence microscopy. The cellular fluorescence intensities were proportional to the methylamine concentration in agar plates within the range 10^{-3} – 10^{1} mM. The fluorescence intensities were measured from at least 50 cells and averaged. Error bars show standard deviations of 5 shots of different fields. The Similar results were obtained from three independent experiments. (C) Intracellular localization of Venus-Ynr1 on plant leaves. Venus-Ynr1 fusion protein was expressed under the control of the native *YNR1* promoter in cells living on growing or wilting leaves of *A. thaliana* shown in the upper images. White arrowheads show dot-like structures of Venus-Ynr1, and yellow arrowheads show the diffuse Venus fluorescence within the vacuole. Bar, 2 µm.

Venus-Ynr1 protein fully restored the growth of *ynr1Δ* strain on nitrate as a solo nitrogen source (data not shown). When Venus-Ynr1 expressing cells were inoculated on young leaves of growing plant (2-3 weeks after germination), I observed cytosolic fluorescence (Figure 2-3C). On the other hand, I detected dot-like structures of Venus-Ynr1 and diffuse vacuolar fluorescence in cells inoculated onto aged leaves of wilting plant (2-3 months after germination) (Figure 2-3C). These results prompted us to hypothesize that Ynr1 is subjected to autophagic degradation induced by the adaptation to the change of leaf environment.

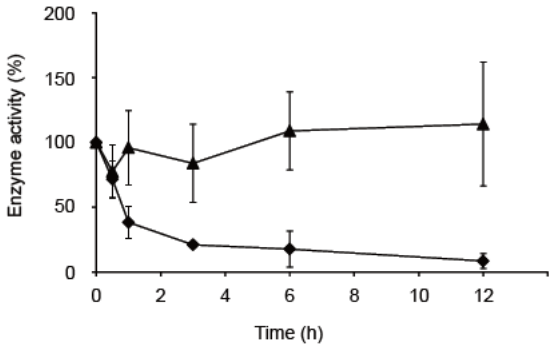

Figure 2-4. Ynr1 enzyme activity decreases rapidly after nitrogen-source shift. Symbols: ◆, 10mM methylamine; ▲, 10mM nitrate. Experiments were repeated three times. Enzyme activity is expressed as the relative value to each of the values measured at the time point 0 h: (◆) 73.2 and (▲) 87.9 U (μmol/mg protein). Error bars show the standard deviations of three independent experiments.

Ynr1 activity decreased after the shift from nitrate- to methylamine-containing medium

To understand the adaptation mechanism of the yeast for environmental change on leaves over the course of host plant aging, I decided to examine the dynamics of Ynr1 *in vitro*. First, I monitored the enzyme activity of Ynr1 following a shift from nitrate- to methylamine-containing liquid medium. Specifically, the wild-type *C. boidinii* was grown on 10 mM nitrate as the sole nitrogen source (nitrate medium), and then transferred to 10 mM methylamine (methylamine medium) or nitrate medium (as a control). The enzymatic activity of Ynr1 decreased rapidly within 1 h of the shift from nitrate to methylamine medium. By contrast, transfer to nitrate medium did not significantly affect enzymatic activity (Figure 2-4).

Ynr1 is transported to the vacuole via autophagy after the shift to methylamine

Because Ynr1 enzyme activity decreased after the nitrogen-source shift, I hypothesized that Ynr1 was subjected to autophagic degradation. To elucidate the molecular basis of autophagic degradation of Ynr1 after the nitrogen-source shift, I used a strain in which Venus-Ynr1 fusion protein was expressed under the *YNR1* promoter. Once Venus-Ynr1 is delivered to the vacuole, the Venus moiety is proteolytically detached from the rest of the fusion protein, after which it is relatively stable and can be detected by immunoblot analysis[57].

I cultivated wild-type yeast as well as *atg1Δ* and *atg8*Δ cells, which are impaired in all autophagic processes, on medium containing on nitrate, and then shifted the cells to methylamine medium or medium without a nitrogen source (nitrogen starvation). Twelve hours after the shift from nitrate medium to methylamine medium, the cleaved form of Venus was detected in wild-type cells, but not in *atg1Δ* cells or *atg8Δ* cells (Figure 2-5A). In a similar manner, when the cells were subjected to nitrogen-starvation conditions to induce bulk autophagy, the cleaved form of Venus was detected in the wild-type strain but not the *atg1*Δ

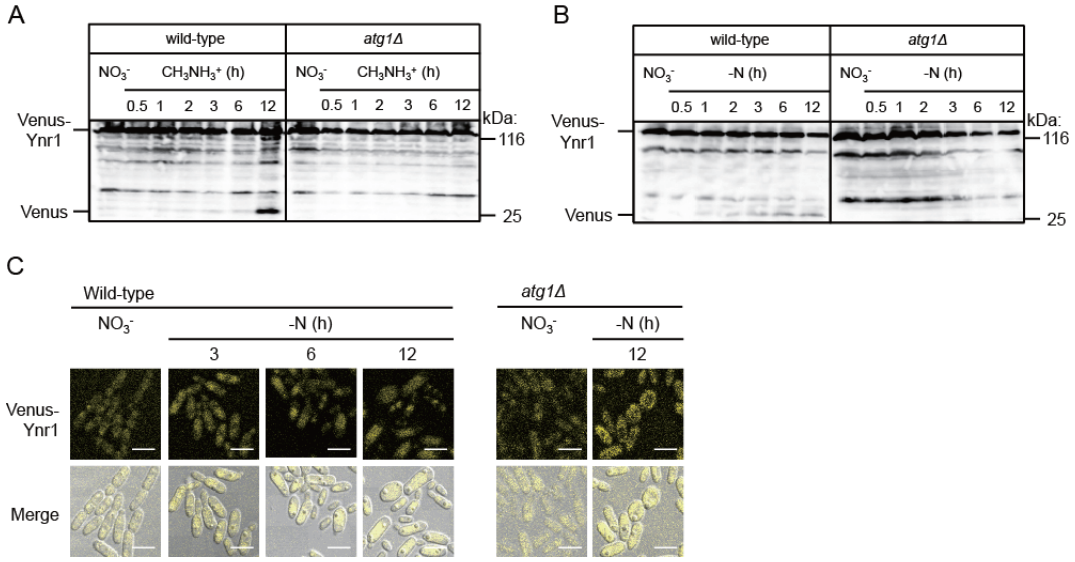

Figure 2-5. Ynr1 transport to the vacuole is defective in *atg1Δ* cells. (A) Immunoblot analysis of Venus-tagged Ynr1 in *C. boidinii* wild-type, *atg1Δ* and *atg8Δ* cells transferred from nitrate to methylamine medium. (B) Immunoblot analysis of Venus-tagged Ynr1 in *C. boidinii* wild-type and *atg1Δ* cells transferred from nitrate medium to nitrogen-starvation conditions. (C) Microscopic images of Venus-Ynr1 expressed in wild-type and *atg1Δ* cells during the shift from nitrate medium to nitrogen-starvation conditions. Merged images are combined images of Venus yellow fluorescence and DIC images. Bar, 5 μm.

strain (Figure 2-5B).

Interestingly, the band intensities of the cleaved form of Venus, detected after the medium transfer from nitrate to methylamine, were more intense than those detected after the shift to nitrogen-starvation conditions (Figure 2-5B). These results suggest that Ynr1 is more effectively subjected to degradation after a nitrogen-source shift from nitrate to methylamine than under conditions that induce bulk autophagy.

I also used fluorescence microscopy to monitor the fate of Venus-Ynr1 following the medium shift. After the transition from nitrate to nitrogen-starvation medium, Venus fluorescence was detected within the vacuole in wild-type cells, but remained in the cytosol in *atg1Δ* cells (Figure 2-5C). These morphological results were also consistent with the biochemical analysis, which indicated that Venus-Ynr1 is transported to the vacuole via autophagy after the shift of nitrogen source.

Transport of Ynr1 to the vacuole requires the selective autophagy factor Atg11

Atg11 is required for selective autophagy pathways, including the Cvt pathway, mitophagy, and pexophagy. It functions as a scaffold protein for recruitment of cargo to the phagophore assembly site (PAS) for packaging into vesicles[47]. I investigated whether Ynr1 is transported to the vacuole in an Atg11-dependent manner. In *atg11Δ* cells, the band intensity of the cleaved form of Venus was clearly weaker than that in wild-type cells after the medium shift from nitrate to methylamine (Figure 2-6A).

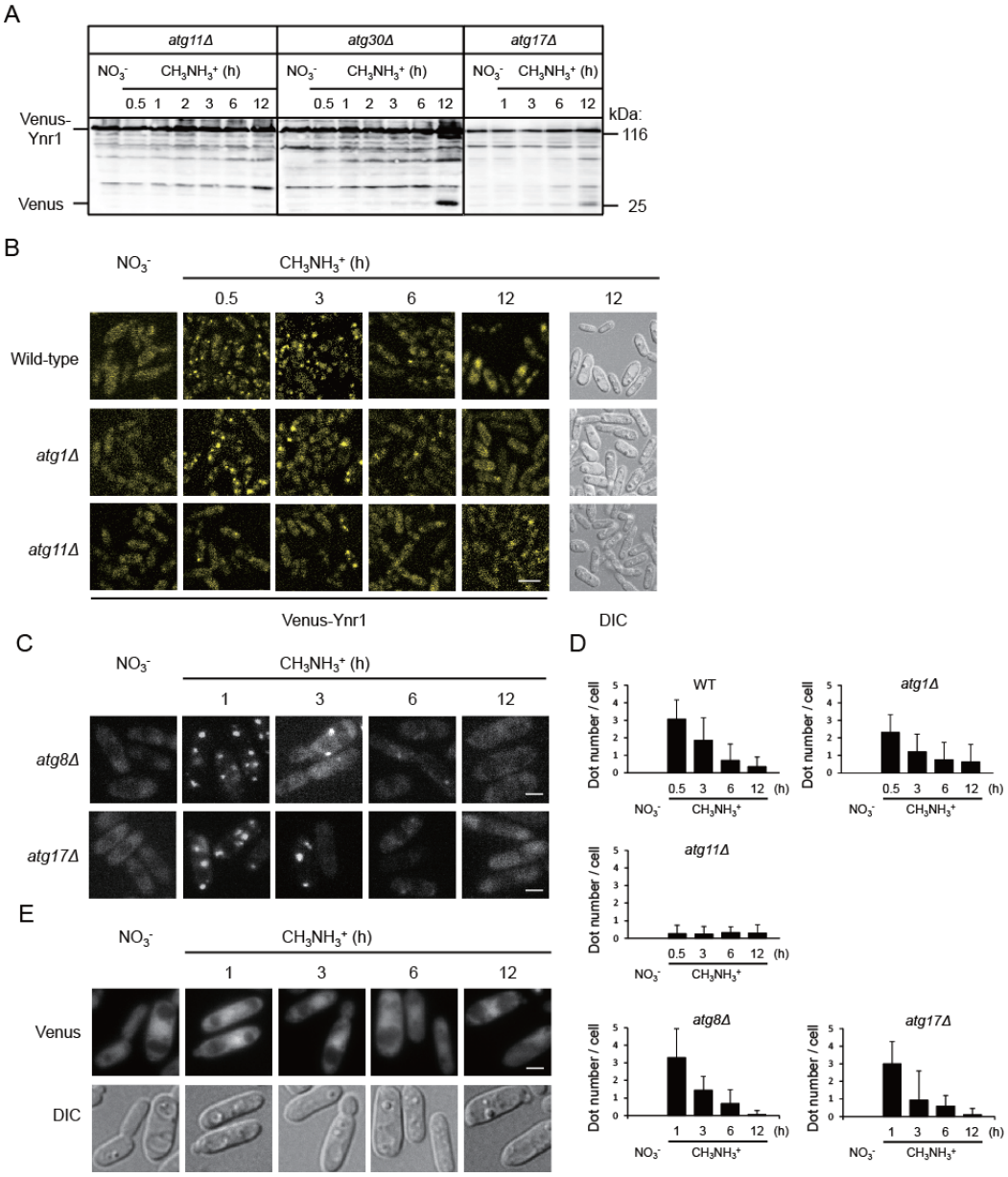

Figure 2-6. Ynr1 transport to the vacuole is dependent on the selective autophagy factor Atg11. (A) Immunoblot analysis of Venus-tagged Ynr1 in *atg11Δ*, *atg30Δ* and *atg17Δ* strains transferred from nitrate to methylamine medium. (B) Fluorescent images of Venus-Ynr1–expressing *C. boidinii* wild-type, *atg1Δ*, and *atg11Δ* cells during the nitrogen-source shift from nitrate to methylamine. Bar, 5 μm. (C) Fluorescence images of Venus-Ynr1–expressing *C. boidinii atg8Δ* and *atg17Δ* cells during the nitrogen-source shift from nitrate to methylamine. Bar, 2μm. (D) Quantitation of the number of Venus-Ynr1 puncta per cell, estimated from analysis of the fluorescent images shown in (B and C). For each sample, a minimum of 50 cells were analyzed. Error bars show standard deviations. (E) Fluorescence image of cells expressing Venus under the control of the *ACT1* promoter. Bar, 2μm.

Amo1 is a peroxisomal amine oxidase, which has a peroxisomal targeting signal type 2 (PTS2) motif with the consensus sequence of (R,K)-(L,V,I)-X5-(H,Q)-(L,A,F). During adaptation to methylamine medium in the methylotrophic yeast *Hansenula polymorpha*[28], Amo1 was induced and transported to the peroxisomes. Atg11 is also necessary for pexophagy[58]. Therefore, I asked whether Atg11-dependent transport of Venus-Ynr1 was

independent of pexophagy. In the methylotrophic yeast *Pichia pastoris*, Atg30 is required for pexophagy, but not for the Cvt pathway or mitophagy[59]. Twelve hours after the medium shift, I detected the cleaved form of Venus in *atg30Δ* cells, as well as in wild-type cells, indicating that Ynr1 transport to the vacuole is independent of pexophagy (Figure 2-6A). Ynr1 was also degraded in the *atg17*Δ strain, which is impaired in non-selective bulk autophagy (Figure 2-6A).

I also observed the localization of Venus-Ynr1 by fluorescence microscopy. When cells were cultured on nitrate medium, Venus-Ynr1 was found dispersed in the cytosol (Figure 2-6B). In wild-type cells, 0.5 h after the shift from nitrate to methylamine medium, Venus-Ynr1 formed dots, which were detectable for further 3 h. Subsequently, the Venus fluorescence was localized inside the vacuole until 12 h after the shift. In *atg1Δ* (Figure 2-6B) and *atg8Δ* (Figure 2-6C) cells, in contrast, Venus-Ynr1 was not transported to the vacuole. Atg11 and Atg17 serve as scaffold proteins for phagophore formation in the selective and non-selective autophagic pathways, respectively. The frequency of Venus-Ynr1 dot formation was low in *atg11Δ* cells, (Figure 2-6B and 2-6D), but normal in *atg17Δ* cells (Figure 2-6C and 2-6D). Thus, trafficking of Venus-Ynr1 to the vacuole depended on selective autophagy but not on non-selective autophagy. Indeed, after the medium shift, Venus expressed in the cytosol did not exhibit vacuolar fluorescence (Figure 2-6E) indicating that starvation-induced autophagy did not occur. These biochemical and morphological data confirmed that Ynr1 is selectively transported to the vacuole in Atg11-dependent manner.

Ynr1 is transported to the vacuole via the Cvt pathway during adaptation from nitrate to methylamine medium

I interpreted Venus-Ynr1 dot formation as a sign of sequestration into autophagosomes. To test this idea, I constructed wild-type cells expressing both mCherry-Ynr1 and Atg11-Venus, and examined the subcellular localization of both proteins. Following the shift from nitrate to methylamine, mCherry-Ynr1 and Atg11-Venus were co-localized to an extent that increased over time (Figure 2-7A and 2-7B). Atg8 is an autophagosome marker that has been used previously to follow the dynamics of autophagy[60], and co-localization of mCherry-Ynr1 and Venus-Atg8 was also observed in the wild-type strain (Figure 2-7C). These results suggested that Ynr1 is selectively recruited and sequestered into autophagic vesicles for its transport to the vacuole.

To examine the involvement of Cvt pathway in the Ynr1 transport to the vacuole, I constructed wild-type cells expressing both mCherry-Ynr1 and Venus-Ape1. When the cells were shifted from nitrate to methylamine medium, mCherry-Ynr1 often localized with Venus-Ape1 (Figure 2-7D). I also observed co-localization of mCherry-Ynr1 and Ape4-Venus, another member of the Cvt complex[53] (Figure 2-7E). These results demonstrate that Ynr1

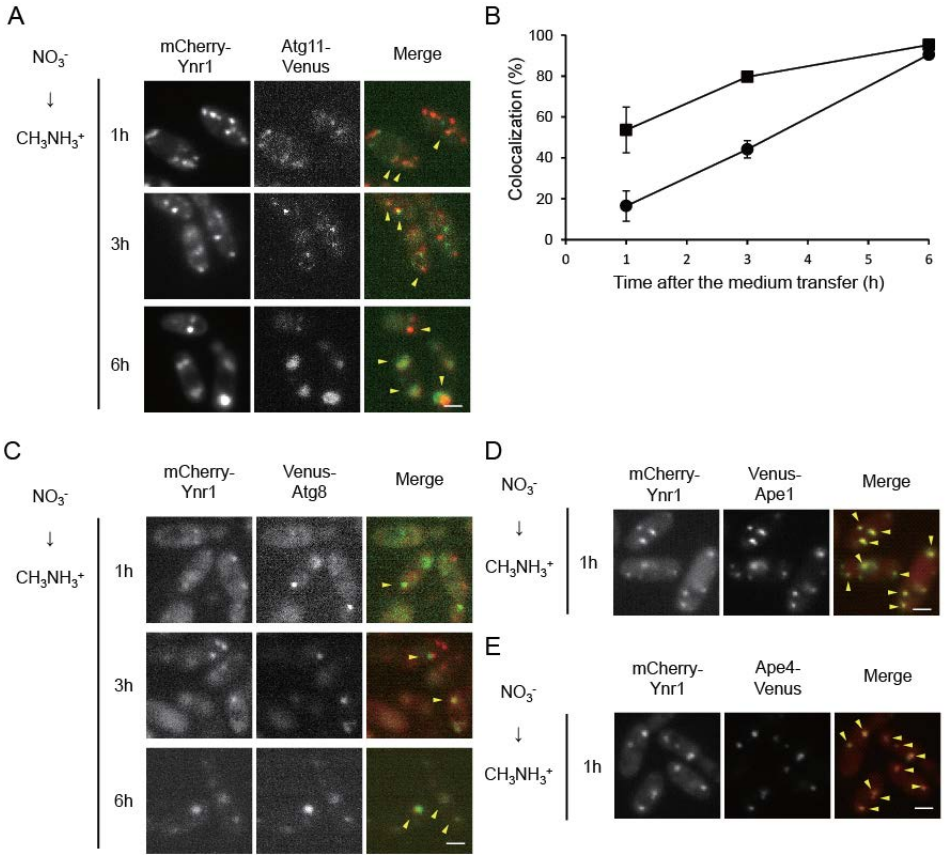

Figure 2-7. Sequestration and transportation of Ynr1 via the Cvt pathway after the shift from nitrate to methylamine. (A) Microscopic images of *C. boidinii* wild-type cells expressing Atg11-Venus and mCherry-Ynr1. The cells were subjected to the nitrogen-source shift from nitrate to methylamine. Yellow arrowheads indicate co-localization of Atg11-Venus and mCherry-Ynr1. Merged images are combined images of Venus green fluorescence and mCherry red fluorescence images. Bar, 2 μm. (B) Quantitation of co-localization of Atg11-Venus and mCherry-Ynr1 in the *C. boidinii* wild-type strain used for the microscopic imaging analysis shown in (A). Percentages represent the ratio of the number of co-localized puncta to the number of Atg11-Venus puncta or mCherry-Ynr1 puncta. Symbols: ■, ratio of the number of co-localized puncta to the number of Atg11-Venus puncta; ●, ratio of the number of co-localized puncta to the number of mCherry-Ynr1 puncta. For each sample, a minimum of 50 cells was analyzed. Error bars show standard deviations of dot measurements of all cells. (C) Fluorescence images of cells expressing both mCherry-Ynr1 and Venus-Atg8. Yellow arrows indicate co-localization of Atg8-Venus and mCherry-Ynr1. Bar, 2 μm. (D) Co-localization of Venus-Ape1 and mCherry-Ynr1 in wild-type cells 1 h after the nitrogen-source shift from nitrate to methylamine. Yellow arrowheads indicate co-localized puncta. Bar, 2 μm. (E) Fluorescence images of both mCherry-Ynr1– and Ape4-Venus–expressing cells. Yellow arrows indicate co-localization of Ape4-Venus and mCherry-Ynr1. Bar, 2 μm.

forms dots associated with the Cvt complex, is sequestered into Cvt vesicles, and is ultimately delivered to the vacuole. These data indicated that Ynr1 forms a complex for its degradation with other vacuolar enzymes for biosynthesis.

Methylamine efficiently induced degradation of Ynr1 via selective autophagy

Next, I investigated the induction of selective autophagy during the shift of nitrogen source from nitrate to several compounds other than methylamine. Cells expressing both mCherry-Ynr1 and Venus-Ape1 were observed by fluorescence microscopy. One hour after the medium change, among the four tested nitrogen sources only methylamine caused the

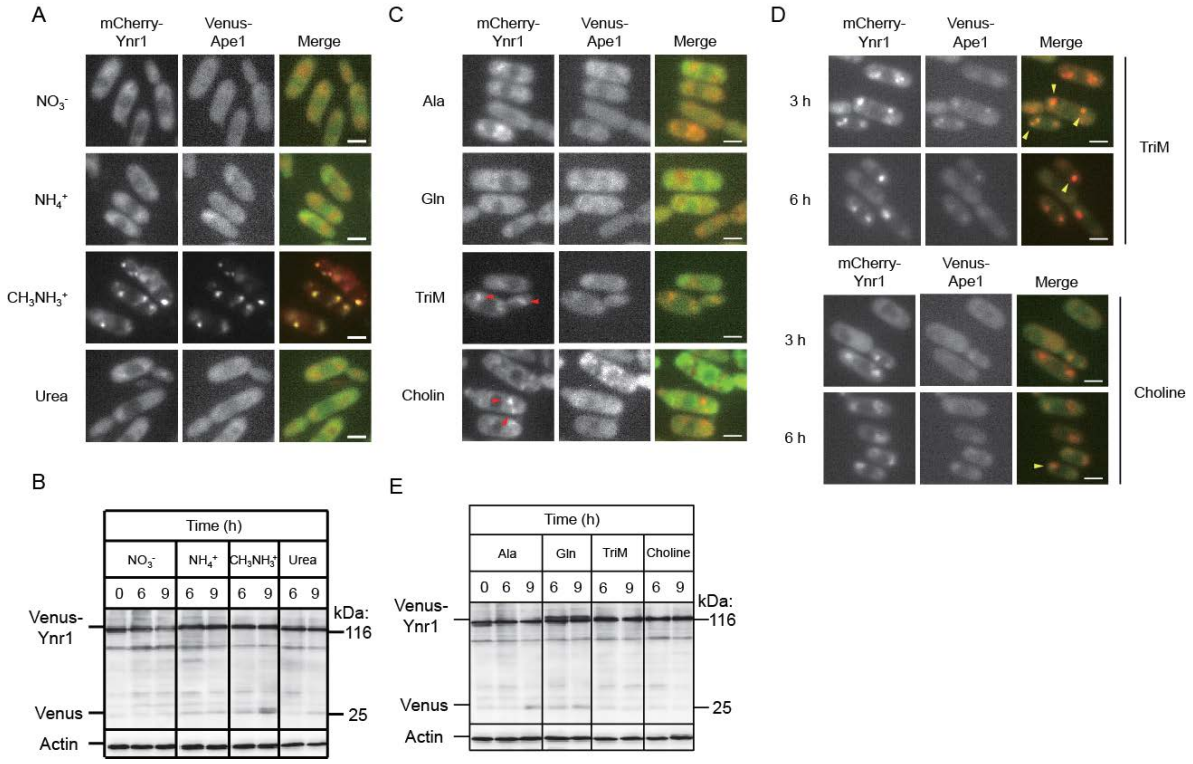

Figure 2-8. Methylamine effectively induced transport of Venus-Ynr1 via the Cvt pathway. (A) Microscopic images of *C. boidinii* wild-type cells expressing mCherry-Ynr1 and Venus-Ape1. Cells were observed 1 h after a nitrogen-source shift from nitrate to methylamine, ammonium, or urea, as well as nitrate as its control. Merged images are combined images of Venus and mCherry fluorescence images. Bar, 2 μm. (B) Immunoblot analysis of Venus Ynr1 in *C. boidinii* wild-type cells transferred from nitrate to four different media indicated. (C) Microscopic images of *C. boidinii* wild-type cells expressing mCherry-Ynr1 and Venus-Ape1. Cells were observed 1 h after the nitrogen-source shift from nitrate to L-alanine, glutamine, trimethylamine, or choline. Red arrowheads show dot formations of mCherry-Ynr1. Bar, 2 μm. (D) Microscopic images of *C. boidinii* wild-type cells expressing mCherry-Ynr1 and Venus-Ape1. Images were taken 3 and 6 h after the nitrogen-source shift from nitrate to trimethylamine or choline. Yellow arrowheads indicate co-localized puncta. Bar, 2 μm. (E) Immunoblot analysis of Venus- Ynr1 in *C. boidinii* wild-type cells transferred from nitrate to these four different media. Abbreviation: L-Ala; L-alanine, Gln; glutamine, TriM; trimethylamine.

formation of the mCherry-Ynr1-dot, which colocalized with Venus-Ape1 (Figure 2-8A). I also examined Ynr1 dynamics by immunoblot analysis using Venus-Ynr1 expressing cells. After 9 hours of the medium shift, the band intensity of a cleaved form of Venus detected with cells adapted for methylamine medium was stronger than those adapted for the other media (Figure 2-8B). These results suggest that Ynr1 degradation was effectively induced only when the nitrogen source changed from nitrate to methylamine.

In addition, I also checked the effects of other compounds, including glutamine, alanine, trimethylamine and choline, on the induction of mCherry-Ynr1 dot formation. Metabolism of trimethylamine and choline produce methylamine as a metabolite[27]. One hour after the shift from nitrate to choline- or trimethylamine-containing medium, a small number of dot-like structures of mCherry-Ynr1 were detected (Figure 2-8C). Therefore, I continued to observe the Ynr1 dynamics under the fluorescence microscope, and found that both trimethylamine and choline induced dot formation of mCherry-Ynr1, which was detectable

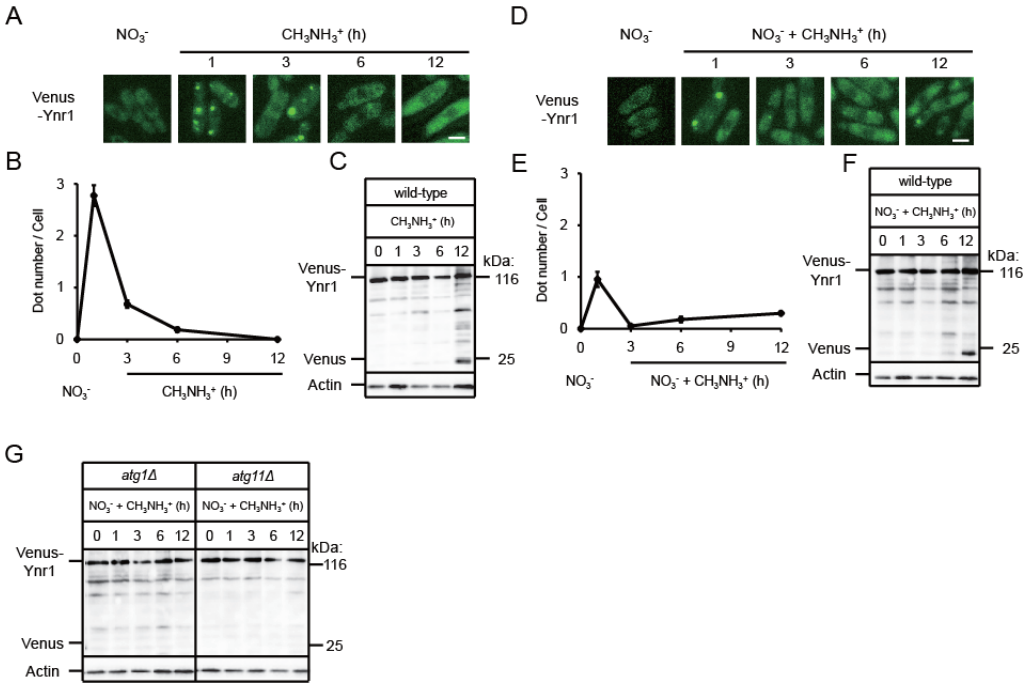

Figure 2-9. Ynr1 was transported to the vacuole even in the presence of nitrate. Venus-Ynr1 expressing wild-type (A-F), *atg1*Δ, and *atg11*Δ (G) cells, were first cultured on SD medium supplemented with nitrate and transferred to SD medium containing methylamine (A-C) or methylamine plus nitrate (D-G). Cells were collected at the indicated time point after the medium shift. (A, D) Fluorescent images of Venus-Ynr1 expressing *C. boidinii* wild-type cells. Bar, 2 μm. (B, E) Quantitation of the number of Venus-Ynr1 puncta per cell, determined from analysis of the fluorescent images shown in (A) or (D). For each sample, a minimum of 50 cells were analyzed. Error bars show standard deviations. (C, F, G) Immunoblot analysis of Venus-Ynr1.

even 6 h after the medium transfer (Figure 2-8D). Distinct from the case with methylamine, however, Venus-Ape1 formed very small dots both in number and size in the presence of trimethylamine or choline, and not all mCherry-Ynr1 dots colocalized with Venus-Ape1. Furthermore, I examined the Venus-Ynr1 expression by immunoblot analysis. However, none of the tested compounds induced the formation of a distinct band of free Venus as observed in the case with methylamine (Figure 2-8E). These results indicate that the presence of methylamine effectively induces the dot formation of mCherrry-Ynr1.

Ynr1 was transported to the vacuole even in the coexistence with nitrate

Neither the enzyme activity nor the transcript level of nitrate reductase Ynr1 was affected by nitrate in the coexistence with other nitrogen sources (Figure 1-5). In order to examine the regulation of Ynr1 degradation in the presence of multiple nitrogen sources, intracellular dynamics of Venus-Ynr1 was investigated during the medium shift from nitrate to methylamine or methylamine plus nitrate. As shown in Figure 2-6B and 2-9A, nitrogen source shift from nitrate to methylamine induced dot formation of Venus-Ynr1 followed by vacuolar transport via the Atg11-dependent Cvt pathway, and degradation, detected as a cleaved form

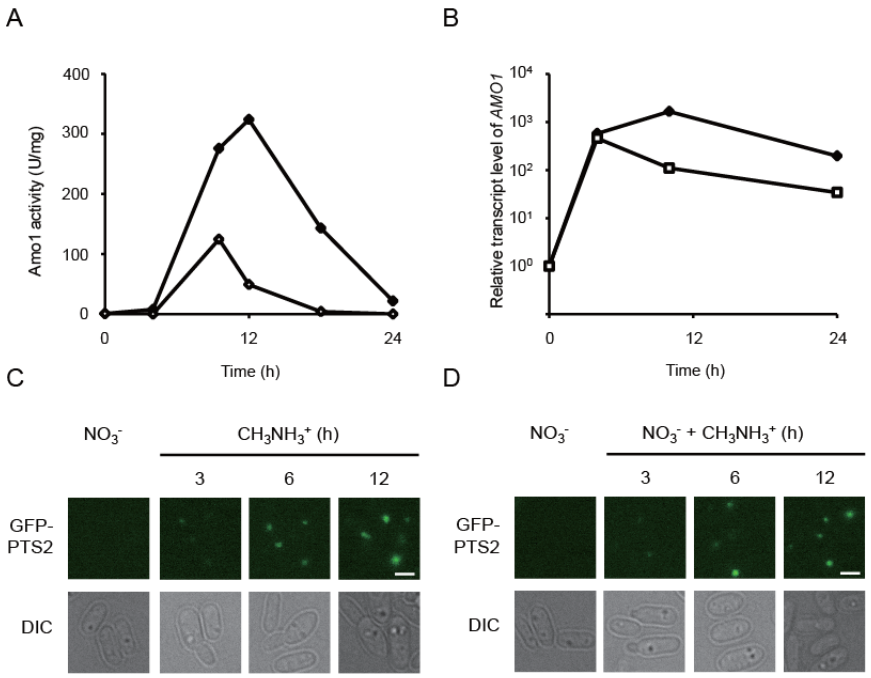

Figure 2-10. Effect of nitrate on peroxisome biogenesis induced by methylamine. (A) Amo1 activity. (B) Relative transcript level of *AMO1*. *C. boidinii* cells were first cultured on SD ammonium medium, transferred to SD medium containing methylamine or methylamine plus nitrate, and then harvested at the indicated time point. Symbol: closed diamonds; Methylamine, open squares; Methylamine plus nitrate. Similar results were obtained from two independent experiments and average values of the duplicate experiments are shown. (C and D) Microscopic images of PTS2-GFP expressing cells during methylamine-induced peroxisome proliferation. Cells were pre-cultured in SD ammonium medium and shifted to SD medium containing methylamine (C) or methylamine plus nitrate (D). Subsequently, the yeast cells were observed by fluorescence microscopy at the indicated time points. DIC represents the image from differential interference contrast microscope.

of Venus after 12 h (Figure 2-5A and 2-9C). Although the dot number of Venus-Ynr1 per cell was smaller than that observed after the nitrogen source shift from nitrate to methylamine, the shift to methylamine plus nitrate medium induced dot formation of Venus-Ynr1 (Figure 2-9A, 2-9B and 2-9D, 2-9E), followed by degradation of the cleaved form of Venus (Figure 2-9F). In addition, the degradation of Venus-Ynr1 was not observed in *atg1*Δ or *atg11*Δ cells (Figure 2-9G). These results indicate that methylamine-induced degradation of Ynr1 occurred even when nitrate was present in the medium.

Nitrate did not affect methylamine-induced peroxisome biogenesis

Amo1 is known to be a peroxisomal enzyme that is highly induced by methylamine[27]. Therefore, the effect of nitrate on methylamine-induced peroxisome proliferation was investigated. I first followed the Amo1 activity and *AMO1* transcript level over time in the presence of methylamine or methylamine plus nitrate. These results showed that Amo1 activity increased after 10 h of incubation in both media, and that the *AMO1* transcript level was up-regulated 4 h after medium transfer (Figure 2-10A and 2-10B), followed by the increase of the enzyme activity.

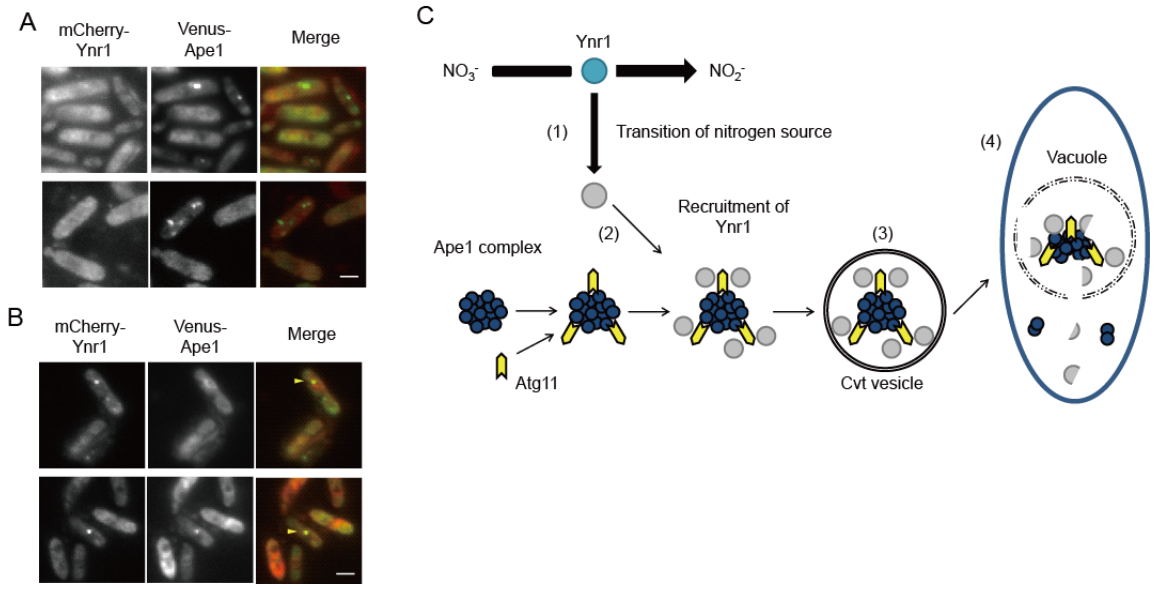

Figure 2-11. Co-localization of mCherry-Ynr1 and Venus-Ape1 in *C. boidinii* cells inoculated on wilting plant leaves. (A) and (B) Microscopic images of *C. boidinii* cells expressing mCherry-Ynr1 and Venus-Ape1 on (A) growing or (B) wilting *A. thaliana* leaves. Yellow arrowheads indicate co-localization of Atg11-Venus and mCherry-Ynr1. Merged images are combined images of Venus green fluorescence and mCherry red fluorescence images. Bar, 2 μm. (C) Ynr1 turnover on plant leaves via the Cvt pathway. On growing plant leaves, *C. boidinii* utilizes nitrate as the nitrogen source, and active Ynr1 (blue) catalyzes reduction of nitrate to nitrite. The transcriptional level of *YNR1* is adjusted in accordance with the plant's daily light–dark cycle. As the plant gets older, methylamine (and other compounds) leaks from the plant surface and can be used as a nitrogen source by *C. boidinii*. (1). At this stage, inactive Ynr1 (gray) is recruited to the Ape1 complex (2) in atg11-dependent manner. After sequestration of Ynr1 inside the Cvt vesicle (3), the vesicle fuses with the vacuole, releasing the Cvt body into the vacuolar lumen (4). Released Ynr1 is subjected to degradation.

As shown previously, CbAmo1 also has a putative peroxisomal targeting signal type 2 (PTS2) motif at its N terminus. In order to investigate the PTS2-dependent transport of peroxisomal proteins and peroxisome dynamics, a strain expressing PTS2-GFP was constructed and incubated in medium containing methylamine or methylamine plus nitrate. During peroxisome biogenesis induced by methylamine, clear green PTS2-GFP puncta were observed 6 h after the medium shift under both conditions (Figure 2-10C and 2-10D).

Taken together, the coexistence of nitrate with methylamine did not have a clear effect on Amo1 activity, transcript level of *AMO1*, or transport of peroxisomal proteins containing PTS2, suggesting that nitrate had no negative impact on methylamine-induced proliferation of peroxisomes.

Ynr1 is degraded via the Cvt pathway on wilting plant leaves

Finally, I monitored the localization of mCherry-Ynr1 and Venus-Ape1 in *C. boidinii* cells grown on plant leaves. As shown in Figure 2-11A and 2-11B, Venus-Ape1 formed dots in cells grown on both young and wilting plant leaves. On the other hand, dot-like structures of mChrry-Ynr1 were observed only on wilting plant leaves (Figure 2-11A), although the

number and size of these dots were smaller than those detected in cells grown in methylamine-containing liquid media. These results support the idea that the active form of Ynr1 catalyzes reduction of nitrate to nitrite in the cytosol of cells growing on young plant leaves, whereas on old leaves Ynr1 is transported to the vacuole as a new cargo of the biosynthetic Cvt vesicles, and degraded (Figure 2-11C).

Discussion

Asporogenous yeasts that inhabit plant surfaces are speculated to evolve other strategies than forming spores, in order to survive environmental changes in their ecological niche. Here I show that nitrate is used by the yeast *C. boidinii* on younger leaves while methylamine becomes more important nitrogen source in older leaves, and demonstrate that nitrate reductase Ynr1 essential for yeast proliferation on young leaves was transported to and degraded in the vacuole mediated by an Atg11-dependent selective pathway similar to the Cvt pathway on aged leaves. The Cvt pathway is a constitutive biosynthetic pathway, and Ape1 transport to vacuole was indeed suggested on young leaves (Figure 2-11A and 2-11B). On aged leaves, Ynr1 became a cargo member of Cvt vesicles, and was degraded in the vacuole (Figure 2-2C and 2-11B). Because Amo1 is transported to peroxisomes and catalyzes methylamine metabolism on aged leaves, it is logical for Ynr1 degradation to be independent of pexophagy.

Regulation of autophagy in *C. boidinii* plays a critical role in the daily environmental adaptation during growth on young leaves[6]. Under such conditions, some type of autophagy (e.g., the Cvt pathway) was constitutively activated, as judged by cleavage of Venus-Atg8 and lipidation of Atg8, but Ynr1 escaped degradation. By contrast, both peroxisome proliferation and pexophagy are regulated by the daily cycle of methanol concentration, the main carbon source for this organism on plant leaves. Pexophagy occurs only during the light period when the methanol concentration is low[6], and this specific degradation of peroxisomes, mediated by Atg30, is necessary for proliferation of this yeast on young growing plant leaves. In addition to the plant daily light-dark cycle, I herein showed the importance of regulation of autophagy in order to adjust a dynamically changing environment in response to aging of host plant. Ynr1, which functions on young leaves, is not degraded via autophagy on young plant leaves. However, on wilting plant leaves, it becomes a cargo for the constitutive Cvt pathway, which has shown to occur on plant. And also, results propose a new role of Cvt pathway for protein degradation, that has been believed to be a biosynthetic pathway. Together with the results of these recent studies, my findings reveal that selective autophagy is strictly controlled in a sophisticated manner. To the best of my knowledge, these findings represent the first description on how eukaryotic microbes surviving on plant surfaces adapt to the environment by regulating multiple autophagic pathways in a sophisticated and strict manner not only during the daily cycle but also during the plant lifespan. Such regulation of autophagy was suggested to exist also in a plant pathogenic fungi during differentiation of appressorium on plant leaf[44].

I also investigated the role of autophagy on Ynr1 activity *in vitro* during a nitrogen-source shift from nitrate to methylamine. Following the nitrogen-source shift, Ynr1

was rapidly inactivated and decreased to ~20% of its enzymatic activity after 6 h. On the other hand, I detected the cleaved form of Venus only 12 h after the medium transfer, indicating that Ynr1 was inactivated prior to its transport to the vacuole for degradation. The enzyme activity decreased at similar rates in the *atg1Δ* and *atg11Δ* strains. Although activation of Ynr1 in *H. polymorpha* has been studied at the level of expression[19,61], inactivation of yeast Ynr1 has not been reported previously. On the other hand, nitrate reductases from higher plants contain a well-conserved serine residue within the hinge 1 region that is phosphorylated in response to light or CO_2[62]. I could neither find a conserved region in Ynr1 nor detect phosphorylation of Ynr1 during the process of adaptation to methylamine. I speculate that inactivated Ynr1 can be distinguished from its active form, and can therefore be recognized by some autophagic receptor protein and thereby recruited to Cvt vesicles for degradation. Atg19, a receptor protein of the Ape I complex, is not present in *C. boidinii*. Thus, the detailed mechanisms underlying inactivation of Ynr1, and specific recruitment of the inactivated enzyme to Cvt vesicles, remain to be elucidated.

By quantitative growth analysis, I showed that the *C. boidinii ynr1*Δ strain could not proliferate on young leaves. Therefore, nitrate sufficient to support yeast proliferation is present on young leaves. It has been widely assumed that nitrate is an abundant compound in many plants, and that plants can store excess nitrate in their tissues, including leaves[63-65]. Furthermore, nitrate assimilation was recently shown to be important in colonization of plant leaves by an aerobic Gram-negative and asporogenous bacterium[39]. Although all of these observations suggested that nitrate available for microbes is present on leaves, my observation of the impaired growth of the *C. boidinii ynr1*Δ strain on plant leaves provides the first demonstration that microbes utilize nitrate on young plant leaves.

Ynr1 expression oscillated during the daily cycle on young leaf, in a cycle similar to the daily oscillations of methanol, methanol-inducible genes, and peroxisome dynamics (Figure 2-2B). Although I could not estimate the nitrate concentration in the phyllosphere in *C. boidinii* strain PYNR, which expressed Venus from the *YNR1* promoter, previous reports have indicated that the nitrate concentration in plant leaves is several times higher in the light than in the dark[66,67]. Furthermore, nitrate reductase activity in leaves is higher in the light period, and it is rapidly inactivated in the dark[68]. Therefore, it is likely that the daily oscillation of *YNR1* expression reflected the daily fluctuation of nitrate concentration in the phyllosphere.

Another important finding of this study is that the importance of nitrogen sources for microbes in the phyllosphere changes during the plant life cycle, and microbes must also adapt to this change. On aged leaves, *C. boidinii* cells express peroxisomal Amo1 and utilize methylamine (and possibly other unidentified nitrogen compounds) that leak from the plant cells. At this stage, Ynr1 is transported to the vacuole for degradation. When I used a *C. boidinii* cell sensor expressing the *AMO1* promoter–driven Venus to assess the local

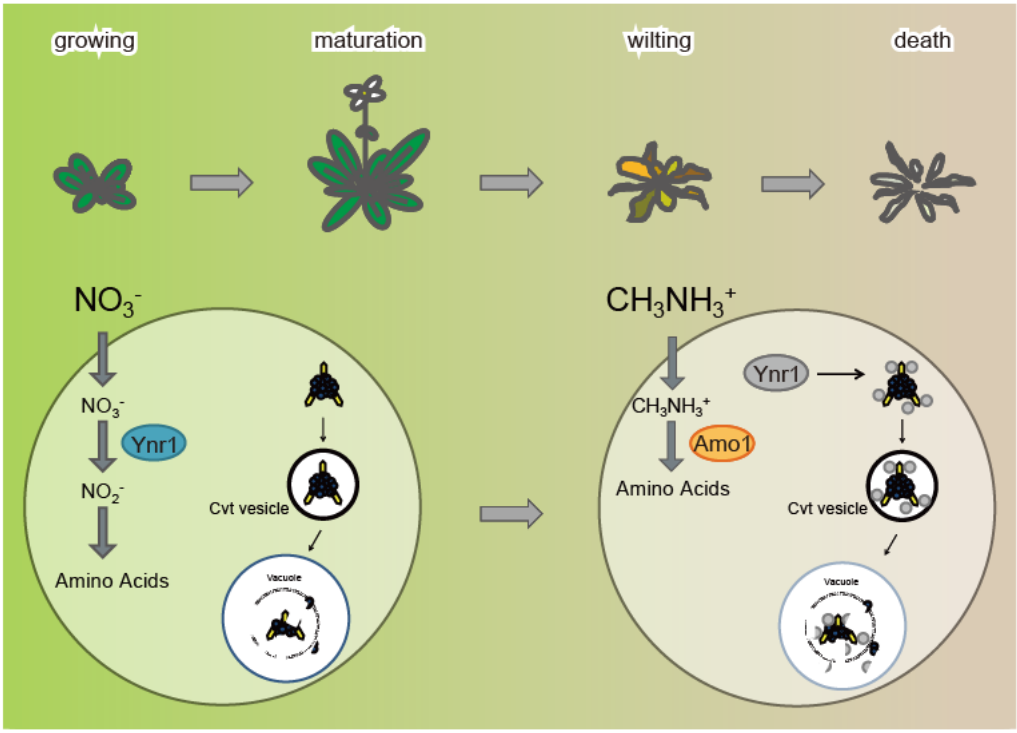

Figure 2-12. Nitrogenmetabolism and regulation of autophagy in the methylotrophic yeast in the phyllosphere. On growing leaves, nitrate can be utilized as nitrogen source. On the other hand, on wilting leaves, methylamine is utilized by *C. boidinii* and Ynr1 is inactivated, incorporated into the Cvt vesicle with other vacuolar hydrolases, and degraded.

methylamine concentration on *A. thaliana* leaves, I did not detect methylamine on growing young leaves (Figure 2-2A). By contrast, on aged plants, methylamine was estimated to be present at a concentration of 4.78×10^{-3} mM. Intracellular nitrogen compounds leak from the aged plant cells, resulting in a dramatic change in the importance of each nitrogen source for phyllospheric microbes. These changes will affect the population and activity of microbes on plant surfaces, mediating microbial substance circulation by acting as a biomass degrader.

To further understand the adaptation mechanisms of the yeast to the change in leaf environment during plant lifespan, I set up and conducted *in vitro* culture experiments, and found that the change of nitrogen source from nitrate to methylamine induced degradation of Ynr1 via selective autophagy. While I could observe induction of *AMO1* expression and the appearance of Ynr1 punctates on aged leaves, these might not be due to simple change of nitrogen source from nitrate to methylamine rather due to complex environmental changes in the phyllosphere.

In conclusion, I elucidated the influence of nitrogen metabolism on the regulation of autophagy in *C. boidinii* on both growing and wilting leaves of *A. thaliana* (Figure 2-12). On growing leaves, *C. boidinii* utilizes nitrate and adjusts the expression levels of *YNR1* in accordance with daily oscillation of nitrate concentration. During the light period, while pexophagy is active on young leaves, Ynr1 escapes from autophagic degradation. In contrast,

on wilting leaves, the yeast responds to the change of leaf environment by expressing peroxisomal Amo1 and degrading cytosolic Ynr1 via the Cvt pathway. Overall, I showed that the composition of available nitrogen sources for phyllospheric microbes change during plant lifespan. Moreover, this study has shed light on a new role of Cvt pathway for protein degradation together with the importance of regulation of autophagy in eukaryotic microbes as the survival strategy on the plant surfaces. These will improve our knowledge and concept of how microbes adjust to changing of environmental conditions and how they survive in nature.

Chapter III

Intracellular sequestration of yeast Hog1 is involved in heat tolerance

Abstract

Yeast high osmolarity glycerol (Hog) pathway plays a central role in stress responses. It has been reported that Hog1 is activated by a variety of stress stimuli including high osmolarity, oxidative stress, heat stress and arsenite, and contributes to cellular adaptation to the change in the external environment. However, intracellular dynamics of Hog1 is almost unknown under those stresses except for the translocation from the cytosol to the nucleus in response to high osmolality. Here I investigated the intracellular dynamics of Hog1 under high temperature condition using four yeast species, *Saccharomyces cerevisiae*, *Candida boidinii*, *Pichia pastoris*, and *Schizosaccharomyces pombe*. When treated with high temperature stress, Hog1-Venus formed dot structures that were observed in all of the tested yeast species except with *S. cerevisiae*. With further analyses on the dot formation of Hog1-Venus in *C. boidinii*, I found that N-terminal region of CbHog1 is necessary and sufficient for its dot formation, and that CbHog1-Venus partially co-localized with stress granules. Growth analysis revealed that ScHog1, forming no dots in the cytosol, negatively affected the cell growth of *C. boidinii* under high temperature conditions. On the other hand, non-functional ScHog1 (i.e., kinase dead, phosphorylation defective, and plasma membrane anchored ScHog1) caused no cytotoxicity, indicating that the importance of intracellular sequestration of Hog1 under high temperature condition is modulation of Hog1 kinase activity in cells.

Introduction

When cells are exposed to environmental stresses, they must first sense the stresse and activate the corresponding signal transduction pathway. Subsequently, the downstream gene expression and/or protein activity are regulated for adaptation to the stress conditions. Mitogen-activated protein kinases (MAPKs) are signaling proteins that are conserved from yeasts to human. They are serine-threonine protein kinases that are activated by some stimuli, such as cytokines, growth factors, hormones, and cellular stresses[13-15]. MAPKs are catalytically inactive in their base form. In order to become active, they are required to be phosphorylated in their activation loops. When cells sense some stimuli, small GTPase Ras is activated for activation of the downstream signaling pathways, including MAPK cascade. Dephosphorylation of MAPK by MAPK phosphatase, on the other hand, leads to the inactivation of MAPK[16].

Hog1, an ortholog of the mammalian MAPK p38, plays a central role as a signaling mediator during osmoregulation in the baker's yeast *Saccharomyces cerevisiae*[13]. Activation of the Hog1 cascade is mediated by two upstream cascades[69]. As the first step, the Sln1/Ypd1/Ssk1 osmosensor activates the Ssk2/Ssk22 MAP kinase kinase kinases (MAPKKKs). The second step of Hog1 activation is independent of the Sln1/Ypd1/Ssk1 osmosensor, but involves a transmembrane Sho1 and Ste11 MAPKKK. Only Pbs2 MAP kinase kinase (MAPKK) and Hog1 MAPK are commonly used in both of the two cascades. Activated Hog1 is localized to the nucleus and mediates upregulation of nearly 600 genes by phosphorylating osmoresponsive transcription factors, such as Msn2/Msn4, Sko1, Hot1, and Smp1[70]. The major role of the yeast MAPK pathway is to elevate the intracellular glycerol level as osmolyte by inducing glycerol synthesis and accumulation. Loss of Hog1 activity results in reduced cell growth on high osmolality media and abnormal cell morphology[71]. In addition to high osmotic condition, Hog1 is partially activated by heat stress through Sho1 branch and loss of Hog1 phosphatase, Ptp2 and Ptp3, resulting in heat sensitivity[72]. However, intracellular dynamics of Hog1 under high temperature condition remains to be investigated.

Heat stress induces several cellular responses in yeast. At high temperature, yeast cells activate the heat-shock response (HSR), a highly conserved transcriptional program. In HSR, heat shock transcription factor Hsf1 and general stress response transcription factor Msn2/Msn4 induce expression of chaperone and other general stress response genes[73]. The cell wall integrity (CWI) pathway responds to perturbations of the cell wall via activation of Mpk1 MAPK pathway[74]. This pathway is also induced by transient heat shock, suggesting that such high temperature conditions destabilize the membrane or cell wall[75]. In addition, heat stress induces the formation of non-translating mRNPs (messenger ribonucleoproteins) such as processing bodies (P-bodies) and stress granules (SGs)[76,77]. These granules harbor the

mRNA decay machinery or various factors, involved in translational repression and transient storage of mRNAs, and thus, play an important role in the quality control of the cytosolic mRNAs[78]. Recently, it has been reported that SGs regulate signaling of the target of rapamycin complex 1 (TORC1), a central kinase that coordinates nutrient availability with eukaryotic cell growth, by sequestering TORC1 into those SGs under high temperature condition[79].

In this chapter, I investigated the intracellular dynamics of Hog1 MAPK under heat stress condition by using four different yeast species: the baker's yeast *Saccharomyces cerevisiae*, the methylotrophic yeasts *Candida boidinii*, *Pichia pastoris*, and the fission yeast *Schizosaccharomyces pombe*. I found a novel localization pattern of Hog1-Venus and its homologous proteins in all the tested yeast species except for *S. cerevisiae* under high temperature condition. Microscopic observation revealed that N-terminal region of CbHog1 is necessary and sufficient for its dot formation, and that CbHog1-Venus partially co-localized with SGs under high temperature condition. Furthermore, when cell growth was compared between *C. boidinii* strain expressing CbHog1 or ScHog1, growth defect was only observed in *C. boidinii* cells expressing ScHog1. It was also found that non-functional ScHog1, i.e., kinase inactive, phosphorylation defective, and plasma membrane anchored ScHog1, showed no negative effect on cell growth under high temperature condition. These results indicate that intracellular sequestration of Hog1 under high temperature condition is important to suppress Hog1 function harboring a kinase activity.

Materials and methods

Yeast strains and culture conditions

Escherichia coli DH10B was used for plasmid propagation. *E. coli* was grown at 37˚C in LB medium (0.5 % yeast extract, 1 % tryptone, 0.5 % NaCl) supplemented, when required, with ampicillin (100 μg/ml). For preparation of solid medium, LB medium was supplemented with 2 % agar.

The yeast strains used in this study are listed in Table 3-1. *S. cerevisiae*, *C. boidinii*, and *P. pastoris* cells were grown on YPD medium (1% Bacto-yeast extract, 2% Bacto-peptone, 2% glucose), SD medium (0.67% Yeast Nitrogen Base without amino acids, 2% glucose), or SD-Trp medium (SD medium supplemented with 1.92 g/L Yeast Synthetic Drop-out Medium Supplements without tryptophan (Sigma-Aldrich)). The pH of SD medium was adjusted to 6.0 with NaOH. To select strain *Cbhog1Δ* (*ura3*), 2.4 μg/ml of uracil or 0.08% wt/vol of 5-fluoroorotidic acid (5-FOA) were added to SD medium. *S. pombe* cells were grown on YES medium (0.5% Bacto-yeast extract, 3% glucose, 75 mg/L adenine, leucine, uracil and lysine). Cultivation was performed at 28˚C under aerobic conditions, and the growth of the yeast cells was monitored by measuring the optical density at 610 nm (OD_{610}). For preparation of solid medium, the above media were supplemented with 2 % agar.

DNA isolation and transformation

Plasmid DNAs from *E. coli* were isolated with Wizard® *Plus* SV Minipreps DNA Purification System (Promega, Madison, WI). Transformation of *E. coli* was performed by the method of Dower *et al*[80]. Yeast DNA was isolated by the method of Cryer *et al*[81]. Transformation of *S. cerevisiae* was performed by using the Fast yeast transformation kit (G-Biosciences, Maryland Heights, MO, USA). Transformation of *C. boidinii* was performed by the modified version of the lithium acetate method[33]. Transformation of *P. pastoris* was performed as follows: A single fresh colony was pre-cultured on 5 mL YPD medium for 24h and the overnight culture was used for inoculation in 80 mL YPD culture in a 500 mL flask, with starting OD_{610} 0.1-0.2, and grown to a cell density of OD_{610} 0.6-1.0. Yeast cells were harvested and treated with 25 mM dithiothreitol in YPD containing 20 mM HEPES-KOH, pH 8.0, for 15 min at 30˚C. The cells were washed twice by 40 mL ice-cold water, once by 30 mL cold 1 M sorbitol, and then resuspended in 1 M sorbitol (2 mL/250 OD unit) which resulted in *P. pastoris* competent cells. 80 μL competent cells were mixed with 0.2-1.0 ng of DNA and transferred to a 0.2 cm gap cuvette (Bio-Rad), and the DNA was introduced by electroporation at 1.5 kV, 25 microfarads, 200 ohms (Gens Pulser, Bio-Rad Corp.). The cells were incubated with 1 mL 1 M sorbitol for 1h. Then, the cells were centrifuged at 5,000 rpm for 1 min and spread onto a SD plate, supplemented with appropriate amino acids and

Table 3-1. Strains used in this study

Designation	Genotype	References
S. cerevisiae		
BY4741	MATa *his3Δ1 leu2Δ0 met15Δ0 ura3Δ0*	Brachmann. (1982)
HS01	BY4741, *Schog1*::*ScHOG1-GFP, LEU2*	This study
C. boidinii		
TK62	*ura3*	Sakai *et al.* (1991)
HC01	TK62, *Cbhog1Δ*::*URA3*	This study
HC02	HC01, *ura3*	This study
HC03	HC02, *ura3*::(P_{CbHOG1}*CbHOG1-Venus, URA3*)	This study
HC04	HC02, *ura3*::(P_{CbACT1}*ScHOG1-Venus, URA3*)	This study
HC05	HC02, *ura3*::(P_{CbHOG1}*CbHOG1Δ(1-10)-Venus, URA3*)	This study
HC06	HC02, *ura3*::(P_{CbHOG1}*CbHOG1Δ(1-17)-Venus, URA3*)	This study
HC07	HC02, *ura3*::(P_{CbHOG1}*CbHOG1(1-20)-Venus, URA3*)	This study
HC08	HC02, *ura3*::(P_{CbHOG1}*CbHOG1(1-50)-Venus, URA3*)	This study
HC09	HC02, *ura3*::(P_{CbACT1}*ScHOG1-K52R-Venus, URA3*)	This study
HC10	HC02, *ura3*::(P_{CbACT1}*ScHOG1-T174A/Y176F-Venus, URA3*)	This study
HC11	HC02, *ura3*::(P_{CbACT1}*ScHOG1 Venus-CAARas2, URA3*)	This study
HC12	TK62, *ura3*::(P_{CbPAB1}*CbPAB1-Venus, URA3*)	This study
HC13	TK62, *Cbpbp1Δ*::*URA3*	This study
HC14	HC13, *ura3*	This study
HC15	TK62, *Cbedc3Δ*::*URA3*	This study
HC16	HC15, *ura3*	This study
HC17	HC16, *Cbpat1Δ*::*URA3*	This study
HC18	HC17, *ura3*	This study
HC19	HC14, *ura3*::(P_{CbPAB1}*CbPAB1-Venus, URA3*)	This study
HC20	HC18, *ura3*::(P_{CbPAB1}*CbPAB1-Venus, URA3*)	This study
BUL	*ura3, leu2*	Sakai and Tani (1992)
SK01	BUL, *leu2*::(P_{CbPAB1}*CbPAB1-Venus, LEU2*)	This study
HC21	SK01, *ura3*::(P_{CbHOG1}*CbHOG1-mCherry, URA3*)	This study
P. pastoris		
PPY12	*arg4 his4*	Sakai *et al.* (1998)
HP01	PPY12, *Pphog1Δ*::Zeo^r	This study
HP02	HP01, *arg4*::(P_{PpHOG1}*PpHOG1-YFP, ARG4*)	This study
S. pombe		
FY14931	*ade6-216 leu1-32 lys1-131 ura4-D18 sty1*::*sty1-GFP-HA*, Kan^r	This study

Table 3-2. Primers used in this study

Designation	DNA sequence (5'→3')
CbHOG1_UP_Fw	GGGCGAATTGGGTACGGCGCCGATGGAAATATGGAAACAGAGATG
CbHOG1_UP_Rv	GGGGGGGCCCGGTACCACCCATACCAACTGGATTTAAA
CbHOG1_DOWN_Fw	CACCGCGGTGGAGCTCAACAACAGCTGTAACAATAATTCAAG
CbHOG1_DOWN_Rv	ACAAAAGCTGGAGCTGAATTCCAACATGTCCAACAACAACAAC
CbPBP1_ UP_Fw	GGCGAATTGGGTACCCCGTGCACTACATTTGCGTTTTAAAAAT
CbPBP1__UP_Rv	GGGGGGCCCGGTACCGAAGTATTTGGGTTACCAGAAGCCATTT
CbPBP1_DOWN_Fw	CACCGCGGTGGAGCTCCATAGGGGTTCAAGAGGACATTATAAATTTTAATG
CbPBP1__DOWN_Rv	ACAAAAGCTGGAGCTCGAATGTTGCTGGAAAATCCATTTTTTGAAG
CbEDC3_ UP_Fw	GGCGAATTGGGTACCCCGTACCGTTCGTGCTATTCATT
CbEDC3_UP_Rv	GGGGGGCCCGGTACCGCCTTTGTTATCGTTGATCCAAATCCATAAG
CbEDC3_DOWN_Fw	CACCGCGGTGGAGCTCCAAATCAAATTGTTTAATCATTTAATCATTTAATCATTTA ATCAT
CbEDC3_DOWN_Rv	ACAAAAGCTGGAGCTCGATAGTGATTTTTCAAAATTTAATAAATCATCTTTTGATA AATC
CbPAT1_ UP_Fw	GGCGAATTGGGTACCCTATCTACCTATATATCAGAATCCTGATATAATACTC
CbPAT1_UP_Rv	GGGGGGCCCGGTACCGTGCATAACTCAAACCTGAATCATTGA
CbPAT1_DOWN_Fw	GGGCGAATTGGGTACGGCGCCGATGGAAATATGGAAACAGAGATG
CbPAT1_DOWN_Rv	GGGGGGGCCCGGTACCACCCATACCAACTGGATTTAAA
CbHOG1_SPR_Fw	CACCGCGGTGGAGCTCAACAACAGCTGTAACAATAATTCAAG
CbHOG1_SPR_Rv	ACAAAAGCTGGAGCTGAATTCCAACATGTCCAACAACAACAAC
CbHOG1_Vn_Fw	GGCGAATTGGGTACCCCGTGCACTACATTTGCGTTTTAAAAAT
CbHOG1_UP_Fw	GGGGGGCCCGGTACCGAAGTATTTGGGTTACCAGAAGCCATTT
CbHOG1_UP_Rv	CACCGCGGTGGAGCTCCATAGGGGTTCAAGAGGACATTATAAATTTTAATG
CbPAT1_DOWN_Fw	CACCGCGGTGGAGCTCCAAGGTTTAGAAGGAAGATTAAATCAAATTTTCCCAC
CbPAT1_DOWN_Rv	ACAAAAGCTGGAGCTCCACGTCCTATATACCCTAATTAGTCATTCA
CbHOG1_SPR_Fw	GATGGAAATATGGAAACAGAGATG
CbHOG1_SPR_Rv	CAACATGTCCAACAACAACAAC
CbHOG1_Vn_Fw	CTTTTGCTCACATGTGATGGAAATATGGAAACAGAGATGAAG
CbHOG1_Vn_Rv	AGAAACCATGTCGACCAGCTGTTGTTGTTGTTGTTGTT
P_{CbACT1}ScHOG1__Fw	ATATTACAAAAGTCGACATGACCACTAACGAGGAATTCATTAG
P_{CbACT1}ScHOG1_ Rv	TTAGAAACCATGTCGACCTGTTGGAACTCATTAGCGTACTG
CbHOG1_Δ(1-10)_Fw	TTTGGTACTATATTTGAAACAACAAATAGATACTC
CbHOG1_ΔN_Rv	CATTTTATTTATATCTATATATATATATGTCTATTGTATATGTCTATTGTC

Continued to the next page

Table 3-2. Continued

Designation	DNA sequence (5'→3')
CbHOG1_Δ(1-17)_Fw	ACAAATAGATACTCAGATTTAAATCCAG
HOG1_ΔC_Fw	GTCGACATGGTTTCTAAAGGTG
CbHOG1__(1-20)_Rv	TCTATTTGTTGTTTCAAATATAGTACCAAATATTTGAGTTC
CbHOG1_ (1-50)_Rv	TTTAATTGCAACATTTTGATTTGTTAATTTATCCTTTGC
CbPab1_Fw	CTTTTGCTCACATGTGGCGCTTAATTTTGGCTGAATC
CbPab1_Rv	AGAAACCATGTCGACGCCGGATTCACCCTTCTTC
ScHOG1_KD_Fw	AAAATCATGAAACCTTTTTCCACTGCA
ScHOG1_KD_Rv	TCTAATGGCAACTGGCTGAGATG
ScHOG1_nP_Fw	GGCTTTGTTTCCACTAGATACTACAGG
ScHOG1_nP_Fw	AGCCATTTGAGGGTCTTGAATTCTTGCTAG
ScHOG1_CAA_Fw	GGTTCTGGTGGTTGTTGTATTATTTCTTAACTGCAGGGAATTTAATCATTTTCAAC
ScHOG1_CAA_Rv	TTTATATAATTCATCCATACCTAAAGTAATACCAG
ScHOG1CTag_Fw	CGGTAACCAGGCCATACAGTACGCTAATGAGTTCCAACAGGTGAGCAAGGGCGAG GAGCT
ScHog1CTag_Rv	GAAGTAAGAATGAGTGGTTAGGGACATTAAAAAAACACGTCGACCTGTATCGCTC AAAAG
Zhog1_UPfw	CGTTTAATAAAGCCAGCCATTTAGATCGTCTAGACTAACCTATACGGGTTTAATGC C
Zhog1_UPrv	TGAAGCTATGGTGTGGAAGACTGCCGGTTTATCCTC
Zhog1_DWfw	TTTGGTCATGAGATCCTGTTCTGCCAAGGACAAGC
Zhog1_DWrv	GGCATTAAACCCGTATAGGTTAGTCTAGACGATCTAAATGGCTGGCTTTATTAAAC G
pPICZ_Zeo_fw	CACACCATAGCTTCAAAATGTTTCTAC
pPICZ_Zeo_rv	GATCTCATGACCAAAATCCCTTAAC
PpHog1IF_fw	GGTACCCGGGGATCCCTAACCTATACGGGTTTAATGCC
PpHog1IF_rv	CAGCTCGAGACTAGTTTGATCCTCAACTTGATGGAAGTC
ScHOG1CTag_Fw	CGGTAACCAGGCCATACAGTACGCTAATGAGTTCCAACAGGTGAGCAAGGGCGAG GAGCT
ScHog1CTag_Rv	GAAGTAAGAATGAGTGGTTAGGGACATTAAAAAAACACGTCGACCTGTATCGCTC AAAAG
Zhog1_UPfw	CGTTTAATAAAGCCAGCCATTTAGATCGTCTAGACTAACCTATACGGGTTTAATGC C
Zhog1_UPrv	TGAAGCTATGGTGTGGAAGACTGCCGGTTTATCCTC

Continued to the next page

Table 3-2. Continued

Designation	DNA sequence (5'→3')
Zhog1_DWfw	TTTGGTCATGAGATCCTGTTCTGCCAAGGACAAGC
Zhog1_DWrv	GGCATTAAACCCGTATAGGTTAGTCTAGACGATCTAAATGGCTGGCTTTATTAAACG
pPICZ_Zeo_fw	CACACCATAGCTTCAAAATGTTTCTAC
pPICZ_Zeo_rv	GATCTCATGACCAAAATCCCTTAAC
PpHog1IF_fw	GGTACCCGGGGATCCCTAACCTATACGGGTTTAATGCC
PpHog1IF_rv	CAGCTCGAGACTAGTTTGATCCTCAACTTGATGGAAGTC

Table 3-3. Plasmids used in this study

Designation	Description	References
for *S. cerevisiae*		
pMO152	EGFP LEU2	Oku *et al*. (In press)
for *C. boidinii*		
SK+SPR	*URA3*	Sakai and Tani. (1992)
pHC100	Hog1-UPregion URA3	This study
pHC101	Hog1-UPregion Hog1-DOWNregion URA3	This study
pHC102	Pbp1-UPregion Pbp11-DOWNregion URA3	This study
pHC103	Edc3-UPregion Edc3-DOWNregion URA3	This study
pHC104	Pat1-UPregion Pat1-DOWNregion URA3	This study
pKK001	P_{CbACT1}Venus URA3	Kawaguchi *et al.* (2011)
pHC200	P_{CbHOG1}CbHOG1-Venus URA3	This study
pHC300	P_{CbACT1}ScHOG1-Venus URA3	This study
pHC201	P_{CbHOG1}CbHOG1Δ(1-10)-Venus URA3	This study
pHC202	P_{CbHOG1}CbHOG1Δ(1-17)-Venus URA3	This study
pHC203	P_{CbHOG1}CbHOG1(1-20)-Venus URA3	This study
pHC204	P_{CbHOG1}CbHOG1(1-50)-Venus URA3	This study
pSPM001	P_{CbACT1} mCherry URA3	Shiraishi *et al*. (2015)
pHC400	P_{CbHOG1}CbHOG1-mCherry URA3	This study
pHC401	P_{CbPAB1}CbPAB1-Venus URA3	This study
pHC402	P_{CbPAB1}CbPAB1-Venus LEU2	This study
pHC500	P_{Cbact1}ScHog1-Venus URA3	This study
pHC501	P_{CbHOG1}ScHOG1-K52R-Venus URA3	This study
pHC502	P_{CbHOG1}ScHOG1-T174A/Y176F-Venus URA3	This study
pHC503	P_{CbHOG1}ScHOG1-Venus-CAARas2 URA3	This study
P. pastoris		
pPICZ A	Zeo^r	This study
pHP001	PpHog1-UPregion PpHog1-DOWNregion Zeocin	This study
pIB1-ARG4	atg1K.D.(D190A)-YFP ARG4	This study
pHP100	P_{PpHOG1}PpHOG1-YFP ARG4	This study

antibiotics, incubated at 28˚C for 2-3 days until colonies appeared. For the first screening, the colonies were picked up and transferred to a new SD plate.

Plasmid construction for expression in *C. boidinii*

The oligonucleotide primers used for PCR reactions are listed in Table 3-2. The plasmids used in this study are listed in Table 3-3. A deletion cassette for the *CbHOG1* gene was constructed as follows: Primer set named CbHOG1_UP_Fw / CbHOG1_UP_Rv was used to amplify 1.0-kb fragment using genomic DNA of *C. boidinii* as template. The PCR product was fused with the 7.6-kb KpnI-cutted SK+SPR by In-fusion HD ® cloning kit (TaKaRa, Kyoto, Japan), yielding pHC100. Primer set CbHOG1_DOWN_Fw / CbHOG1_DOWN_Rv was used to amplify 1.0-kb fragment using genoic DNA of *C. boidinii* as template. The PCR product was fused with the 8.6-kb SacI-cutted pHC100 by In-fusion HD ® cloning kit, yielding CbHOG1 disruption vector pHC101. Deletion cassettes for the *CbPBP1*, *CbEDC3*, and *CbPAT1* genes were constructed in a similar way with primer sets CbPBP1_UP_Fw / CbPBP1_UP_Rv and CbPBP1_DOWN_Fw / CbPBP1_ DOWN _Rv, CbEDC3_UP_Fw / CbEDC3_UP_Rv and CbEDC3_DOWN_Fw / CbEDC3_ DOWN _Rv, and CbPAT1_UP_Fw / CbPAT1_UP_Rv and CbPAT1_DOWN_Fw / CbPAT1_ DOWN _Rv, respectively. The PCR products were fused with KpnI/SacI-cutted SK+SPR by In-fusion HD ® cloning kit (TaKaRa, Kyoto, Japan), yielding pHC102, pHC103, and pHC104, respectively.

CbHOG1 promoter and ORF region without STOP codon was amplified by primer set CbHOG1_Vn_Fw / CbHOG1_Vn_Rv using genomic DNA of *C. boidinii* as template. The PCR product was fused with the 6.4-kb AflIII-SalI fragment of plasmid pKK001 by In-fusion HD ® cloning kit, resulting pHC200. *ScHOG1* ORF region without STOP codon was amplified by primer set P_{CbACT1}ScHOG1_ Fw / P_{CbACT1}ScHOG1_ Rv. The PCR product was fused with the 8.1-kb SalI-cutted pKK001 by In-fusion HD ® cloning kit, resulting in pHC300. pHC401 was prepared in a similar manner with a primer set CbPab1_Fw / CbPab1_Rv. A vector pHC402, encoding CbPab1-Venus under the control of the *PAB1* promoter with *LEU2* (Sakai and Tani, 1992) was constructed by ligation of an AatII-NarI fragment from pHC401 with an AatII-NarI fragment of *LEU2* gene.

pHC201, a deletion mutant of *CbHOG1*, was constructed as follow: Primer set CbHOG1_Δ(1-10)_Fw / CbHOG1_ΔN_Rv was phosphorylated at their 5′-ends with T4 nucleotide kinase, and used to amplify 8.6-kb fragment by inverse PCR using the pHC200 plasmid as template. The PCR product was self-ligated, yielding a vector pHC201. Other deletion mutants of *CbHOG1* were constructed in a similar way with Primer sets CbHOG1_Δ(1-17)_Fw / CbHOG1_ΔN_Rv, HOG1_ΔC_Fw / CbHOG1_ (1-20)_Rv, and HOG1_ΔC_Fw / CbHOG1_ (1-50)_Rv, resulting in the vectors pHC202, pHC203, and pHC204, respectively. Deletion mutants of ScHOG1 were also constructed in a similar manner. Two fragments, the 1.6-kb SalI-EcoRI fragment of the plasmid pSPM001 and the 4.1-kb SalI-EcoRI fragment of the plasmid pHC200 were ligated, yielding a vector pHC400.

pHC501, a kinase inactive *SCHOG1*, was constructed as follows: Primer set

ScHOG1_KD_Fw / ScHOG1_KD_Rv was phosphorylated at their 5′-ends with T4 nucleotide kinase, and used to amplify 8.6-kb fragment by inverse PCR using the pHC500 plasmid as template. The PCR product was self-ligated, yielding a vector pHC501. Other plasmids harboring mutated ScHOG1 were constructed in a similar way with Primer sets ScHOG1_nP_Fw / ScHOG1_nP_Fw and ScHOG1_CAA_Fw / ScHOG1_CAA_Rv, resulting in the vectors pHC502, and pHC503, respectively.

***CbHOG1* gene disruption**

A deletion cassette for the *CbHOG1* gene was amplified by a primer set CbHOG1_SPR_Fw / CbHOG1_SPR_Rv using the pHC101 plasmid as template. The PCR product was transformed into *C. boidinii* TK62 by the modified version of the lithium acetate method[33]. Proper gene disruption was confirmed by colony PCR analysis. The constructed *Cbhog1Δ* strain was converted to uracil auxotrophy by 5-FOA selection, yielding *Cbhog1Δura3* strain. Restoration of the marker gene, *URA3* was confirmed by PCR analysis.

Disruption of the *CbPBP1, CbEDC3* and *CbPAT1* genes. Disruption of components of SG and P-body was performed in a similar manner to the *CbHOG1* gene deletion. Deletion cassettes for the *CbPBP1*, *CbEDC3* and *CbPAT1* genes were amplified by primer sets CbPBP1_UP_Fw / CbPBP1_DOWN_Rv, CbEDC3_UP_Fw / CbEDC3_DOWN_Rv, CbPAT1_UP_Fw / CbPAT1_DOWN_Rv, respectively. The pHC102, pHC103, and pHC104 vectors were used as templates. The PCR product was transformed into *C. boidinii* TK62 by the modified version of the lithium acetate method[33]. Proper gene disruption was confirmed by colony PCR analysis. The constructed *Cbpbp1Δ*, *Cbedc3Δ*, and *Cbpat1Δ* strains were converted to uracil auxotrophy by 5-FOA selection, yielding *Cbpbp1Δura3*, *Cbedc3Δura3*, and *Cbpat1Δura3* strains. Restoration of the marker gene, *URA3* was confirmed by PCR analysis.

Vectors and plasmids for *S. cerevisiae*

The oligonucleotide primers used for PCR reactions are listed in Table 3-2. The plasmids used in this study are listed in Table 3-3. The *S. cerevisiae* strain expressing ScHog1-GFP was constructed in the following way. GFP-LEU2 region was PCR amplified with a primer set ScHOG1CTag_Fw / ScHog1CTag_Rv using pMO152 vector as its template. The fragment containing GFP-LEU2 gene was directly integrated into the C terminal region of the *ScHOG1* gene, resulting in the *S. cerevisiae* strain expressing ScHog1-GFP.

Vectors and plasmids for *P. pastoris*

The oligonucleotide primers used for PCR reactions are listed in Table 3-2. The plasmids used

in this study are listed in Table 3-3. The deletion strain of the *PpHOG1* gene was constructed as follows. Deletion cassettes were amplified with primer sets Zhog1_UPfw / Zhog1_UPrv and Zhog1_DWfw / Zhog1_DWrv, respectively, using genoic DNA of *P. pastoris* as template. The PCR products were linked by PCR with a primer set Zhog1_UPfw / Zhog1_DWrv, resulting in the 2.0-kb fragment containing the upstream and downstream regions of the *PpHOG1* gene. Zeocine marker was PCR amplified using the pPICZ A vector as its template resulting in the 1.9-kb fragment. Those two fragments were fused by In-fusion HD ® cloning kit, yielding *PpHOG1* disruption vector pHP001. The pHP001 vector was cut by XbaI site and transformed into the host strain, PPY12. Proper gene disruption was confirmed by colony PCR analysis.

The vector harboring PpHog1-YFP was constructed as follows. *PpHOG1* promoter and ORF region without STOP codon was amplified by primer set PpHog1IF_fw / PpHog1IF_rv using genomic DNA of *P. pastoris* as template. The PCR product was fused with the 3.4-kb BamHI-SpeI fragment of plasmid pIB1-ARG4 by In-fusion HD ® cloning kit, resulting pHP100. The pHP100 vector was cut by XbaI site and transformed into the host *Pphog1Δ* strain. Proper gene disruption was confirmed by colony PCR analysis.

The *S. pombe sty1Δ* strain expressing Sty1-GFP

The FY14931 strain was provided by the NBRP (YGRC), Japan.

Analysis of intracellular localization of fluorescent proteins under hyperosmotic stress condition

Yeast cells were pre-cultured on 5 mL YPD (for *S.cerevisie*, *C. boidinii* or *P. pastoris*) medium or YES (for *S. pombe*) medium to the stationary phase at 28˚C. Subsequently, 20 μL of these cultures were transferred to 5 mL SD-Trp (for *S. cerevisie* cul), SD (for *C. boidinii* or *P. pastoris*), or YES (for *S. pombe*) medium, and the cells were grown to early-log phase at 28˚C. Then, all of these cultures were centrifuged at 6,000 rpm for 2 min and cells were transferred to 5 mL fresh SD-Trp medium containing 0.5 M NaCl (for *S.cerevisie*), SD medium containing 0.4 M NaCl (for *C. boidinii*), SD medium containing 0.5 M NaCl (for *P. pastoris*), or YES medium containing 1 M KCl (for *S. pombe*) medium at 28˚C for 5 min (for *S.cerevisie*, *C. boidinii* or *P. pastoris*) or 10 min (for *S. pombe*). These cells were harvested by centrifugation for microscopic observation.

Analysis of intracellular localization of fluorescent proteins under heat stress condition

Yeast cells were pre-cultured on 5 mL YPD (for *S.cerevisie*, *C. boidinii* or *P. pastoris*) or YES (for *S. pombe*) medium to the stationary phase at 28˚C. Subsequently, 20 μL of these cultures were transferred to 5 mL SD-Trp (for *S.cerevisie*), SD (for *C. boidinii* or *P. pastoris*), or YES (for *S. pombe*) medium, and the cells were grown to early-log phase at 28˚C. Then, cells were treated with indicated heat stresses. These cells were harvested by centrifugation for microscopic observation.

Fluorescence microscopy

Fluorescence microscopy was performed using an IX81 inverted microscope (Olympus) equipped with an Uplan-Apochromat 100×/1.35 NA oil iris objective lens. Venus and mCherry signals were acquired using a Plan Fluor 100×lens (Carl Zeiss) with pin hole set to 1.02 airy units for YFP acquisition. Images were analyzed on METAMORPH imaging software (Molecular Devices) and Adobe Photoshop CS6 (Adobe). In all figures, the scale bar is 2 μm. Fluorescence observations of cells cultured in vitro were repeated at least twice and three shots of different fields were taken at each time point.

Morphometric analysis

Cell count analysis was performed in which the numbers of cells (n > 50, n; number of cells in one field) observed under fluorescent microscopy (f > 3, f; a field of vision) were counted, and independent examinations were repeated at least three times.

Preparation of cell samples for immunoblot analysis

To prepare samples for Phos-tag SDS-PAGE, harvested cells were suspended in lysis buffer (0.2 N NaOH, 1% (v/v) 2-mercaptoethanol) and incubated at 4°C for 10 min. Next, trichloroacetic acid was added (final concentration 10%). Then, the samples were vortexed, incubated at 4°C for 10 min, and centrifuged. Subsequently, the pellet was washed twice with acetone and resuspended in sample buffer (16.7 mM Tris-HCl pH 6.8, 1% SDS, 10% Glycerol, 1% 2-mercaptoethanol, 1 mM $MnCl_2$) and boiled for 3 min.

SDS-PAGE with or without phos-tag and immunoblot analysis

The prepared samples were electrophoresed on a 6% Phos-tag SDS-PAGE gel (containing 30 μM Phos-tag (Wako), 100 μM $MnCl_2$) or 10% normal SDS-PAGE gel. Western analysis was performed by the method of Towbin *et al*[82]. The proteins on a gel were transferred to a PROTRAN® nitrocellulose transfer membrane (Schleicher & Schuell BioScience, Inc., Dassel, Germany) by tank blotting system (BIO-RAD) at 100 V for 1 h. After the transformation, the transferred membrane was blocked for 1 hour in TBS-T buffer (3 g Tris, 8 g NaCl, 0.2 g KCl,

0.1% Tween 20, pH 8.0) supplemented with 5% skim milk. These blots were incubated with monoclonal anti-GFP antibody (life technologies) at 1:1000 dilution in TBS-T buffer for 1 hour and washed three times with TBS-T. Subsequently, blots were incubated with an anti-mouse IgG (life technologies) at 1:10000 dilution in TBS-T for 1 hour, and washed three times in TBS-T. Immunoreactive bands were detected with the Western Lightning Chemiluminescence Reagent Plus (Perkin-Elmer Life Science) and the signals were detected by Light-Capture II (ATTO).

Results

CbHog1 is necessary for high osmotic stress resistance

To clone the gene *CbHOG1*, a homolog of *ScHOG1*, I searched for draft genome sequences of *C. boidinii*, and found 1194bp ORF encoding protein of 398 amino acids. The predicted amino acid sequence of CbHog1 showed a high degree of identity with ScHog1 (71%) as well as other homologous proteins PpHog1 from *P. pastoris* and SpSty1 from *S. pombe* (Figure 3-1). In order to reveal the functions of *CbHOG1*, this gene was disrupted by replacing the ORF with *URA3* gene as a selective marker. In *S. cerevisiae*, Hog1 is known to be localized to the nucleus after hyperosmotic stress treatment, and the *Schog1*Δ strain shows hyperosmo-sensitivity[13]. In order to observe the localization of CbHog1, I constructed the *Cbhog1*Δ strain expressing CbHog1-Venus under the control of its own promoter.

```
ScHog1      MTTNEEFIRTQIFGTVFEITNRYNDLNPVGMGAFGLVCSATDTLTSQPVAIKKIMKPFSTAVLAKRTYRE 70
CbHog1      --MAQEFTRTQIFGTIFETTNRYSDLNPVGMGAFGLVCAAKDKLTNQNVAIKKVMKPFSTAVLAKRTYRE 68
PpHog1      -MSQEKFTRTQIFGTIFETTARYDELNPVGMGAFGLVCSAKDKLTEQQVAIKKIMKPFSTPVLAKRTYRE 69
SpSty1      ---MAEFIRTQIFGTCFEITTRYSDLQPIGMGAFGLVCSAKDQLTGMNVAVKKIMKPFSTPVLAKRTYRE 67
                  * ******* ** * **  * * ********* * * **   ** ** ****** *********

ScHog1      LKLLKHLRHENLICLQDIFLSPLEDIYFVTELQGTDLHRLLQTRPLEKQFVQYFLYQILRGLKYVHSAGV 140
CbHog1      LKLLNHLRHENLISLDDIFLSPLEDIYFVTELQGTDLHRLLTSRPLEKQFIQYFLYQILRGLKFVHSSGV 138
PpHog1      LKLLNHLRHENLITLTDIFLSPLEDIYIVTELQGTDLHRLLTSRPLEKQFIQYFLYQILRALKYVHSAGV 139
SpSty1      LKLLKHLRHENIISLSDIFISPFEDIYFVTELLGTDLHRLLTSRPLETQFIQYFLYQILRGLKFVHSAGV 137
            **** ****** * * *** ** **** **** ********  **** ** ********* ** *** **

ScHog1      IHRDLKPSNILINENCDLKICDFGLARIQDPQMTGYVSTRYYRAPEIMLTWQKYDVEVDIWSAGCIFAEM 210
CbHog1      IHRDLKPSNILINENCDLKICDFGLARVQDPQMTGYVSTRYYRAPEIMLTWQKYDTEVDIWSAGCIFAEM 208
PpHog1      IHRDLKPSNILINENCDLKICDFGLARIQDHQMTGYVSTRYYRAPEIMLTWQKYDTEVDIWSAGCIFAEM 209
SpSty1      IHRDLKPSNILINENCDLKICDFGLARIQDPQMTGYVSTRYYRAPEIMLTWQKYNVEVDIWSAGCIFAEM 207
            ************************** ** **********************  **************

ScHog1      IEGKPLFPGKDHVHQFSIITDLLGSPPKDVINTICSENTLKFVTSLPHRDPIPFSERFKTVEPDAVDLLE 280
CbHog1      IEGKPLFPGKDHVHQFSIITELLGSPPKDVIDTICSENTLRFVQSLPHRDPIPFNEKFKGVEPEAIDLLS 278
PpHog1      IEGKPLFPGKDHINQFSIITELLGSPPTDVIDTICSENTLRFVQSLPHREPVPLIERFQGVEPVAIDLLE 279
SpSty1      IEGKPLFPGRDHVNQFSIITELLGTPPMEVIETICSKNTLRFVQSLPQKEKVPFAEKFKNADPDAIDLLE 277
            ********* **  ****** *** **  ** **** *** ** ***     *  * *    * * ***

ScHog1      KMLVFDPKKRITAADALAHPYSAPYHDPTDEPVADAKFDWHFNDADLPVDTWRVMMYSEILDFHKIGGSD 350
CbHog1      KMLVFDPRKRVTAEQALEHEYLSPYHDPTDEPVAEEKFDWSFNDADLPVDTWRVMMYSEILDFHQ----- 298
PpHog1      KMLVFDARKRITAEESLAHEYLEPYHDPTDEPVAAEKFDWSFNDADLPVDTWRVMMYSEILDFHQ----- 299
SpSty1      KMLVFDPRKRISAADALAHNYLAPYHDPTDEPVADEVFDWSFQDNDLPVETWKVMMYSEVLSFHN----- 297
            ******  **  *   * * *  ***********   *** * * **** ** ****** * **

ScHog1      GQIDISATFDDQVAAATAAAAQAQAQAQAQVQLNMAAHSHNGAGTTGNDHSDIAGGNKVSDHVAANDTIT 420
CbHog1      ----------------------------------------VEGAEADALQQQVQGQYEHSMTLQQQQQQH 373
PpHog1      ----------------------------------------VEDQ---------------------------- 348
SpSty1      ----------------------------------------MDNELQS----------------------- 349

ScHog1      DYGNQAIQYANEFQQ---------- 435
CbHog1      QIQKQQELQENELLQQQQQQQQQQL 398
PpHog1      -------------------------
SpSty1      -------------------------
```

Figure 3-1. Alignment of the amino acid sequences of Hog1 homolog proteins from 4 yeast species, *S. cerevisiae, C. boidinii, P pastoris* and *S. pombe*. The CLUSTLW program was used to align the amino acid sequences of ScHog1, CbHog1, PpHog1 and SpSty1 from respective yeast strains.

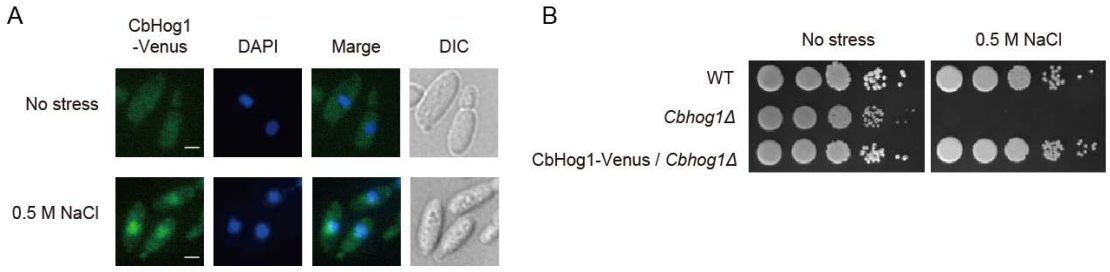

Figure 3-2. CbHog1 is required for yeast tolerance to high salt stress. (A) Microscopic images of the *C. boidinii hog1*Δ strain expressing CbHog1-Venus. Cells were grown to early log phase in SD medium, and shifted to SD medium supplemented with 0.4 M NaCl as high osmotic stress. DAPI was used for nuclear staining. Merged images are combined images of Venus yellow fluorescence and DAPI blue fluorescence images. Bar, 2 μm. (B) Growth assay under high salt condition. The wild type and the indicated mutant strains of *C. boidinii* were grown to early log phase, adjusted to OD_{610} = 1, and 3 μL of each ten-fold serially diluted liquid were dropped onto YPD plates without or with 0.5 M NaCl. Cells were incubated at 28˚C and cell growth was scored after 3 days.

CbHog1-Venus was localized to the nucleus 5 min after the treatment with 0.5 M NaCl (Figure 3-2A). Stress resistance analysis was also performed under high osmotic conditions in the wild type, *Cbhog1Δ* and CbHog1-Venus expressing *Cbhog1Δ* strains. The *Cbhog1Δ* strain exhibited severe growth defect on YPD medium containing 0.5 M NaCl, while CbHog1-Venus completely restored the hyperosmo-sensitivity of *Cbhog1Δ* (Figure 3-2B). These results indicate that CbHog1 plays a central role in osmotic stress tolerance, similar to ScHog1.

CbHog1-Venus forms dot structures under high temperature condition

To examine intracellular dynamics of CbHog1-Venus under high temperature condition, cells were incubated at 42˚C for 30 min. Microscopic observation revealed that *C. boidinii* cells harbored 5~6 dot structures of CbHog1-Venus in the cytosol (Figure 3-3A). In order to examine whether this intracellular dynamics occur in a reversible manner, I observed the localization of CbHog1-Venus after the removal of heat stress. As shown in Figure 3-3B and 3-3C, CbHog1-Venus dots gradually disappeared after the medium shift from high temperature condition to normal temperature and no or very few number of cells harbored Venus dots 60 min after the heat removal, suggesting that dot formation of CbHog1-Venus is a reversible process.

Dot formation of CbHog1-Venus depends on its amino acid sequence

Since the dot formation of CbHog1-Venus under high temperature condition is a novel localization pattern of yeast Hog1, I decided to further investigate the intracellular localization of Hog1 homologue proteins in other three different yeast species, *S. cerevisiae*, *P. pastoris*, and *S. pombe*. To perform microscopic observation, the *Schog1*Δ strain expressing ScHog1-GFP, *Pphog1*Δ strain expressing PpHog1-YFP and *Spsty1*Δ strain expressing

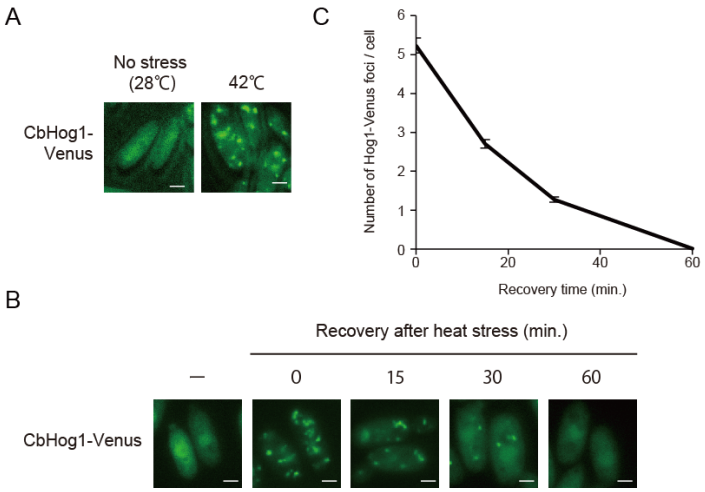

Figure 3-3. Intracellular localization of CbHog1 under high temperature condition. (A) Microscopic images of *C. boidinii hog1*Δ strain expressing CbHog1-Venus under normal and high temperature conditions. Bar, 2 μm. (B) Microscopic images of *C. boidinii hog1*Δ strain expressing CbHog1-Venus after the removal of heat stress. Cells grown to early log phase in SD medium at 28˚C were treated with heat stress (39˚C, 30 min), and then analyzed the intracellular dynamics of CbHog1-Venus by fluorescence microscopy during the recovery phase at 28˚C for 60 min. Bar, 2 μm. (C) Quantification of the number of Venus dots per cell in the *C. boidinii hog1*Δ strain expressing CbHog1-Venus used for the microscopic imaging analysis shown in (B). For each sample, a minimum of 50 cells was analyzed. Error bars show the standard deviations of all cells.

SpSty1-GFP were constructed. I found that all the strains showed similar localization of Hog1 after hyperosmotic stress treatment (Figure 3-4A). On the other hand, after heat stress treatment, all the Hog1-fluorescent proteins except for ScHog1-GFP formed dots in the cytosol in a similar manner to CbHog1-Venus (Figure 3-4A).

In order to elucidate whether the difference of the localization pattern of the Hog1 homologue proteins is due to the difference of the host strains, the *Cbhog1Δ* strain expressing ScHog1-Venus and the *Schog1Δ* strain expressing CbHog1-Venus were constructed. While ScHog1-Venus restored the osmotolerance in a similar manner to CbHog1-Venus (Figure 3-4B), ScHog1-Venus did not form dot in *C. boidinii* under high temperature condition (Figure 3-4C). On the other hand, upon heat stress CbHog1-Venus was detected in dot structures in *S. cerevisiae* (Figure 3-4C). These results indicate that dot formation of CbHog1-Venus under high temperature condition is due to the amino acid sequence of CbHog1, instead of the nature of the host strains.

N-terminal region of CbHog1-Venus is important for its dot formation

In order to determine which amino acid region of CbHog1 was important for its dot formation, I constructed the *Cbhog1*Δ strains expressing Venus-tagged deletion mutants of CbHog1. CbHog1Δ(1-10) and CbHog1Δ(1-17) are the CbHog1 deleted of the first N-terminal 10 and 17 amino acid residues, respectively. CbHog1(1-20) and CbHog1(1-50) are the CbHog1

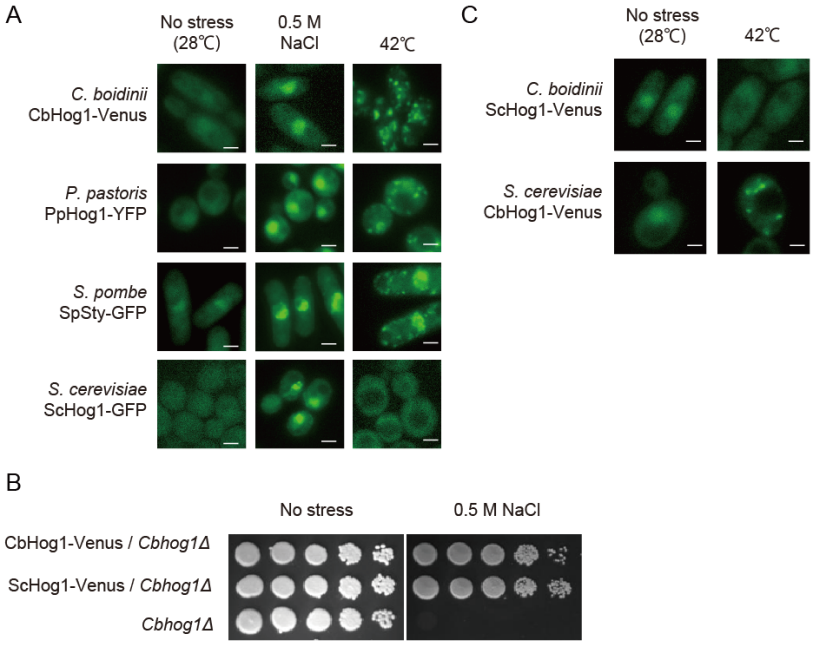

Figure 3-4. Intracellular localization of Hog1 in 4 yeast species under osmotic or heat stress condition. (A) Microscopic images of 4 yeast species expressing Hog1-fluorescent proteins under high salt or heat stress condition. The *S. cerevisiae hog1*Δ strain expressing ScHog1-GFP, *C. boidinii hog1*Δ strain expressing CbHog1-Venus, *P. pastoris hog1*Δ strain expressing PpHog1-YFP, and *S. pombe sty1*Δ strain expressing SpSty1-GFP were analyzed by fluorescence microscopy. Cells were grown to early log and treated with high salt stress (0.5 M NaCl, 5 min), or heat stress (42˚C, 30 min). Bar, 2 μm. (B) Growth under high salt condition. *C. boidinii hog1*Δ strain expressing CbHog1-Venus under the control of its own promoter, *C. boidinii hog1*Δ strain expressing ScHog1-Venus under the control of the *CbACT1* promoter, and *C. boidinii hog1*Δ strains were grown to early log phase, adjusted to OD610 = 1, and 3 μL of each ten-fold serially diluted liquid were dropped onto YPD plates without or with 0.5 M NaCl. Cells were incubated at 28˚C and cell growth was scored after 3 days. (C) Microscopic images of the *C. boidinii hog1*Δ strain expressing ScHog1-Venus under the control of the *CbACT1* promoter and *S. cerevisiae* strain expressing CbHog1-Venus under the control of the *CbHOG1* promoter. Cells were grown to early log phase in SD medium, and treated with heat stress (42˚C, 30 min). Bar, 2 μm.

consisting of the N-terminal 20 and 50 amino acid residues, respectively. CbHog1Δ(1-17)-Venus did not form dot after heat stress (Figure 3-5A), that is, the amino acid region 1-17 is necessary for dot formation of CbHog1-Venus. On the other hand, CbHog1(1-50)-Venus formed dots upon heat stress (Figure 3-5A), suggesting that the N-terminal region of the first 50 amino acid residues is sufficient for the dot formation. Judging from the prediction of protein structure based on the homology remodeling, the N-terminal region of Hog1 is assumed to form β-sheet structure with high hydrophobicity which could contribute to dot formation (Figure 3-5B).

Heat stress induces sequestration of CbHog1 into stress granules

Subsequently, I investigated the intracellular localization of the CbHog1-Venus induced by high temperature stress. Stress granules (SGs) are the cytosolic aggregations composed of proteins and RNAs that appear in response to external stresses including heat shock and severe ethanol stresses[83,84]. Recently, it has been reported that yeast SGs formed upon heat

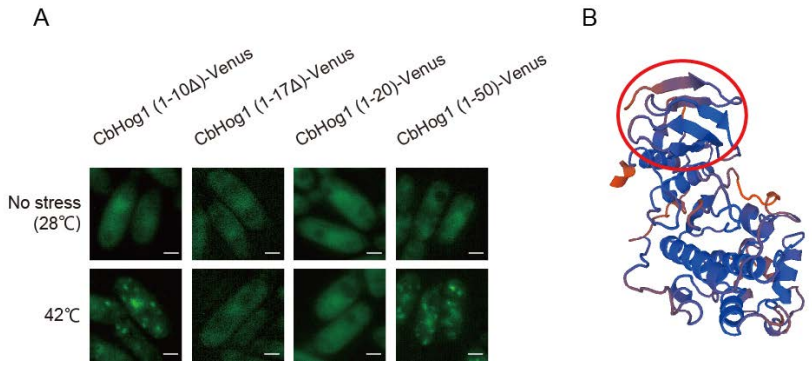

Figure 3-5. N-terminal region of Hog1 is important for dot formation. (A) Microscopic images of the *C. boidinii hog1*Δ strains expressing CbHog1Δ(1-10)-Venus, CbHog1Δ(1-17)-Venus, CbHog1(1-20)-Venus or CbHog1(1-50)-Venus. Cells were grown to early log phase in SD medium, and treated with heat stress (42˚C, 30 min). Bar, 2 μm. (B) Predicted structure of CbHog1 by homology remodeling (SWISS-MODEL : http://swissmodel.expasy.org/). The amino acid region about 1-50 residues is enclosed in red line.

stress sequestered the target of rapamycin complex 1 (TORC1) and blunted its signaling[79].

To examine the contribution of SGs on Hog1 dot formation, I searched *C. boidinii* draft genome sequence and found possible homologs of the major components of SGs, the poly-A binding protein Pab1, and the Pab1 binding protein Pbp1. Amino acid sequence of these proteins showed high homologies to those in *S. cerevisiae* (Table 3-4). The *C. boidinii* strain expressing CbPab1-Venus or CbPbp1-mCherry was constructed for examination of the intracellular distributions of SGs. Similar to *S. cerevisiae*, high temperature condition induced the dot formation of both CbPab1-Venus and CbPbp1-mCherry, showing co-localization of these two SG marker proteins in the cytosol (Figure 3-6A). These results indicate that SGs in *C. boidinii*, as well as other eukaryotes, are highly dynamic structures that respond to environmental conditions. To ascertain the possibility that CbHog1-Venus dots are associated with SGs, *C. boidinii* cells expressing CbHog1-mCherry and CbPab1-Venus were prepared. When treated with high temperature condition at 42˚C, both of CbHog1-mCherry and CbPab1-Venus formed dots and significantly colocalized, while at 37˚C only CbHog1-mCherry showed dot structures in the cytosol (Figure 3-6B).

Table 3-4. Comparison of amino acid sequences of P-body and SG components in *C. boidinii* with those in *S. cerevisiae*

	protein	identity (%)	similarity (%)
P-body components	Edc3	25	57
	Pat1	28	55
SG components	Pab1	56	76
	Pbp1	23	55

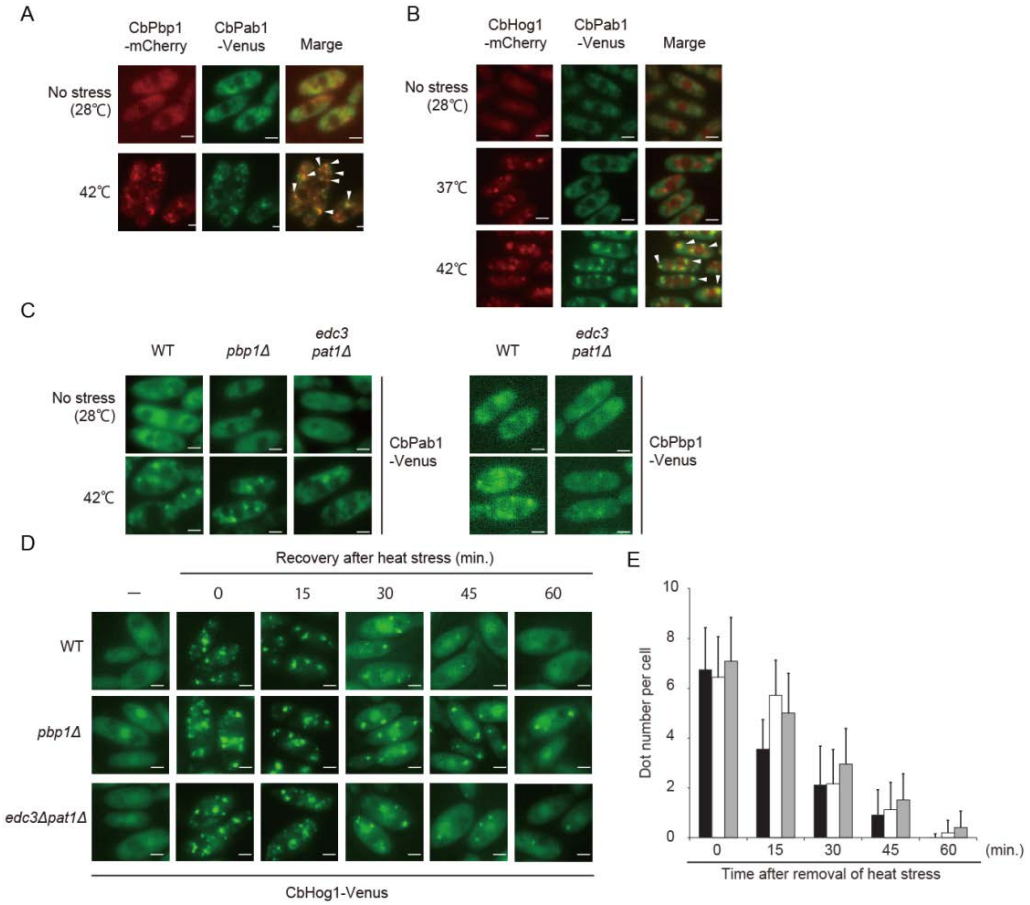

Figure 3-6. Sequestration of CbHog1 into SGs under heat stress and its recovery after heat removal. (A) Microscopic images of the *C. boidinii* strain expressing two SG marker proteins, CbPbp1-mCherry and CbPab1-Venus. Cells were grown to early log phase, and treated with heat stress at 42ºC for 30 min. Merged images are combined images of mCherry red fluorescence and Venus green fluorescence images. Arrowheads indicate representative dots in which CbPbp1-mCherry colocalized with CbPab1-Venus. Bar, 2 μm. (B) Microscopic images of the *C. boidinii* strain expressing CbHog1-mCherry and CbPab1-Venus. Cells were grown to early log phase, and treated with indicated heat stress for 30 min. Merged images are combined images of mCherry red fluorescence and Venus green fluorescence images. Arrowheads indicate representative dots in which CbHog1-mCherry colocalized with CbPab1-Venus. Bar, 2 μm. (C) Microscopic images of the *C. boidinii* wild-type and *edc3pat1Δ* strains expressing SG marker proteins, CbPab1-Venus or CbPbp1-Venus. Cells were grown to early log phase, and treated with heat stress at 42ºC for 30 min. Bar, 2 μm. (D) Microscopic images of the *C. boidinii* wild-type and mutant strains expressing CbHog1-Venus after the removal of heat stress. Cells grown to early log phase in SD medium at 28˚C were treated with heat stress (42˚C, 30 min), and then analyzed the intracellular dynamics of CbHog1-Venus by fluorescence microscopy during the recovery phase at 28˚C for 60 min. Bar, 2 μm. (E) Quantification of the number of Venus dots per cell in the *C. boidinii* wild-type and mutant strains expressing CbHog1-Venus used for the microscopic imaging analysis shown in (D). For each sample, a minimum of 50 cells was analyzed. Error bars show the standard deviations of all cells.

To further investigate the contribution of SGs on Hog1 dot formation, the *C. boidinii pbp1Δ* strain was constructed. Similar to *S. cerevisiae*, disruption of the *PBP1* gene was unable to inhibit heat stress-induced formation of SGs (Figure 3-6C). In the *pbp1Δ* strain Hog1 dot formation was detected in a similar manner to the wild-type strain, while disassembly of Hog1 dots after removal of heat stress was delayed in *pbp1Δ* cells (Figure 3-6D and 3-6E). Based on a previous research with the budding yeast[83], I constructed *C.*

boidinii cells lacking the Processing body (P-body) scaffold protein, Edc3, and the putative anion transporter, Pat1, which caused significant decrease of SG formation under heat stress condition (Figure 3-6C). Comparison of amino acid sequences of these components with homologues in *S. cerevisiae* was also shown in Table 3-4. Similar to the *pbp1Δ* strain, disruption of these two components necessary for SG formation also led to delay in the disassembly of Hog1 dots after heat removal (Figure 3-6D and 3-6E). These results suggest that localization to SGs plays important role on the relocation of CbHog1 from SGs to cytosol after removal of heat stress.

Hog1 kinase activity and its phosphorylation negatively affects on the cellular survivability under high temperature condition

In order to investigate the physiological significance of CbHog1 dot formation, I looked for a difference in phenotype between the *Cbhog1*Δ strain expressing CbHog1-Venus or ScHog1-Venus. Both of the strains restored the osmotolerance (Figure 3-4B). Immunoblot analysis showed no significant difference in expression level of Hog1 between the two strains (data not shown). Growth assay on yeast osmotic stress resistance was performed using the wild type, *C. boidinii hog1*Δ strain expressing CbHog1-Venus, *C. boidinii hog1*Δ strain expressing ScHog1-Venus and *C. boidinii hog1*Δ strain. Cells spotted on the YPD plates were incubated at 37˚C for 24 h as heat stress, transferred to the normal growth condition at 28˚C for 48 h and analyzed the cell growth. The *Cbhog1*Δ strain expressing ScHog1-Venus was more sensitive to heat stress than the *Cbhog1*Δ strain expressing CbHog1-Venus and *Cbhog1*Δ strain (Figure 3-7A), suggesting that dot formation of Hog1 is important for heat tolerance in *C. boidinii*.

Next, I constructed the mutant *Cbhog1*Δ strains expressing ScHog1 K52R-Venus, deficient in Hog1 kinase activity, and expressing ScHog1 T174A/Y176F-Venus, defective in Hog1 phosphorylation, to investigate the involvement of Hog1 kinase activity and its phosphorylation on the heat tolerance. Neither the ScHog1 K52R-Venus nor the ScHog1 T174A/Y176F-Venus caused negative effect on the *C. boidinii* cell growth under high temperature condition (Figure 3-7B). These results suggested that both kinase activity and phosphorylation of Hog1 were necessary to negatively regulate the cellular survival under high temperature condition.

Intracellular sequestration of Hog1 enhances the cellular survival under high temperature stress

Plasma membrane targeting of Ras proteins requires posttranslational modification of the C-terminal CaaX box (C = cysteine, A = aliphatic, X = any amino acid) and either palmitoylation or the presence of a polybasic domain[85-87]. To test whether anchoring of active

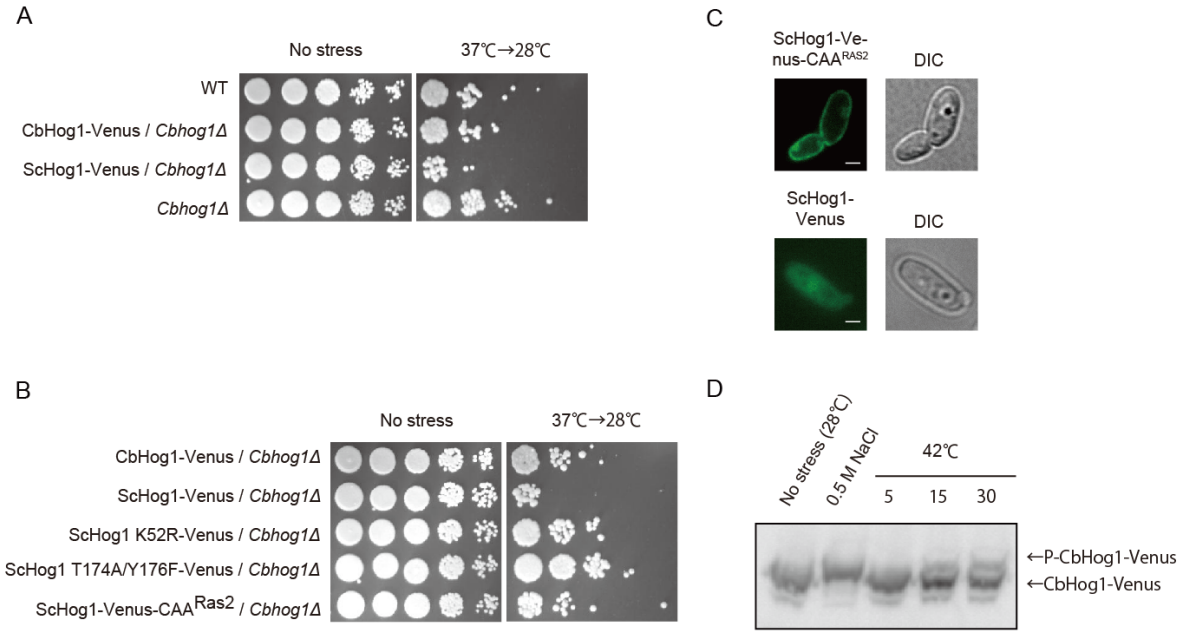

Figure 3-7. Intracellular sequestration of Hog1 enhances yeast heat tolerance. (A) Growth assay on yeast heat resistance. The wild type strain, *C. boidinii hog1*Δ strain expressing CbHog1-Venus, *C. boidinii hog1*Δ strain expressing ScHog1-Venus, and *C. boidinii hog1*Δ strain were grown to early log phase, adjusted to OD_{610} = 1, and 3 μL of each ten-fold serially diluted liquid were dropped onto YPD plates. Subsequently, one plate was incubated at 28˚C, the other plate was treated with heat stress (37˚C, 24 h) before incubation at 28˚C. Then, cell growth was scored after 2 or 3 days, respectively. (B) Growth assay on yeast heat resistance. The *C. boidinii hog1*Δ strain expressing CbHog1-Venus, *C. boidinii hog1*Δ strain expressing ScHog1-Venus, *C. boidinii hog1*Δ strain expressing ScHog1K52R-Venus, *C. boidinii hog1*Δ strain expressing ScHog1 T174A/Y176F-Venus and *C. boidinii hog1*Δ strain ScHogg1-Venus-CAA^{Ras2} were grown to early log phase, adjusted to OD_{610} = 1, and 3 μL of each ten-fold serially diluted liquid were dropped onto YPD plates. Subsequently, one plate was incubated at 28˚C, the other plate was treated with heat stress (37˚C, 24 h) before incubation at 28˚C. Then, cell growth was scored after 2 or 3 days, respectively. (C) Microscopic images of *C. boidinii* cells expressing ScHog1-Venus-$CAAX^{RAS2}$. The mutant strain expressing ScHog1-Venus-$CAAX^{RAS2}$ under the control of the *CbACT1* promoter showed its Venus fluorescence in the plasma membrane, while the *C. boidinii* cells expressing normal ScHog1-Venus under the control of the *CbACT1* promoter showed cytosolic Venus fluorescence. Cells were grown to early log phase in SD medium, and harvested for microscopic observation. Bar, 2 μm. (D) Immunoblot analysis of Venus-tagged Hog1 with phos-tag SDS-PAGE under osmotic (0.5 M NaCl, 5 min) or heat stress (42˚C, 5, 15 or 30 min) condition.

Hog1 to plasma membrane can suppress its negative effect on cell growth, I constructed *C. boidinii* cells expressing ScHog1-Venus-$CAAX^{RAS2}$. ScHog1-Venus-$CAAX^{RAS2}$ can be activated by phosphorylation but is anchored to the plasma membrane (Figure 3-7C). Growth assay revealed that ScHog1-Venus-$CAAX^{RAS2}$ had no growth defect under heat stress condition, suggesting that ScHog1 anchored to the plasma membrane could suppress cellular cytotoxicity of active form of ScHog1 (Figure 3-7C). Taken together, these results indicate that non-functional (kinase inactive, phosphorylation-sites mutated and plasma membrane anchored) ScHog1 is able to repress the negative impact on cell growth under high temperature condition.

In *S. cerevisiae*, Hog1 is partially activated by heat stress[72]. In order to determine whether Hog1 is also activated under high temperature condition in *C. boidinii*, Phosphate-affinity (Phos-tag) SDS–PAGE followed by immunoblotting with the anti-GFP antibody was performed. I analyzed total cell lysate of CbHog1-Venus expressing *Cbhog1Δ* strain treated with or without indicated stress. Cells treated with 0.5M NaCl for 10 min as hyperosmotic stress exhibited up-shifted band (Figure 3-7D), suggesting that Hog1 is phosphorylated by hyperosmotic stress in *C. boidinii* in a similar manner to *S. cerevisiae*[13]. Moreover, Cells treated with heat stress partially exhibited up-shifted bands, indicating that Hog1 is partially phosphorylated by heat stress in *C. boidinii* similarly in *S. cerevisiae*[72]. These results suggested that intracellular sequestration of yeast Hog1 phosphorylated in active form under high temperature conditions is considered to be one of the cellular strategies to suppress its physiological function.

Discussion

Intracellular dynamics of yeast Hog1 has been studied mainly on its translocation from the cytosol to the nucleus in response to high osmotic stress. Here I show a novel localization pattern of yeast Hog1 under high temperature condition. Upon heat stress CbHog1 formed dot structures in the cytosol that partially colocalized with stress granules (Figure 3-6B). This drastic change of intracellular localization of Hog1 homolog was also observed in other yeast species, *P. pastoris* and *S. pombe*, but not in *S. cerevisiae* (Figure 3-4A). These results suggest that dot formation of Hog1 is a well conserved phenomenon in yeasts.

Microscopic observation revealed that CbHog1 localized to SGs (Figure 3-6A). According to a previous study[79], it is possible to speculate that sequestration of CbHog1 into SGs under heat stress is an important strategy for yeast to control its signaling as a kinase. It is worth noting that localization of CbHog1 with SGs was partial and CbHog1-Venus formed dots at more mild heat stress (37˚C, 30 min) in which almost no SGs were formed (Figure 3-6B). These results suggest that CbHog1 forms dots earlier than SGs formation and that CbHog1 localizes with other cytosolic components. I asked the possible component to P-bodies whose formation is known to be induced by a variety of stress stimuli[88] and constructed *C. boidinii* cells expressing CbHog1-mCherry and CbEdc3-Venus. Although both CbHog1-mCherry and CbEdc3-Venus formed dots upon heat stress at 37˚C and 42˚C, those proteins did not colocalize under tested conditions (data not shown). Intracellular location of Hog1 under high temperature condition other than SGs remains to be elucidated.

The intracellular dynamics of CbHog1-Venus and ScHog1-Venus upon heat stress did not change by exchanging the host yeasts (Figure 3-4C). These results suggest that formation of cytosolic dots of Hog1-fluorecent protein did not depend on the host yeast, but on the amino acid sequence of Hog1 protein. I found a critical amino acid region of CbHog1 on dot formation under high temperature condition. The results demonstrated that the amino acid region of CbHog1 1-17 is necessary and CbHog1 1-50 is sufficient for dot formation of CbHog1-Venus (Figure 3-5A). The tertiary structure of CbHog1 predicted by homology-modeling showed that the amino acid region 1-50 forms β-sheet structure (Figure 3-5B), which is hydrophobic. It has been reported that some RNA binding proteins, that are constituent of SGs, reversibly aggregated through its glycine-rich domain[89]. Hence it is inferred that the hydrophobicity of N-terminal β-sheet region of CbHog1 drives its dots formation. In order to find critical amino acid residues for Hog1 dot formation, I compared amino acid sequences of the four Hog1 homolog proteins at the N-terminal region. However, no conserved amino acid sequence except for *S. cerevisiae* was found. Since the first 17 amino acid residues were necessary for dot formation, I designed 2 mutant CbHog1 (I14A and T17A substitutions) and performed microscopic observation. However, those two mutants

showed dot formation of CbHog1-Venus in a similar manner under high temperature condition (data not shown).

Physiological significance of dot formation of yeast Hog1 was investigated. The results demonstrated that, although ScHog1-Venus showing no dots, had cytotoxicity under heat stress condition, non-functional ScHog1-Venus (kinase dead and phosphorylation defective mutants) did not cause growth defect (Figure 3-7B). Previous study also described the negative effect of hyperactivated Hog1 due to the lack of two protein phosphatases, Ptp2 and Ptp3, on cell growth at elevated temperature[72]. I also revealed that the plasma membrane anchored ScHog1 lost its cytotoxicity under high temperature condition (Figure 3-7B), indicating that intracellular sequestration of Hog1 is crucial to suppress its function as kinase. Therefore, sequestration of Hog1 to SGs and other intracellular compartments functions in inactivation of Hog1 kinase activity. Microscopic observation of CbHog1-Venus during recovery from heat stress indicated another possible role of SGs. In two mutant strains lacking a component of SGs, Pbp1, and showing low ability to form SGs, CbHog1-Venus dots remained longer in the cytosol after removal of heat stress (Figure 3-6D and -6E), suggesting that sequestration into SGs is important for proper relocation of Hog1 for the subsequent environmental stresses. Taking the fact that CbHog1-Venus partially colocalized with SGs under heat stress into consideration (Figure 3-6B), SG is one possible cytosolic structure that sequesters activated CbHog1 to control its kinase activity.

One interesting finding was that SpSty1-GFP formed cytosolic dots, but at the same time, seemed to be localized into nucleus during heat stress (Figure 3-4A). These results suggest that SpSty1 is suppressed its function by sequestration into the cytosolic compartments, and simultaneously upregulates gene expression in the nucleus in adaptation to high temperature condition. Compared with the other yeast species, showing only dot structures (*C. boidinii* and *P. pastoris*) or no localization change (*S. cerevisiae*), SpSty1 might play more significant and active role in yeast heat tolerance. My speculation can be supported by previous studies that found that ScHog1 is important only for rapid recovery from heat stress[72], while the *STY1* deletion mutant was not able to grow at high temperature[90].

In conclusion, I elucidated that intracellular sequestration of yeast Hog1 is important for heat tolerance. Partially phosphorylated Hog1 due to heat stress has a possibility to negatively affect cell survivability. In order to inhibit the cytotoxicity, Hog1 is temporarily colocalized into SGs to control its function as kinase. Considering the fact that non-functional Hog1 proteins, i.e., kinase inactive, phosphorylation-site dead, and plasma membrane anchored Hog1, show no negative effect on cell growth under high temperature condition, sequestration of active form of Hog1 is critical to yeast heat resistance. Overall, I showed that a novel localization pattern of yeast Hog1 under heat stress is a sign for its intracellular sequestration to control its kinase activity.

Conclusion

This study aimes to gain insight on nitrogen utilization and stress response in the methylotrophic yeast *Candida boidinii*.

In Chapter I, I elucidated the regulation of nitrate and methylamine metabolism in *C. boidinii*. *In vitro* experiments revealed that the transcript level of Ynr1 gene was induced by nitrate and nitrite, and was not repressed by the coexistence with other nitrogen sources. On the other hand, the transcript level of Amo1 gene, which was induced by methylamine, was significantly repressed by the coexistence with ammonium or glutamine.

In Chapter II, I described yeast nitrogen metabolism and its autophagic regulation in the plant leaf environment. On young leaves of *Arabidopsis thaliana*, Ynr1 was necessary for yeast proliferation, and the yeast utilized nitrate as nitrogen source. In contrast, on older leaves, methylamine metabolism was induced in *C. boidinii*, and Ynr1 was subjected to degradation. Biochemical and microscopic analysis of Ynr1 *in vitro* during a shift of nitrogen source from nitrate to methylamine revealed that Ynr1 was transported to the vacuole being the cargo for biosynthetic Cvt pathway, and degraded.

In Chapter III, I revealed that sequestration of yeast Hog1 into stress granules is involved in heat tolerance. When treated with high temperature stress, CbHog1 formed dot structures that co-localized with stress granules (SGs). I also disclosed that the N terminal region of Hog1 is necessary and sufficient for its co-localization with SGs. Growth assay showed that ScHog1, this sequestration of Hog1 into SGs under high temperature condition control the Hog1 kinase activity.

References

1 Morris, C., Kinkel, L., Lindow, S., Hecht-Poinar, E. & Elliott, V. Fifty years of phyllosphere microbiology: significant contributions to research in related fields. *Phyllosphere Microbiol.* 365-375 (2002).

2 Mizuno, M., Yurimoto, H., Yoshida, N., Iguchi, H. & Sakai, Y. Distribution of pink-pigmented facultative methylotrophs on leaves of vegetables. *Biosci. Biotechnol. Biochem.* **76**, 578-580 (2012).

3 Whipps, J. M., Hand, P., Pink, D. & Bending, G. D. Phyllosphere microbiology with special reference to diversity and plant genotype. *J. Appl. Microbiol.* **105**, 1744-1755 (2008).

4 Lindow, S. E. & Brandl, M. T. Microbiology of the phyllosphere. *Appl. Environ. Microbiol.* **69**, 1875-1883 (2003).

5 Mizuno, M., Yurimoto, H., Iguchi, H., Tani, A. & Sakai, Y. Dominant colonization and inheritance of *Methylobacterium* sp. strain OR01 on perilla plants. *Biosci. Biotechnol. Biochem.* **77**, 1533-1538 (2013).

6 Kawaguchi, K., Yurimoto, H., Oku, M. & Sakai, Y. Yeast methylotrophy and autophagy in a methanol-oscillating environment on growing *Arabidopsis thaliana* leaves. *PLoS One* **6**, e25257 (2011).

7 Knief, C., Ramette, A., Frances, L., Alonso-Blanco, C. & Vorholt, J. A. Site and plant species are important determinants of the *Methylobacterium* community composition in the plant phyllosphere. *ISME J* **4**, 719-728 (2010).

8 Lodish, H., Berk, A., Matsudaira, P., Kaiser, C. A., Krieger, M., Scott, M. P., Zipursky, L. & Darnell, J. *Molecular Cell Biology, 5th edn*. London: Macmillan (2008).

9 Stevenson, F. J. Cycles of soils: carbon, nitrogen, phosphorus, sulfur, micronutrients. *John Wiley & Sons* (1999).

10 Barea, J. M., Pozo, M. J., Azcon, R. & Azcon-Aguilar, C. Microbial co-operation in the rhizosphere. *J. Exp. Bot.* **56**, 1761-1778 (2005).

11 Ruiz-Rueda, O., Hallin, S. & Baneras, L. Structure and function of denitrifying and nitrifying bacterial communities in relation to the plant species in a constructed wetland. *FEMS Microbiol. Ecol.* **67**, 308-319 (2009).

12 Remus-Emsermann, M. N., Tecon, R., Kowalchuk, G. A. & Leveau, J. H. Variation in local carrying capacity and the individual fate of bacterial colonizers in the phyllosphere. *ISME J.* **6**, 756-765 (2012).

13 Brewster, J. L. & Gustin, M. C. Hog1: 20 years of discovery and impact. *Sci. Signal.* **7**, re7 (2014).

14 Herskowitz, I. MAP kinase pathways in yeast: for mating and more. *Cell* **80**, 187-197

(1995).

15 Horvitz, H. R. & Sternberg, P. W. Multiple intercellular signalling systems control the development of the *Caenorhabditis elegans* vulva. *Nature* **351**, 535-541 (1991).

16 Cobb, M. H. & Goldsmith, E. J. How MAP kinases are regulated. *J. Biol. Chem.* **270**, 14843-14846 (1995).

17 Barnett, J. A., Payne, R. W. & Yarrow, D. Yeasts: Characteristics and identification. *Cambridge University Press* (1983).

18 Siverio, J. M. Assimilation of nitrate by yeasts. *FEMS Microbiol. Rev.* **26**, 277-284 (2002).

19 Brito, N., Avila, J., Perez, M. D., Gonzalez, C. & Siverio, J. M. The genes *YNI1* and *YNR1*, encoding nitrite reductase and nitrate reductase respectively in the yeast *Hansenula polymorpha*, are clustered and co-ordinately regulated. *Bioche. J.* **317**, 89-95 (1996).

20 Avila, J., Gonzalez, C., Brito, N. & Siverio, J. M. Clustering of the *YNA1* gene encoding a Zn(II)2Cys6 transcriptional factor in the yeast *Hansenula polymorpha* with the nitrate assimilation genes *YNT1*, *YNI1* and *YNR1*, and its involvement in their transcriptional activation. *Biochem. J.* **335**, 647-652 (1998).

21 Avila, J., González, C., Brito, N., Machín, F., Pérez, M. D. & Siverio, J. M. A second Zn(II)(2)Cys(6) transcriptional factor encoded by the *YNA2* gene is indispensable for the transcriptional activation of the genes involved in nitrate assimilation in the yeast *Hansenula polymorpha*. *Yeast* **19**, 537-544 (2002).

22 Pignocchi, C., Berardi, E. & Cox, B. S. Nitrate reduction and the isolation of Nit-mutants in *Hansenula polymorpha*. *Microbiology* **144**, 2323-2330 (1998).

23 Gonzalez, C. & Siverio, J. M. Effect of nitrogen source on the levels of nitrate reductase in the yeast *Hansenula anomala*. *J. Gen. Microbiol.* **138**, 1445-1451 (1992).

24 Hipkin, C. R., Kau, D. A. & Cannons, A. C. Evidence that the glutamine-stimulated loss of nitrate reductase protein from the yeast *Candida nitratophila* is not the result of inducer exclusion. *Biochem. J.* **295**, 611-615 (1993).

25 de Barros Pita, W., Leite, F. C., de Souza Liberal, A. T., Simoes, D. A. & de Morais, M. A., Jr. The ability to use nitrate confers advantage to *Dekkera bruxellensis* over *S. cerevisiae* and can explain its adaptation to industrial fermentation processes. *Antonie Van Leeuwenhoek* **100**, 99-107 (2011).

26 Garcia-Lugo, P., González, C., Perdomo, G., Brito, N., Avila, J., de La Rosa, J. M. & Siverio, J. M.. Cloning, sequencing, and expression of *H.a.YNR1* and *H.a.YNI1*, encoding nitrate and nitrite reductases in the yeast *Hansenula anomala*. *Yeast* **16**, 1099-1105 (2000).

27 Zwart, K., Veenhuis, M., van Dijken, J. P. & Harder, W. Development of amine

oxidase-containing peroxisomes in yeasts during growth on glucose in the presence of methylamine as the sole source of nitrogen. *Arch. Microbiol.* **126**, 117-126 (1980).

28 Faber, K. N., Haima, P., Gietl, C., Harder, W., Ab, G. & Veenhuis, M. The methylotrophic yeast *Hansenula polymorpha* contains an inducible import pathway for peroxisomal matrix proteins with an N-terminal targeting signal (PTS2 proteins). *Proc. Natl. Acad. Sci. U.S.A.* **91**, 12985-12989 (1994).

29 Kumar, S., Lefevre, S. D., Veenhuis, M. & van der Klei, I. J. Extension of yeast chronological lifespan by methylamine. *PloS one* **7**, e48982 (2012).

30 Sakai, Y., Kazarimoto, T. & Tani, Y. Transformation system for an asporogenous methylotrophic yeast, *Candida boidinii*: cloning of the orotidine-5'-phosphate decarboxylase gene (*URA3*), isolation of uracil auxotrophic mutants, and use of the mutants for integrative transformation. *J. Bacteriol.* **173**, 7458-7463 (1991).

31 Sasano, Y., Yurimoto, H. & Sakai, Y. Gene-tagging mutagenesis in the methylotrophic yeast *Candida boidinii*. *J. Biosci. Bioeng.* **104**, 86-89 (2007).

32 Sakai, Y., Goh, T. K. & Tani, Y. High-frequency transformation of a methylotrophic yeast, *Candida boidinii*, with autonomously replicating plasmids which are also functional in *Saccharomyces cerevisiae*. *J. Bacteriol.* **175**, 3556-3562 (1993).

33 Sakai, Y. & Tani, Y. Directed mutagenesis in an asporogenous methylotrophic yeast: cloning, sequencing, and one-step gene disruption of the 3-isopropylmalate dehydrogenase gene (*LEU2*) of *Candida boidinii* to derive doubly auxotrophic marker strains. *J. Bacteriol.* **174**, 5988-5993 (1992).

34 Bustin, S. A., Johnson, G. & Agrawal, S. G. MIQE - guidelines for developing robust real-time PCR assays. *MYCOSES* **55**:30 (2012).

35 Bradford, M. M. A rapid and sensitive method for the quantitation of microgram quantities of protein utilizing the principle of protein-dye binding. *Anal. Biochem.* **72**, 248-254 (1976).

36 Santi, C., Bogusz, D. & Franche, C. Biological nitrogen fixation in non-legume plants. *Ann. Bot.* **111**, 743-767 (2013).

37 Hobbie, E. A. & Hogberg, P. Nitrogen isotopes link mycorrhizal fungi and plants to nitrogen dynamics. *New Phytol.* **196**, 367-382 (2012).

38 Delmotte, N., Knief, C., Chaffron, S., Innerebner, G., Roschitzki, B., Schlapbach, R., von Mering, C. & Vorholt, J. A. Community proteogenomics reveals insights into the physiology of phyllosphere bacteria. *Proc. Natl. Acad. Sci. U.S.A.* **106**, 16428-16433 (2009).

39 Parangan-Smith, A. & Lindow, S. Contribution of Nitrate Assimilation to the Fitness of P*seudomonas syringae* pv. syringae B728a on Plants. *Appl. Environ. Microbiol.* **79**, 678-687 (2013).

40 Cooper, T. G. Nitrogen metabolism in *Saccharomyces cerevisiae*. *Cold Spring Harbor Monograph Archive* **11**, 39-99 (1982).

41 Veenhuis, M., van der Klei, I. J., Titorenko, V. & Harder, W. *Hansenula polymorpha*: an attractive model organism for molecular studies of peroxisome biogenesis and function. *FEMS Microbiol. Lett.* **100**, 393-403 (1992).

42 Spong, A. P. & Subramani, S. Cloning and characterization of *PAS5*: a gene required for peroxisome biogenesis in the methylotrophic yeast *Pichia pastoris*. *J. Cell Biol.* **123**, 535-548 (1993).

43 Sakai, Y., Koller, A., Rangell, L. K., Keller, G. A. & Subramani, S. Peroxisome degradation by microautophagy in *Pichia pastoris*: identification of specific steps and morphological intermediates. *J. Cell Biol.* **141**, 625-636 (1998).

44 Asakura, M., Ninomiya, S., Sugimoto, M., Oku, M., Yamashita, S., Okuno, T., Sakai, Y. & Takano, Y. Atg26-mediated pexophagy is required for host invasion by the plant pathogenic fungus *Colletotrichum orbiculare*. *Plant Cell* **21**, 1291-1304 (2009).

45 Reggiori, F. & Klionsky, D. J. Autophagy in the eukaryotic cell. *Eukaryot. Cell* **1**, 11-21 (2002).

46 Mizushima, N., Yoshimori, T. & Ohsumi, Y. The role of Atg proteins in autophagosome formation. *Annu. Rev. Cell Dev. Biol.* **27**, 107-132 (2011).

47 Suzuki, K. Selective autophagy in budding yeast. *Cell Death Differ.* **20**, 43-48 (2013).

48 Kanki, T. & Klionsky, D. J. Mitophagy in yeast occurs through a selective mechanism. *J. Biol. Chem.* **283**, 32386-32393 (2008).

49 Singh, R., Kaushik, S., Wang, Y., Xiang, Y., Novak, I., Komatsu, M., Tanaka, K., Cuervo, A. M & Czaja, M. J. Autophagy regulates lipid metabolism. *Nature* **458**, 1131-1135 (2009).

50 Kraft, C., Deplazes, A., Sohrmann, M. & Peter, M. Mature ribosomes are selectively degraded upon starvation by an autophagy pathway requiring the Ubp3p/Bre5p ubiquitin protease. *Nat. Cell Biol.* **10**, 602-610 (2008).

51 Bernales, S., Schuck, S. & Walter, P. ER-phagy: selective autophagy of the endoplasmic reticulum. *Autophagy* **3**, 285-287 (2007).

52 Hutchins, M. U. & Klionsky, D. J. Vacuolar localization of oligomeric alpha-mannosidase requires the cytoplasm to vacuole targeting and autophagy pathway components in *Saccharomyces cerevisiae*. *J. Biol. Chem.* **276**, 20491-20498 (2001).

53 Yuga, M., Gomi, K., Klionsky, D. J. & Shintani, T. Aspartyl aminopeptidase is imported from the cytoplasm to the vacuole by selective autophagy in *Saccharomyces cerevisiae*. *J. Biol. Chem.* **286**, 13704-13713 (2011).

54 Scott, S. V. *et al.* Cytoplasm-to-vacuole targeting and autophagy employ the same machinery to deliver proteins to the yeast vacuole. *Proc. Natl. Acad. Sci. U.S.A.* **93**, 12304-12308 (1996).

55 Lynch-Day, M. A. & Klionsky, D. J. The Cvt pathway as a model for selective autophagy. *FEBS lett.* **584**, 1359-1366 (2010).

56 Boer, E., Schroter, A., Bode, R., Piontek, M. & Kunze, G. Characterization and expression analysis of a gene cluster for nitrate assimilation from the yeast *Arxula adeninivorans*. *Yeast* **26**, 83-93 (2009).

57 Bjorkoy, G. *et al.* Monitoring autophagic degradation of p62/SQSTM1. *Methods Enzymol.* **452**, 181-197 (2009).

58 Sakai, Y., Oku, M., van der Klei, I. J. & Kiel, J. A. K. W. Pexophagy: Autophagic degradation of peroxisomes. *Biochim. Biophys. Acta* **1763**, 1767-1775 (2006).

59 Manjithaya, R., Nazarko, T. Y., Farré, J.-C. & Subramani, S. Molecular mechanism and physiological role of pexophagy. *FEBS lett.* **584**, 1367-1373 (2010).

60 Cheong, H. & Klionsky, D. J. Biochemical methods to monitor autophagy-related processes in yeast. *Methods Enzymol.* **451**, 1-26 (2008).

61 Navarro, F. J., Perdomo, G., Tejera, P., Medina, B., Machín, F., Guillén, R. M., Lancha, A. & Siverio, J. M. The role of nitrate reductase in the regulation of the nitrate assimilation pathway in the yeast *Hansenula polymorpha*. *FEMS Yeast Res.* **4**, 149-155 (2003).

62 Su, W., Huber, S. C. & Crawford, N. M. Identification in vitro of a post-translational regulatory site in the hinge 1 region of Arabidopsis nitrate reductase. *Plant Cell* **8**, 519-527 (1996).

63 Kaiser, W. M., Kandlbinder, A., Stoimenova, M. & Glaab, J. Discrepancy between nitrate reduction rates in intact leaves and nitrate reductase activity in leaf extracts: what limits nitrate reduction in situ? *Planta* **210**, 801-807 (2000).

64 Shimada, Y. & Ko, S. Nitrate in vegetables. *Chugoku. Gakuen. J.* **3**, 7-10 (2004).

65 Umar, S., Iqbal, M. & Abrol, Y. Are nitrate concentrations in leafy vegetables within safe limits? *Curr. Sci.* **92**, 355-360 (2007).

66 Mann, A. F., Hucklesby, D. P. & Hewitt, E. J. Effective of aerobic and anaerobic conditions on the invivo nitrate reductase assay in spinach leaves. *Planta* **146**, 83-89 (1979).

67 Man, H. M., Abd-El Baki, G. K., Stegmann, P., Weiner, H. & Kaiser, W. M. The activation state of nitrate reductase is not always correlated with total nitrate reductase activity in leaves. *Planta* **209**, 462-468 (1999).

68 Ramarao, C. S., Srinivasan & Naik, M. S. Inactivation of nitrate reductase from wheat and rice leaves. *Phytochemistry* **20**, 1487-1491 (1981).

69 Posas, F., Witten, E. A. & Saito, H. Requirement of STE50 for osmostress-induced activation of the STE11 mitogen-activated protein kinase kinase kinase in the high-osmolarity glycerol response pathway. *Mol. Cell. Biol.* **18**, 5788-5796 (1998).

70 Hohmann, S. Osmotic stress signaling and osmoadaptation in yeasts. *Microbiol. Mol. Biol. Rev.* **66**, 300-372 (2002).

71 Galcheva-Gargova, Z., Derijard, B., Wu, I. H. & Davis, R. J. An osmosensing signal transduction pathway in mammalian cells. *Science* **265**, 806-808 (1994).

72 Winkler, A., Arkind, C., Mattison, C. P., Burkholder, A., Knoche, K. & Ota, I. Heat stress activates the yeast high-osmolarity glycerol mitogen-activated protein kinase pathway, and protein tyrosine phosphatases are essential under heat stress. *Eukaryot. cell* **1**, 163-173 (2002).

73 Morano, K. A., Grant, C. M. & Moye-Rowley, W. S. The response to heat shock and oxidative stress in *Saccharomyces cerevisiae*. *Genetics* **190**, 1157-1195 (2012).

74 Kamada, Y., Jung, U. S., Piotrowski, J. & Levin, D. E. The protein kinase C-activated MAP kinase pathway of *Saccharomyces cerevisiae* mediates a novel aspect of the heat shock response. *Genes Dev.* **9**, 1559-1571 (1995).

75 Bermejo, C., Rodríguez, E., García, R., Rodríguez-Peña, J. M., Rodríguez de la Concepción, M. L., Rivas, C., Arias, P., Nombela, C., Posas, F. & Arroyo, J. The sequential activation of the yeast HOG and SLT2 pathways is required for cell survival to cell wall stress. *Mol. Biol. Cell* **19**, 1113-1124 (2008).

76 Brengues, M., Teixeira, D. & Parker, R. Movement of eukaryotic mRNAs between polysomes and cytoplasmic processing bodies. *Science* **310**, 486-489 (2005).

77 Kedersha, N. Stoecklin, G., Ayodele, M., Yacono, P., Lykke-Andersen, J., Fritzler, M. J., Scheuner, D., Kaufman, R. J., Golan, D. E. & Anderson, P. Stress granules and processing bodies are dynamically linked sites of mRNP remodeling. *J. Cell Biol.* **169**, 871-884 (2005).

78 Borbolis, F. & Syntichaki, P. Cytoplasmic mRNA turnover and ageing. *Mech. Ageing Dev.* **152**, 32-42 (2015).

79 Takahara, T. & Maeda, T. Transient sequestration of TORC1 into stress granules during heat stress. *Mol. Cell* **47**, 242-252 (2012).

80 Dower, W. J., Miller, J. F. & Ragsdale, C. W. High efficiency transformation of E. coli by high voltage electroporation. *Nucleic acids research* **16**, 6127-6145 (1988).

81 Cryer, D. R., Eccleshall, R. & Marmur, J. Isolation of yeast DNA. *Methods Cell Biol.* **12**, 39-44 (1975).

82 Towbin, H., Staehelin, T. & Gordon, J. Electrophoretic transfer of proteins from polyacrylamide gels to nitrocellulose sheets: procedure and some applications. *Proc. Natl. Acad. Sci. U.S.A.* **76**, 4350-4354 (1979).

83 Buchan, J. R., Yoon, J. H. & Parker, R. Stress-specific composition, assembly and kinetics of stress granules in *Saccharomyces cerevisiae*. *J. Cell Sci.* **124**, 228-239 (2011).

84 Kato, K., Yamamoto, Y. & Izawa, S. Severe ethanol stress induces assembly of stress granules in *Saccharomyces cerevisiae*. *Yeast* **28**, 339-347 (2011).

85 Casey, P. J., Solski, P. A., Der, C. J. & Buss, J. E. p21ras is modified by a farnesyl isoprenoid. *Proc. Natl. Acad. Sci. U.S.A.* **86**, 8323-8327 (1989).

86 Deschenes, R. J., Stimmel, J. B., Clarke, S., Stock, J. & Broach, J. R. RAS2 protein of *Saccharomyces cerevisiae* is methyl-esterified at its carboxyl terminus. *J. Biol. Chem.* **264**, 11865-11873 (1989).

87 Hancock, J. F., Paterson, H. & Marshall, C. J. A polybasic domain or palmitoylation is required in addition to the CAAX motif to localize p21ras to the plasma membrane. *Cell* **63**, 133-139 (1990).

88 Shah, K. H., Zhang, B., Ramachandran, V. & Herman, P. K. Processing body and stress granule assembly occur by independent and differentially regulated pathways in *Saccharomyces cerevisiae*. *Genetics* **193**, 109-123 (2013).

89 Wolozin, B. Regulated protein aggregation: stress granules and neurodegeneration. *Mol. Neurodegener.* **7**, 56 (2012).

90 Millar, J. B., Buck, V. & Wilkinson, M. G. Pyp1 and Pyp2 PTPases dephosphorylate an osmosensing MAP kinase controlling cell size at division in fission yeast. *Genes Dev.* **9**, 2117-2130 (1995).

Acknowledgements

First of all, I wish to express my deepest gratitude to Professor Yasuyoshi Sakai, Division of Applied Life Sciences, Graduate School of Agriculture, Kyoto University, for his directions and valuable discussion during the entire course of this work. His ideas/thoughts always stimulated my scientific interests and enhanced my ability of logical thinking.

I would like to express my sincere gratitude to Professor Shuichi Kawai, Dean of Graduate School of Advanced Integrated Studies in Human Survivability, Kyoto University, for his helpful advice, valuable discussions, and continuous warm encouragement during the course of this 5-year programme 'Shishu-kan'. Sincere appreciation goes to my supervisor, Professor Yosuke Yamashiki, Graduate School of Advanced Integrated Studies in Human Survivability, Kyoto University, for his valuable discussion and warm encouragement especially on the 4th year's overseas fieldwork. This programme enabled me to enhance my technical and personal skills with broad perspectives.

I would like to show my great appreciation to Associate Professor Hiroya Yurimoto, Division of Applied Life Sciences, Graduate School of Agriculture, Kyoto University, for his invaluable support and direct supervisions from the initial to the final stages of this research work. He had always given me accurate advice which I could rely on.

I am forever indebted to Adjunct Associate Professor Jun Hoseki, Division of Applied Life Sciences, Graduate School of Agriculture, Kyoto University, for generously sharing his knowledge and expertise, especially in the field of molecular and cell biology. He was always there and ready to offer his assistance and impart the latest discoveries of methods and ideas.

I wouldn't be able to complete this paper without significant contribution of Assistant Professor Masahide Oku, Division of Applied Life Sciences, Graduate School of Agriculture, Kyoto University. His recommendations especially on the autophagy related experiments were greatly appreciated.

I would like to extend my thanks to Assistant Professor Kosuke Kawaguchi, Graduate School of Medicine and Pharmaceutical Sciences, Toyama University, for teaching me a number of vital techniques and procedures from basic to very advanced ones.

I am grateful to all of the previous and present-members of Laboratory of Microbial Biotechnology, Division of Applied Life Sciences, Graduate School of Agriculture, Kyoto

University, for their friendship and cooperation throughout this study. Special thanks are due to Dr Hiroyuki Iguchi, Dr Delia Saffian, Dr Saori Oda, Ms Shiori Katayama, Mr Shin Ohsawa, Mr Yuki Oku, Mr Yusuke Yoshida and Mr Tomoyuki Takeya for their great collaborations. I also want to show my appreciation especially to Mr Takahiro Hioki and Ms Akari Habata for giving me opportunities to improve my teaching skill during technical supervisions.

I would like to take this opportunity to say that I have had fruitful years as a graduate student at Kyoto University. Although the 5 years flew by like an arrow with my hectic laboratory work, Shishu-kan programme and other extracurricular activities, I managed to keep my mental and physical health with colleagues, friends, supervisors and supporters.

And at the end but not least, I would like to thank my family. Though none of you have really contributed scientifically but your unceasing encouragement and support are deeply appreciated.

Publications

1. **Shiraishi K**, Oku M, Kawaguchi K, Uchida D, Yurimoto H, Sakai Y.
   "Yeast nitrogen utilization in the phyllosphere during plant lifespan under regulation of autophagy"
   Sci Rep. 106:1148-1152. 2015

2. **Shiraishi K**, Oku M, Uchida D, Yurimoto H, Sakai Y.
   "Regulation of nitrate and methylamine metabolism by multiple nitrogen sources in the methylotrophic yeast *Candida boidinii*"
   FEMS Yeast Res. 15: fov084. 2015

3. **Shiraishi K**, Hioki T, Yurimoto H, Sakai Y.
   "Intracellular sequestration of yeast Hog1 is involved in heat tolerance"
   Manuscript in preparation.

Publications not related to this thesis

1. **Shiraishi K**.
   "Report on the Joint Australian and Japan RNA Meeting 2014 (in Japanese)"
   Magazine of the RNA Society of Japan. 31: 20-21. 2014

2. **Shiraishi K**, Sakai Y.
   "Report on the Science Council of Japan Public Symposium - Food Security and Safety - (in Japanese)"
   Bioscience & Industry.
   In press (2017).